Function and regulation of insect olfactory receptors

Dissertation

To fulfil the
requirements for the degree of
„Doctor of Philosophy“(PhD)

Submitted to the Council of the Faculty
of Biology and Pharmacy
of the Friedrich Schiller University Jena

by Latha Mukunda Shivalingaiah (M.Sc.)

born on January 1st, 1985 in Mysore, India

Reviewers

1, Prof. Dr. Bill Hansson

2, Prof. Dr. Stefan Heinemann

3, PD. Dr. Juergen Krieger

Date of public defense

September 22nd, 2014

Dedicated to my eldest brother

Thank you for giving me education

Table of Contents

Introduction

Myriads of chemical cues are present in the environment and many have to be decoded and interpreted by different organisms. Confronted with multitude of cues, animals rely on their sensory systems to perceive signals in the environment they live. The major sensory systems include olfaction (smell), gustation (taste), vision, touch and hearing. For insects, olfaction is an exceptionally important sense.

Insects are one of the most diverse and dominant group of organisms on earth and can be found anywhere on this planet. They are evolutionarily successful as have developed a remarkable adaptability to different habitats, where they play a critical role in the function of ecological systems where they serve as food resource, pollinators, predators, parasites and disease vectors. With their olfactory system insects detect a vast array of odors with remarkable sensitivity and discrimination power. The olfactory system is important for insect behavior as it detects chemical signals from the environment and responds to biologically meaningful chemical signals related to food, prey and mates. Although there is much progress in the field of insect olfaction we still lack a deep understanding of the mechanisms leading to the exceptional sensitivity displayed. Such knowledge contributes to the understanding of the odor mediated behavior of insects and thus potentially also to the development of new strategies to control their behavior. Hence it is of great importance to know the details of signal transduction pathways in the insect olfactory system as this will augment our understanding of insect olfactory neurobiology and might ultimately help in formulating manipulation strategies to regulate and manage the behavior of insects.

Drosophila adult olfactory organs

Insects are well suited model systems for studying olfaction as they are morphologically well understood and have readily accessible components in the olfactory system (Schneider.D, 1969). The olfactory system of *Drosophila melanogaster* is well characterized and serves as a model for understanding insect olfaction. In *Drosophila* there are two pairs of bilateral olfactory organs, the antenna and the maxillary palp situated on the anterior part of the head (Figure 1A). These organs are covered by

innervated hair like structures called sensilla. There are approximately 400 sensilla on each antenna and 60 on each maxillary palp. Based on the morphology, sensilla can be divided into three groups namely the club-shaped basiconic, the long and pointed trichoid and the smallest peg-shaped coeloconic sensilla (Figure 1B). The maxillary palps contain only the basiconic type of sensilla. Each sensillum houses one to four olfactory sensory neurons (OSNs) (Figure 1C). *Drosophila* antennae house around 1200 and the palp about 120 OSNs, which all express members of the olfactory receptor gene family (Vosshall and Stocker, 2007).

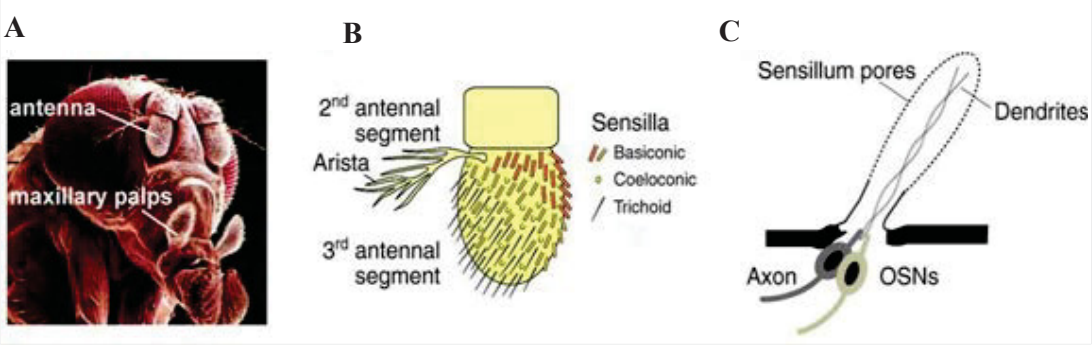

Figure 1: The olfactory system in *Drosophila* A) Head of *Drosophila melanogaster* showing olfactory appendages, the antenna and the maxillary palps. SEM image from Jürgen Berger, Max Planck Institute for Developmental Biology, Tübingen, Germany. B) Scheme of olfactory sensillum distribution on the third antennal segment C) Anatomy of a sensillum. Each sensillum is innervated by 2-4 OSNs, which send their axons to the antennal lobe and their dendrites into the lumen of the sensillum. The sensillum has pores that allow odorants to reach the neurons. (Adapted from Pellegrino and Nakagawa, 2009).

Olfactory information is first detected by the OSNs (Figure 2A). These OSNs send their dendrites into the lymph-filled sensillum lumen. The sensillum wall is equipped with pores through which odor molecules can enter the sensillum lymph, which contains proteins involved in odorant detection. These are odorant-binding proteins (OBPs) and chemosensory proteins (CSPs) which both are thought to transport lipophilic olfactory molecules, and odorant-degrading-enzymes (ODEs) which degrade odorant molecules for slow termination of signals (Figure 2B). The dendritic membrane of OSNs contains the different types of chemoreceptors: odorant receptors (ORs), variant ionotropic glutamate-like receptors (IRs) and gustatory receptors (GRs) (Figure 2C). There are further proteins involved in the process of olfaction such as sensory membrane proteins (SNMPs). The chemosensory receptors identified in *Drosophila melanogaster* are unrelated to vertebrate olfactory receptors. There are about 60 OR genes expressed in the OSNs of basiconic and

trichoid sensilla. Around 73 GR genes are expressed in the taste organs all over the body. These include the CO_2 sensing Gr21a and the Gr63a found in antennal basiconic sensilla. The 61 IR genes are mainly found in coeloconic sensilla (Benton et al., 2009). This study is focused on insect ORs.

Insect olfactory receptors

The first olfactory receptors (ORs) were cloned from rat olfactory epithelium by Linda Buck and Richard Axel (Buck and Axel, 1991). ORs are characterized by a seven transmembrane (7-TM) topology and are members of the G protein-coupled receptor (GPCR) superfamily. Insect ORs were discovered in 1999 by three independent groups (Clyne et al., 1999; Gao and Chess, 1999; Vosshall et al., 1999). Although the functional organization of the olfactory system in vertebrates and insects show similarities, insect ORs do not possess any significant homology to known GPCRs including mammalian ORs (Clyne et al., 1999). Like in vertebrates, insect ORs show 7-TM domains and the identified ORs are highly divergent within species. Extensive *in vitro* and *in vivo* structural studies have revealed that, insect ORs show an inverted membrane topology compared to conventional GPCRs, with a cytoplasmic N-terminus and an extracellular C-terminus (Benton et al., 2006; Wistrand et al., 2006; Lundin et al., 2007; Smart et al., 2008). The insect ORs consist of a conventional ligand binding odorant receptor (OrX) that define the specificity and a highly conserved coreceptor (Or83b) now called Orco (Neuhaus et al., 2005; Vosshall and Hansson, 2011). Orco is broadly expressed in the OSNs and is essential for olfaction *in vivo* (Larsson et al., 2004). The stoichiometry of this heteromeric complex is still unknown.

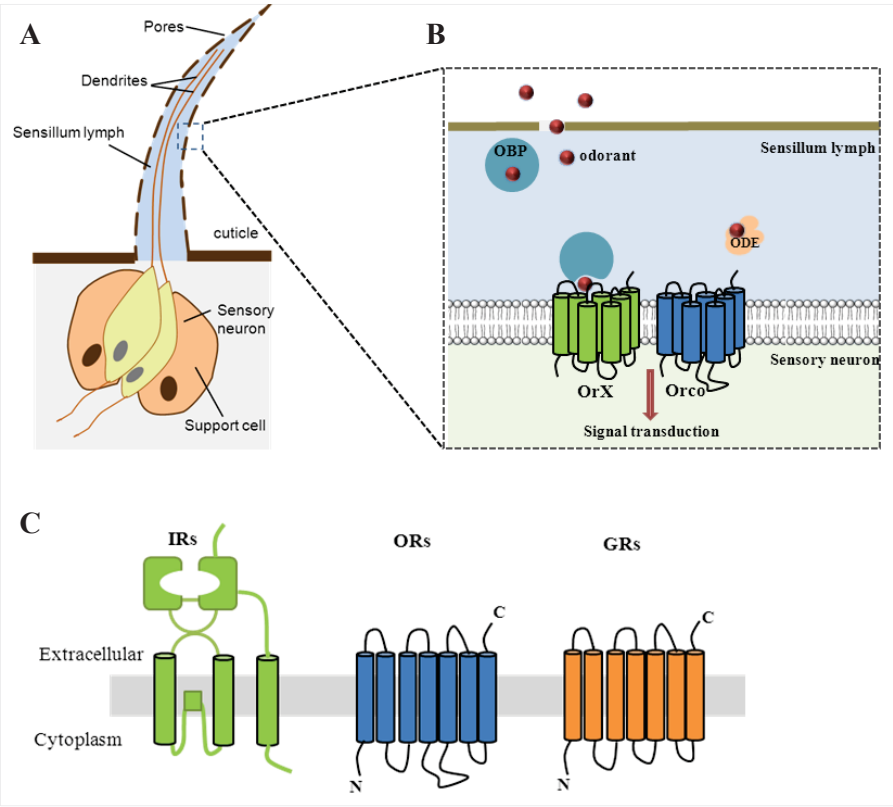

Figure 2: **The protein constituents involves in perireceptor events**: A) Scheme of the general structure of an insect olfactory sensillum B) simplified functional scheme of primary events in insect olfaction showing three major olfactory proteins: odorant binding protein (OBP), odorant degrading enzyme (ODE) and olfactory receptor (ORs) (Modified from Sanchez-Gracia et al., 2009) C) Three insect chemosensory receptor families expressed in the dendrites of antennal OSNs variant ionotropic receptors (IRs), odorant receptors (ORs) and gustatory receptors (GRs).

Insect olfactory signaling

Olfactory signaling in mammalian OSNs involves odorant binding to the olfactory receptor, which in turn induces activation of a G protein signaling cascade. G_s proteins activate the adenylyl cyclase to increase the level of intracellular cyclic nucleotide, 3'-5'-cyclic adenosine monophosphate (cAMP) which directly binds and activates the olfactory cyclic nucleotide–gated channel (CNGC). Opening of the CNG channel allows a flow of cations into the neuron thus producing an action potential and depolarization of the OSN (Figure 3A).

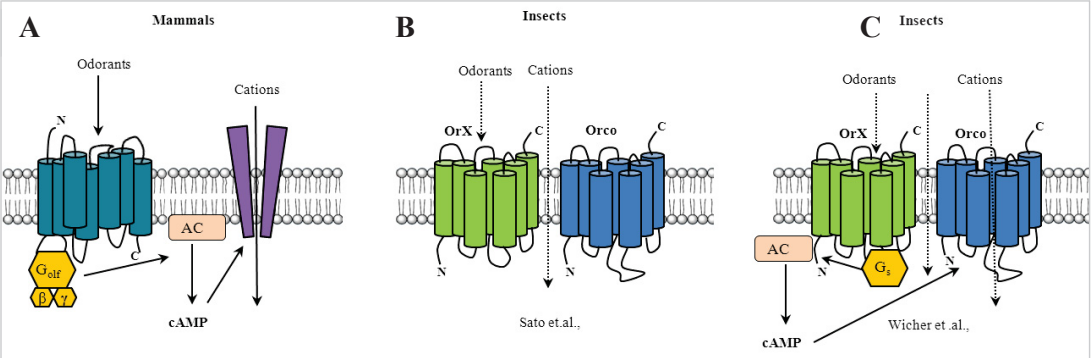

Figure 3: Models of insect olfactory signal transduction: A) Canonical G-protein mediated signaling in the mammalian olfactory system involves odorant binding to the olfactory receptors, which activate G protein (G_{olf}), adenylyl cyclase (AC) and a cyclic nucleotide–gated channel (CNGC). The opening of the CNG channel due to increase in intracellular cAMP levels leads to depolarization of the neuron. B) In Sato et. al., the insect OrX-Orco heteromer complex forms a ligand gated non-selective cation channel that is activated directly by binding of an odor molecule. C) According to Wicher et .al, the ligand binding OrX is a G protein coupled receptor that leads to an increase in cAMP through stimulatory G proteins (G_s). Odor activation of OrX triggers two pathways: a fast ionotropic pathway and a slow metabotropic one.

To understand the mode of olfactory signaling in insects, several studies have been performed on heterologous expression systems. Heterologously expressed cells confer the benefit of studying ORs in isolation and can be subjected to pharmacological analysis. Since the ORs are not in their native environment as in the insect OSN the conclusions should be complemented by experiments with OSNs.

Using patch-clamp to measure ion currents in cultured cells expressing insect ORs and Orco, two independent studies from Sato et al., and Wicher et al., provided evidence for the idea that insect ORs are ligand gated cation channels activated by odorants (Figure 3B, C) (Sato et al., 2008; Wicher et al., 2008). Coexpression of Orco with a tuning OR from *B. mori*, *D. melanogaster* and *A. gambei* conferred similar odorant dependent non-selective ion channel activity in heterologous expression systems (HeLa cells, HEK293 cells and *Xenopus* oocytes). In addition to this, the study from Wicher et al, showed that odor activation of OrX triggers two pathways, a fast ionotropic and a slow metabotropic. The metabotropic pathway includes G_s coupling of OrX leading to production of cAMP, which in turn activates Orco (Figure 3C). The study also demonstrated that Orco acts as an ion channel by itself. The contribution of the metabotropic pathway still remains to be elucidated as the role of G proteins in the signaling mechanism is still highly debated. Several groups have worked on this matter and the results are still ambiguous regarding

definite role of G proteins in insect olfaction. Studies done by (Wicher et al., 2008; Kain et al., 2009; Deng et al., 2011) provide evidence for a role of G proteins in insect olfactory signal transduction, whereas studies from (Sato et al., 2008; Smart et al., 2008; Wicher et al., 2008; Yao and Carlson, 2010) show strong evidence for an ionotropic current (Figure 4).

Odorant coreceptor Orco

Orco is a functional requisite in the insect heteromeric complex (OrX-Orco), required for neuronal surface trafficking and for proper signal transduction (Larsson et al., 2004). Orco forms a common subunit of odorant gated ion channels in insects but is not directly involved in odorant binding. Orco can be activated by cAMP and by a recently identified family of chemical compounds, namely VUAA1 (N-(4-ethylphenyl)-2-((4-ethyl-5-(3-pyridinyl)-4H-1,2,4-triazol-3-yl)thio)acetamide), analogue VUAA4 and, OLC12 (Orco ligand candidate 12) (Wicher et al., 2008; Jones et al., 2011; Chen and Luetje, 2012; Taylor et al., 2012). This VUAA-based family of non-odorant agonists can activate a diversity of insect OrX-Orco complex as well (Taylor et al., 2012).

When heterologously expressed, Orco can form a functional non-specific cation channel in absence of a conventional ligand binding receptor. However, Orco lacks resemblance to any known family of ion channels. Very little is known about amino acid positions important for the gating and cation selectivity properties of Orco channels. Amino acid deletions in the sixth membrane domain of DmelOrco which contains a GYG motif found in the potassium channel selectivity filter altered the ion selectivity (Wicher et al., 2008). Site directed mutagenesis studies done on the *BmOR-Orco* complex showed that a subset of conserved Glu, Asp and Tyr residues in both subunits were essential for channel activity in the OrX-Orco complex. Three mutations D299 and E356 in *Bm/Or1* and Y464 in TM7 of *Bm/Orco* altered the current-voltage relationships and the K^+ selectivity (Nakagawa et al., 2012). A similar study done by substitution of the conserved amino acid Asp466 in WT *Dmel/Orco* to glutamic acid in TM7 (D466E) resulted in a mutant being two fold more sensitive to the Orco agonist VUAA1 in cells expressing Orco and to the Or ligands methyl hexanoate and eugenol in presence of a conventional OR (Kumar et al., 2013). The main finding of this study was that the conserved D466 plays a critical role in Orco activation.

A recent study by Sargsyan et al., 2011, showed that Orco protein from *Drosophila* bears five putative protein kinase C (PKC) phosphorylation sites. Mutation of these sites abolished the sensitivity to cAMP in cell culture experiments as well as *in vivo* in single sensillum recordings. The Orco channel is thus regulated by phosphorylation via PKC, which is activated by the phospholipase C (PLC) intermediate in the inositol 1,4,5-triphosphate/diacyl glycerol (IP_3/DAG) and cAMP transduction cascade (Sargsyan et al., 2011) (Figure 4). This supports the hypothesis that Orco is metabotropically activated via cAMP, which requires basal PKC phosphorylation (Getahun et al., 2013).

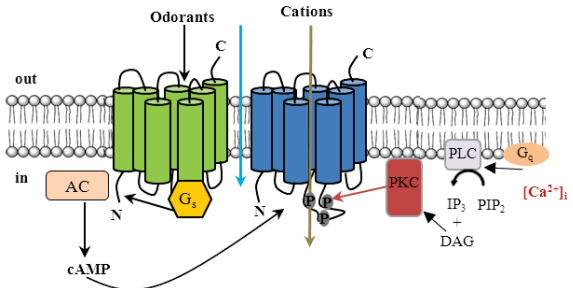

Figure 4: Model of the insect odorant signaling pathway showing ionotropic and metabotropic cascades. Odorant binding to the ligand binding receptor OrX triggers a fast and less sensitive ionotropic pathway (blue arrow), which is followed by a more sensitive and slower metabotropic pathway (brown arrow). Odor stimulation of OrX activates the G_s proteins, which trigger adenylyl cyclases (AC) leading to an increased cAMP level. As a result Orco is activated and thereby the metabotropic response. Orco sensitivity is modulated by protein kinase C (PKC) mediated Orco phosphorylation. Abbreviations: ATP, adenosine triphosphate; cAMP, cyclic adenosine monophosphate; DAG, diacylglycerol; IP_3, inositol 1, 4, 5-trisphosphate; PIP_2 phosphatidylinositol 4, 5-bisphosphate; PLC, phospholipase C.

Subunit stoichiometry of ORs

Formation of ion channels by insect ORs raise obvious questions regarding their subunit contribution to the channel structure. With lacking crystal structure of OR complexes, studies in heterologous systems may provide preliminary insight regarding the number of subunits required for the functional OR complex. Reports from (Neuhaus et al., 2005; Benton et al., 2006) give substantial information on heteromeric interactions between Orco and the ligand binding Or22a receptor. Recent FRET measurement studies on insect cells confirm the homomeric and heteromeric interactions between OrX and Orco proteins (German et al., 2013).

Channelrhodopsin (ChR) is a 7-TM domain protein, which acts as a cation channel. Recent reports using protein crystallization reveal a dimeric structure where the cation

conduction pathway is located at the dimer interface between transmembrane helices 3 & 4 (Mueller et al., 2011; Kato et al., 2012). In order to study the pore forming subunits of insect ORs and the Orco channel the ChR2 crystal structure serves as a suitable prototype. Another possible approach to study oligomerisation would be by constructing and functionally testing concatemers, which are basically two or more subunits that are joined together and where a new protein sequence is introduced to connect the subunits (Steinbach and Akk, 2011).

ORs and sensitivity

As mentioned above, three receptor types are involved in insect olfaction namely the ORs, GRs and IRs. The ORs and the GRs are evolutionarily related but the IRs are derived from the ionotropic glutamate receptor family. Typical response profiles of conventional ORs are fruit odors and pheromones. The IRs detect mainly acids and amines (Benton et al., 2009), while GRs taste chemicals (eg., sugars, bitter substances, salts and pheromones) and sense CO_2.

The occurrence of ORs is limited to mainly flying insects (Missbach et al., 2014), where they show a remarkable sensitivity to odor detection. For example, moth ORs exhibit a very high degree of sensitivity to pheromone and non-pheromone volatiles (Hansson, 1995). In *Manduca sexta* trace amounts of pheromones are sufficient to induce males to initiate flight behaviors for hundreds of meters in pursuit of a potential mate. Recent reports by Getahun et al., 2012 from *Drosophila* OSN recordings show that OR expressing neurons respond faster and with higher sensitivity to brief stimulations compared to IR-and GR expressing neurons. The role of increased sensitivity in OR-expressing neurons probably reflects evolutionary selection pressure for maximized and efficient sensitivity to odors by insects during their flight (Getahun et al., 2012). The sensitivity of ORs requires Orco activation, which occurs through metabotropic autoregulation (Getahun et al., 2013). However the molecular mechanisms underlying the sensitivity of the insect olfactory system are still not well understood.

Cellular calcium and calmodulin

Calcium is an ubiquitous intracellular messenger, which plays a versatile role in a vast array of cellular processes. The basal intracellular calcium levels in neurons at rest are usually 50 to 100 nM but are raised by 10 to 100 times during neuronal activity (Berridge et al., 2000). The handling of intracellular Ca^{2+} ions is critical for normal function of the cells and one of the crucial steps in this process is the subsequent rapid removal of excessive calcium from the cytosol. The clearance of intracellular Ca^{2+} overload is necessary for cell homeostasis. Increase in the intracellular calcium levels can originate from external sources, which include channels that span the plasma membrane such as voltage operated (VOCC), receptor operated (ROCs) and store-operated (SOCC) Ca^{2+}channels. Intracellular Ca^{2+} can also be released into the cytosol from intracellular organelles, the most important being endoplasmic or sarcoplasmic reticula. Calcium release by internal stores is mediated by inositol trisphosphate receptors (IP_3R) and ryanodine receptors (RyR). In order to curb excessive calcium, cells strive to maintain low cytosolic calcium by actively pumping out the calcium, by buffering using calcium-binding proteins or by compartmentalizing calcium into intracellular stores. Calcium ions are removed from the cytosol by the Plasma membrane Ca^{2+}/ATPase (PMCA) pumps and the sodium-calcium exchanger (NCX). Calcium is also sequestered into intracellular stores of the endoplasmic/sarcoplasmic reticulum by sarco(endo)plasmic reticulum calcium ATPase (SERCA) pumps. Alternatively calcium is sequestered in the mitochondrial lumen by opening of mitochondrial uniporter channels. Another method involved in removing free calcium ions from the cytosol is by calcium binding proteins which buffer calcium. Calcium modulated protein (CaM), Calmodulin is one such ubiquitous cytosolic calcium binding protein involved in the binding and regulation of calcium influx and extrusion (Schwaller, 2012; Grienberger and Konnerth, 2012; Berridge et al., 2000). Figure 5 shows events in cell calcium signaling.

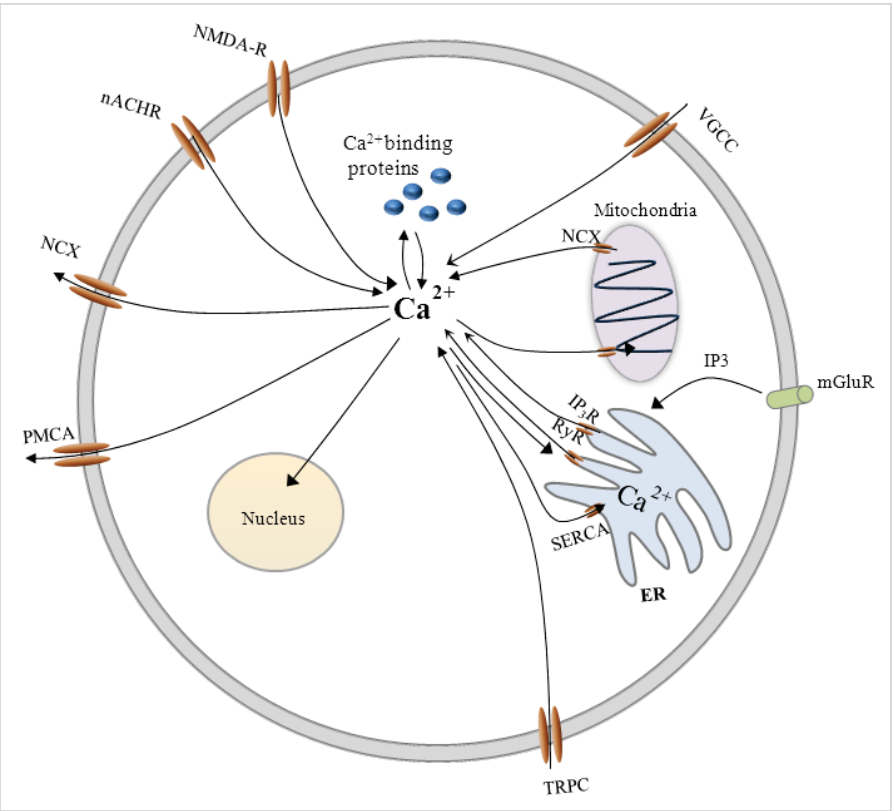

Figure 5: Calcium signaling in a neuronal cell: Calcium influx sources are nicotinic acetylcholine receptors (nAChR), NMDA-type glutamate receptors, transient receptor potential type C channels (TRPC) and voltage-gated calcium channels (VGCC). Calcium efflux is mediated by the plasma membrane calcium ATPase (PMCA), the sodium-calcium exchanger (NCX) and the sarco-endoplasmic reticulum calcium ATPase (SERCA). Intracellular calcium is sensed and buffered by calcium binding proteins. Mitochondria also play an important role in maintaining calcium homeostasis. Calcium release by internal stores is mediated by inositol trisphosphate receptors (IP_3R), ryanodine receptors (RyR). This figure is modified from (Grienberger and Konnerth, 2012).

CaM is a ubiquitous adaptor protein which is evolutionarily conserved and expressed in all eukaryotic cells. It contains two globular domains (N- and C-terminal) joined by a linker. Each domain consists of a calcium binding EF-hand pair. The C- terminal EF-hand pair has a 10 fold higher affinity for Ca^{2+} than the N-terminal hand pair (Martin et al., 1985). CaM is an extremely fast Ca^{2+} buffer (Faas et al., 2011) and acts as a calcium sensor in the regulation of Ca^{2+} pumps as it effectively maintains low and steady levels of intracellular free calcium.

CaM is known to directly modulate numerous types of ion channels, including voltage-gated Ca^{2+} channels and olfactory cyclic nucleotide-gated channels (CNG). CaM plays a preeminent role in intrinsic mechanisms of calcium dependent regulation in voltage gated

calcium channels (Ca_v) (Van Petegem et al., 2005). In the mammalian olfactory system the Ca^{2+} ions bind to calmodulin and the olfactory cyclic nucleotide-gated channels (CNG) are directly inhibited by Ca^{2+}-calmodulin. This inhibition has important implication for olfaction (Tsung-Yu and King-Wai, 1994). Since insect ORs function as non-selective cation channels, the binding of ligand to the ORs leads to Ca^{2+} influx into the cells through Orco or the OrX-Orco complex. What mechanism is involved in the termination of olfactory response is yet to be answered. CaM protein appears to be one of the suitable candidates in studying the molecular and cellular mechanisms involved in insect olfactory signal transduction.

Objectives of the dissertation

Insects have a remarkably sensitive and sophisticated olfactory system providing information regarding the surrounding chemical world. The insect ORs are the most sensitive olfactory receptors recorded. Studying the molecular mechanism involved in insect olfaction provides insights into how olfactory input is translated into behavior. The present study was aimed at understanding the fundamental questions about 'function and regulation of insect olfactory signaling'. Using heterologously expressed cells, olfactory receptors can be studied in isolation and can be subjected to pharmacological analysis. I have performed all investigations in two heterologous systems, namely Chinese Hamster Ovary (CHO) cells and Human embryonic kidney (HEK293) cells to address the questions of interest.

The first manuscript was aimed at investigating functional properties of a synthetic oligomeric construct of *Drosophila* Orco. In order to study channel properties we engineered a simple oligomeric construct; an Orco dimer (Orco di) and stably expressed it in mammalian CHO cell lines. With calcium imaging and patch clamp experiments we showed that Orco di forms a functional ion channel and shows similar properties to those channels formed by Orco wt proteins **(Manuscript 1).**

During the course of this research I also worked on the functional characterization of the olfactory receptors Or56a and Or33a. The main aim of this investigation was the validation of Or56a as a specific receptor for the microbial odor geosmin in heterologously expressed cells (Manuscript 2). This study showed that the receptor Or56a plays an important role for innate behavior in *Drosophila.* Because of their significance

these receptors were also further used to study regulation of insect ORs in manuscript 4 **(Manuscript 2).**

Another study included investigation of the role of *Manduca* Orco in pheromone transduction. The pheromone receptors of *Manduca* belong to the most sensitive receptors known. These receptors are however difficult to study in heterologous system as they are less well expressed. In manuscript 3 we examine the effect of the Orco agonist VUAA1 in *Manduca* Orco using heterologous system HEK293 cells **(Manuscript 3).**

(Manuscript 4) was aimed at understanding the regulation of functional insect ORs. The hypothesis of this study was 'Calmodulin inhibition affects insect odorant receptor function'. In this manuscript we investigated the effect of CaM activity on the Ca^{2+} response of the insect ORs upon agonist stimulation. By using pharmacological analysis, overexpression of CaM mutants and by site directed mutagenesis on a putative calmodulin binding site of Orco protein we studied the modulation of insect ORs by CaM inhibition.

(Manuscript 5) was aimed to find correlates to sensitization in heterologously expressed OR proteins. By monitoring Ca^{2+} responses and current production, we examined whether repeated weak stimulation triggered a sensitization event in heterologously expressed insect ORs. In addition we investigated the role of CaM in sensitization.

Overview of Manuscripts

Manuscript I

Dimerisation of the *Drosophila* odorant co-receptor Orco – a functional study

Latha Mukunda, Sofia Lavista-Llanos, Bill S. Hansson, Dieter Wicher

Frontiers in Cellular Neuroscience (Under revision May 2014)

We engineered a simplest oligomeric construct, Orco dimer (Orco di) and investigated its channel properties. With calcium imaging and patch clamp experiments we show that Orco di forms a functional ion channel. In addition, calcium measurements with coexpression of Or22a show that Orco di interacts with OrX protein Or22a, similar to Orco wt. Furthermore the function of Orco di was seen to be modulated by CaM in a similar manner as the function of Orco wt. Hence we show that the construct Orco di shows similar properties to those channels formed by Orco wt proteins. This is compatible with the hypothesis that Orco wt may act as homodimers.

Author contributions:

Conceived and designed experiments: L. Mukunda, S. Lavista-Llanos, B. S. Hansson, D. Wicher

Performed experiments: L. Mukunda (Construct generation, Bioinformatic analysis, Ca^{2+} imaging of CHO cells, 95%), (electrophysiology 95%), S. Lavista-Llanos (design of construct)

Analyzed the data: L. Mukunda (100%)

Wrote the manuscript: L. Mukunda (70%), D. Wicher. The manuscript was refined in consultation with the authors of the paper.

Manuscript II

A conserved dedicated olfactory circuit for detecting harmful microbes in *Drosophila*

Marcus C. Stensmyr*, Hany K.M. Dweck*, Abu Farhan*, Irene Ibba*, Antonia Strutz, Latha Mukunda, Jeanine Linz, Veit Grabe, Kathrin Steck, Sofia Lavista-Llanos, Dieter Wicher, Silke Sachse, Markus Knaden, Paul G. Becher, Yoichi Seki, and Bill S. Hansson

**These authors contributed equally to the work*

Cell, 2012, 151(6): 1345-1357.

(Published)

Geosmin is a volatile compound released by bacteria, fungi and a cyanobacterium which is known to induce induce slight aversion in flies when added in small amount. In this study we describe a functionally segregated olfactory circuit in *Drosophila melanogaster* that is exclusively activated by geosmin to alert the flies to the presence of harmful microbes. Comprehensive electrophysiological experiments showed that geosmin is detected exclusively by single class of olfactory sensory neurons, ab4B which co express odorant receptors Or56a and Or33a. Functional imaging and deorphanization studies showed that Or56a is the specific receptor for geosmin. We further show that geosmin detection pathway is evolutionarily conserved across genus *Drosophila* and it plays a crucial role for detection and avoidance of toxic feeding and breeding substrates infected with bacteria and mold.

Author contributions:

Designed & performed experiments: M.C. Stensmyr, H.K.M. Dweck, A. Farhan, I. Ibba, A. Strutz, L. Mukunda (Ca^{2+} imaging of CHO cells, 5%), J. Linz, V. Grabe, K. Steck, S. Lavista-Llanos, D. Wicher, S. Sachse, M. Knaden, P.G.Becher, Y. Seki, and B.S. Hansson

Wrote the manuscript: M.C. Stensmyr, H. K.M. Dweck, A. Farhan, I. Ibba, A., B. S. Hansson. The manuscript was refined in consultation with the authors of the paper.

Manuscript III

***In situ* tip-recordings found no evidence for an Orco-based ionotropic mechanism of pheromone-transduction in Manduca sexta.**

Andreas Nolte*, Nico W. Funk*, Latha Mukunda, Petra Gawalek, Achim Werckenthin, Bill S .Hansson, Dieter Wicher, Monika Stengl

**These authors contributed equally to the work*

PLoS One. 2013 8(5):e62648.

(Published)

In this study we examined whether Orco-dependent ionotropic pathway is responsible for the pheromone transduction in *Manduca sexta.* To study the function of Orco in pheromone transduction we examined the effect of Orco agonist VUAA1 on HEK293 (Human embryonic kidney) cells expressing *Manduca* Orco. Calcium imaging experiments showed significant increase in intracellular Ca^{2+} concentration upon stimulation with VUAA1 in cells thus confirming *Manduca* Orco forms spontaneously active Ca^{2+} permeable cation channel in heterologous system akin to D. *melanogaster.* These measurements demonstrate that VUAA1 acts as an agonist for *Manduca* Orco ion channel in heterologous expression system. With in situ long-term tip recordings from pheromone-sensitive trichoid sensilla of intact *M. sexta* we found no evidence for the role of *Msex*/Or–*Msex/* Orco-dependent ionotropic transduction pathway.

Author contributions:

Conceived and designed experiments: A. Nolte, N. W. Funk, B. S. Hansson, D. Wicher, M. Stengl

Performed experiments: A. Nolte, N. W. Funk, P. Gawalek (Tip recordings), L. Mukunda (Ca^{2+} imaging of HEK cells 10%)

Analyzed the data: A. Nolte, N. W. Funk, L. Mukunda, A. Werckenthin, D. Wicher

Wrote the manuscript: A. Nolte, N. W. Funk, M. Stengl. The manuscript was refined in consultation with the authors of the paper.

Manuscript IV

Calmodulin modulates insect odorant receptor function

Latha Mukunda, Fabio Miazzi, Sabine Kaltofen, Bill S. Hansson, Dieter Wicher
Cell Calcium, 2014, 55(4):191-9

(Published)

In this study using Ca^{2+} imaging to monitor OR activity we investigated the effect of calmodulin (CaM) inhibition on the function of OR proteins. Stimulation of *Drosophila* olfactory sensory neurons with the synthetic OR agonist VUAA1 in presence of CaM inhibitor W7 elicited reduced and prolonged Ca^{2+} response. A similar response was seen in Orco proteins heterologously expressed in CHO cells with use potent CaM inhibitors and also upon overexpression of CaM-EF hand mutants. Furthermore, with cells expressing Orco CaM mutant bearing a point mutation in putative CaM binding site (K339N), the Ca^{2+} responses were similar to the observed effect with application of CaM inhibitors. We also show that in CHO cells coexpressing *Drosophila* ORs (Or22a/Orco, Or47a/Orco, and Or56a/Orco) CaM inhibition did not show a generalized effect on Ca^{2+} responses. This study provides evidence that CaM activity affects the function of Orco channels and may have specific effect on OrX/Orco complex.

Author contributions:

Conceived and designed experiments: D. Wicher, L. Mukunda, F. Miazzi, B. S. Hansson

Performed experiments: L.Mukunda (Bioinformatic analysis, site direct mutagenesis, Ca^{2+} imaging of CHO cells, 80%), F. Miazzi (antennal preparations and imaging in flies), S. Kaltofen (fly antennal preparations).

Analyzed the data: L.Mukunda (80%), F. Miazzi

Wrote the manuscript: D. Wicher, L.Mukunda (20%), F. Miazzi. The manuscript was refined in consultation with the authors of the paper.

Manuscript V

Sensitization in heterologously expressed ORs

Latha Mukunda*, Vardanush Sargsyan*, Bill S. Hansson, Dieter Wicher

**These authors contributed equally to the work*

(In preparation)

Sensitization is a process where repeated weak stimulation of ORs produces an enhanced response. Using electrophysiological and calcium imaging methods we demonstrate that OR sensitization can be monitored with heterologously expressed OR proteins. Repeated stimulation of heterologously expressed Orco using agonist VUAA1 showed increased current production and enhanced Ca^{2+} responses respectively. This sensitization process can be abolished by CaM inhibition thus suggesting a role of CaM in mediating sensitization. This study provides a system to study the mechanism of sensitization in heterologous expression system.

Author contributions:

Conceived and designed experiments: D. Wicher, L. Mukunda, V. Sargsyan, B. S. Hansson

Performed experiments: L. Mukunda (Ca^{2+} imaging of CHO cells 50%), V. Sargsyan (electrophysiology)

Analyzed the data: L. Mukunda (50%), V. Sargsyan

Wrote the manuscript: L. Mukunda (70%), D. Wicher. The manuscript was refined in consultation with the authors of the paper.

Manuscript I

Dimerisation of the *Drosophila* odorant co-receptor Orco –a functional study

Dimerisation of the *Drosophila* odorant co-receptor Orco – a functional study

Latha Mukunda, Sofia Lavista-Llanos, Bill S. Hansson, Dieter Wicher
Max Planck Institute for Chemical Ecology, Department Evolutionary Neuroethology, Hans-Knöll-St. 8, D-07745 Jena, Germany

Corresponding author: Dieter Wicher, Max Planck Institute for Chemical Ecology, Hans-Knöll-St. 8, D-07745 Jena, Germany, Tel.: +49 3641 571415, e-mail: dwicher@ice.mpg.de

Abstract

Odorant receptors (ORs) detect volatile molecules and transform this external information into an intracellular signal. Insect ORs are heteromers composed of two seven transmembrane proteins, an odor-specific OrX and a coreceptor (Orco) protein. These ORs form ligand gated cation channels that conduct also calcium. The sensitivity of the ORs is regulated by intracellular signaling cascades. Heterologously expressed Orco proteins form also non-selective cation channels that cannot be activated by odors but by synthetic agonists such as VUAA1. The stoichiometry of OR or Orco channels is unknown. In this study we engineered the simplest oligomeric construct, the Orco dimer (Orco di) and investigated its functional properties. Two Orco proteins were coupled via a 1-transmembrane protein to grant for proper orientation of both parts. The Orco di construct and Orco wild type proteins were stably expressed in CHO (Chinese Hamster Ovary) cells. Their functional properties were investigated and compared by performing calcium imaging and patch clamp experiments. With calcium imaging experiments using allosteric agonist VUAA1 we demonstrate that the Orco di construct - similar to Orco wt -forms functional calcium conducting ion channel. This was supported by patch clamp experiments. The function of Orco di was seen to be modulated by CaM in a similar manner as the function of Orco wt. In addition, Orco di interacts with the OrX protein, Or22a. The properties of this complex are comparable to Or22a/Orco wt couples. Taken together, the properties of the Orco di construct are similar to those of channels formed by Orco wt proteins. Our results are thus compatible with the view that Orco wt channels are dimeric assemblies.

Keywords: odorant receptor, coreceptor, concatameric dimer, calmodulin, Orco channel

Introduction

Olfactory receptors are transmembrane proteins that transfer information of external volatile molecules into an intracellular signal. Insect possess three classes of these receptors, odorant receptors (ORs), gustatory receptors (GRs) and variant ionotropic glutamate receptors (IRs). The insect OR gene family encodes proteins comprising seven transmembrane domains as G protein coupled receptors (GPCRs). Compared to vertebrate ORs, insect ORs are inversely inserted into the plasma membrane (Benton et al., 2006; Lundin et al., 2007; Smart et al., 2008) and are formed by heterodimeric complexes of a ligand binding olfactory receptor protein (OrX) and a highly conserved odorant co-receptor (Orco) (Neuhaus et al., 2005; Benton et al., 2006). Insect ORs operate as ligand-gated ion channels (Sato et al., 2008; Wicher et al., 2008), which are tuned by intracellular signaling (Wicher et al., 2008; Kain et al., 2009; Deng et al., 2011; Getahun et al., 2013; Ignatious Raja et al., 2014).

Orco has a chaperone function as it supports the dendritic localization of OrX proteins (Larsson et al., 2004), and it contributes to the OR ion channel pore formation (Nichols et al., 2011; Pask et al., 2011; Nakagawa et al., 2012). In the absence of OrX proteins, Orco forms a homomeric ion channel (Wicher et al., 2008; Jones et al., 2011). A FRET study demonstrated homodimeric and heterodimeric interactions between Orco and OrX proteins (German et al., 2013). It is, however, not excluded that dimers may dimerise to form tetramers as observed for orai1 channels (Penna et al., 2008). Whether Orco channels form dimers as the heteromeric OR channels remains elusive.

Channelrhodopsin (ChR) is another type of a seven transmembrane domain protein that acts as ion channel. Protein crystallization revealed a dimeric structure (Mueller et al., 2011; Kato et al., 2012). The conductance pathway of ChR2 is located at the dimer interface with transmembrane helices 3 and 4 (Mueller et al., 2011). Dimerisation has been observed for GPCR proteins, either as homomeric interaction of muscarinic acetylcholine receptors or as heteromeric coupling of $GABA_B$ receptors (Wicher, 2010). Artificial homo as well as heterodimerization of GPCR proteins was performed by linking the C terminus of one protein to the N terminus of the other, spaced by a membrane spanning linker leading to functional constructs that were well expressed in heterologous cells (Terpager et al., 2009).

In the present study we ask whether a dimeric Orco construct would display channel properties and if so, whether these properties differ from those of Orco wild type (Orco wt) channels. For this purpose we engineered an Orco dimer (Orco di) and expressed it in Chinese

hamster ovary (CHO) cells. By means of calcium imaging and patch clamp experiments we show that the dimeric construct displays similar properties as Orco wt channels.

Materials and methods

Synthetic dimer construct

The Orco dimer construct (3.6kb) was generated by fusion of two *Drosophila melanogaster* Orco subunits as a single open reading frame into pcDNA3.1(-) mammalian expression vector (Invitrogen). To grant a correct orientation of the seven transmembrane domains of each of two Orco subunits, they were coupled with a 177 amino acid long 1- transmembrane protein human sodium channel, type I, beta subunit (SCN1B) (NM_001037.4). SCN1B was synthesized by Eurofins MWG Operon and cloned into Topo pcR2.1 vector (Invitrogen). The oligonucleotides used for generating Orco dimer contained XhoI /SacI restriction sites: Orco F 5'- GAT CTC GAG CTA TGA CAA CCT CGA TGC AGC C - 3' Orco R 5'-CGA GCT CTT TCT TGA GCT GCA CCA GCA CCA TAA AGT AGG T-3' or NotI/ HindIII restriction sites: Orco F 5'- TTG CGG CCG CCT ATG ACA ACC TCG ATG CAG CCG AGC -3' Orco R 5'- TCG AAG CTT GTT ACT TGA GCT GCA CCA GCA -3'. The PCR products were T: A cloned into Topo vector separately (Invitrogen). The two Orco units were then subcloned into pcDNA3.1 (-) vector containing SCN1B. All the sequence analysis was done via double strand DNA sequencing at Eurofins MWG Operon. Sequence congruence was 100%.

Cell culture and calcium imaging

CHO cells stably expressing Orco wt or Orco dimer were purchased from cytobox UG (Konstanz, Germany) and grown in cytobox™ CHO select medium containing puromycin. The cells were grown on poly-L-lysine (0.01%, Sigma-Aldrich) coated coverslips. The culture conditions and transient transfection protocol were done as described by (Wicher et al., 2008) .Cells for imaging were loaded with fura-2 by incubation in 1 ml CHO select medium containing 5µM fura-2/acetomethylester (Molecular Probes, Invitrogen) for 30 min. Excitation of fura-2 at 340 and 380 nm was performed with a monochromator (Polychrome V, T.I.L.L. Photonics, Gräfelfing, Germany) coupled via an epifluorescence condenser into an Axioskop FS microscope (Carl Zeiss, Jena, Germany) with a water immersion objective (LUMPFL 40xW/IR/0.8; Olympus, Hamburg, Germany). Emitted light was separated by a 400-nm dichroic mirror and filtered with a 420-nm long-pass filter. Free intracellular Ca^{2+}

concentration ($[Ca^{2+}]_i$) was calculated according to the equation $[Ca^{2+}]_i = K_{eff}(R-R_{min})/(R_{max}-R)$.

K_{eff}, $R_{min,}$ and R_{max} were determined as mentioned in (Mukunda et al., 2014). Fluorescence images were acquired using a cooled CCD camera controlled by TILLVision 4.0 software (T.I.L.L. Photonics). The resolution was 640x480 pixels in a frame of 175x130 µm (40x/IR/0.8 objective). Image pairs were obtained by excitation for 150 ms at 340 nm and 380 nm; background fluorescence was subtracted. CHO cells were stimulated using VUAA1, OLC12, and via pipette.

Patch-clamp electrophysiology

Current measurements and data acquisition from CHO cells were performed in whole cell configuration using EPC10 patch-clamp amplifier controlled by PatchMaster software (HEKA Elektronik, Lambrecht, Germany). Pipettes having resistances 3-4 MΩ were pulled from borosilicate capillaries (Sutter Instruments, Novato, CA, USA). The pipette solution for whole-cell recordings contained (in mM) 140 KCl, 4 NaCl, 1 $CaCl_2$, 2 Mg-ATP, 0.05 Na-GTP, 5 EGTA, 10 HEPES (pH 7.3), and the bath solution contained (in mM) 140 NaCl, 5 KCl, 1 $CaCl_2$, 1 $MgCl_2$, 10 HEPES, 10 glucose (pH 7.4). For application of the agonist pneumatic picopump PV830 (World precision Instruments, USA) was used and the cells were continuously perfused with bath solution in the recording/perfusion chamber (RC-27,Warner Instruments Inc, Hamden, CT, USA).

Chemicals

VUAA1 (N-(4-ethylphenyl)-2-((4-ethyl-5-(3-pyridinyl)-4H-1,2,4-triazol-3-yl)thio)acetamide) was synthesized by the working group "Mass Spectrometry/Proteomics" of the Max-Planck Institute for chemical ecology (Jena, Germany). OLC12 was kindly provided by Charles Luetje, University of Miami, FL, USA. W-7 hydrochloride was purchased from Tocris bioscience (Wiesbaden-Nordenstadt, Germany). Ruthenium red (RR) was purchased from Sigma Aldrich (Steinheim, Germany).

Data analysis

The transmembrane domain prediction was performed by TTHMM server v.2.0 (CBS, Denmark) and TopPred 0.01- Topology prediction of membrane proteins (Mobyle@Pasteur, France). For electrophysiology data analysis the software IgorPro (WaveMetrics, Lake Oswego, OR, USA) was used. Statistical analysis was performed in Prism 4 software (GraphPad Software, Inc., La Jolla, CA, USA). All data represent mean ± SEM.

Results

Orco di was generated by fusing two Orco proteins of *Drosophila melanogaster* into a single open reading frame and subsequent cloning into a pcDNA 3.1(-) mammalian expression vector (Figure 1). To grant an equal orientation of each of the seven transmembrane proteins, we coupled the single transmembrane human sodium channel beta subunit SCN1B between the two Orco subunits.

Orco wt and Orco di were stably expressed in CHO cells. To study and to compare their functional properties we performed calcium imaging experiments using the ratio metric dye fura-2. Stimulation of the receptors with the synthetic Orco agonist VUAA1 (Jones et al., 2011) led to rapid increases in free intracellular Ca^{2+} concentration $[Ca^{2+}]_i$ for both Orco wt and di expressing cells (Figure 2A). A higher maximum increase observed in Orco wt (Figure 2B) may result from a more pronounced functional expression of the protein within the plasma membrane. For both Orco wt and Orco di the responses to VUAA1 terminated within 50 s, and the time constant τ of the decay in $[Ca^{2+}]_i$ was not significantly different (Figure 2C). To demonstrate that the observed Ca^{2+} signals resulted from Ca^{2+} influx into the cells, we stimulated Orco di expressing cells in a Ca^{2+}-free bath solution. Under these conditions $[Ca^{2+}]_i$ remained constant (Figure 2D). The presence of Ruthenium red (RR) which has been previously shown to inhibit insect OR's (Nakagawa et al., 2005; Sato et al., 2008; Jones et al., 2011; Nichols et al., 2011) also abolished any Ca^{2+} signal upon VUAA1 application (Figure 2E). These observations are in line with previous findings in Orco wt expressing cells (Mukunda et al., 2014) and indicates that Orco di forms Ru red-sensitive Ca^{2+} permeable ion channels.

Heterologously expressed Orco proteins show constitutive channel activity leading to enhanced resting $[Ca^{2+}]_i$ (Wicher et al., 2008). Compared with non-transfected cells the Ca^{2+} resting levels in cells expressing Orco wt and Orco di appeared to be significantly enhanced, at comparable levels (Figure 2F). Thus Orco di channels seem to show a similar constitutive activity as the Orco wt channels.

To compare the transmembrane currents conducted by Orco wt and Orco di we performed patch clamp experiments using the whole cell configuration. While receptor stimulation with VUAA1 in the non-invasive calcium imaging approach induced robust and reproducible responses, it appeared to be less efficient in the patch clamp recordings. Also for *Drosophila* Orco expression in *Xenopus* oocytes the used VUAA1 concentration of 100 µM was just

above the threshold and below the EC_{50} of 190 µM (Chen and Luetje, 2012). We thus used the more potent OR agonist OLC12 (EC_{50} = 35 µM; Chen and Luetje, 2012) which induced transient inward currents in Orco wt and Orco di expressing cells. (Figure 3A, B). The currents induced by OLC12 had similar amplitude in Orco wt (mean 220 pA) and Orco di (mean 140 pA) expressing cells (Figure 3C). The current decay was slower for Orco di (τ = 14 ± 2.9 s) compared to Orco wt (τ = 7.6 ± 0.7 s) (Figure 3D) which indicates a slower closure of the dimer channels. In conclusion, the patch clamp measurements demonstrate that Orco di gives rise to a membrane current upon agonist stimulation.

In a previous study (Mukunda et al., 2014) we have seen that calmodulin (CaM) modulates Orco channel activity. In order to check if this regulation is conserved in Orco di we stimulated cells expressing Orco di with VUAA1 in the presence of CaM inhibitor W7 (Figure 4A). Application of W7 reduced the calcium responses to VUAA1 stimulation (Figure 4B) and significantly increased the decay time constant of the Ca^{2+} response (Figure 4, C). These effects are in line with the results obtained for Orco wt (Mukunda et al., 2014), and demonstrate conservation of the CaM regulation in the dimeric Orco construct.

In heterologous expression systems Orco forms heterodimeric complexes with ligand binding OrX proteins (Neuhaus et al., 2005; Benton et al., 2006). To test whether Orco di interacts with a ligand binding odorant receptor OrX, we next coexpressed Or22a in Orco wt and in Orco di expressing cells. The $[Ca^{2+}]_i$ signals obtained from cells coexpressing Or22a displayed a slower decay than cells solely expressing Orco, as previously observed (Mukunda et al., 2014). The amplitude of $[Ca^{2+}]_i$ in Or22a/wt expressing cells was larger than in cells expressing Or22a/di (Figure 5A, B). The decay of the Ca^{2+} signals was similar for Orco wt and Orco di expressing cells (Figure 5C). The calcium measurements with coexpression of Or22a show that Orco di interacts with OrX proteins to form a functional OR channel.

Discussion

Orco is an integral part of insect ORs and is required for the correct insertion of OrX proteins in the dendritic membrane of the receptor neurons (Larsson et al., 2004). In addition to forming heteromers with OrX proteins with an as yet unknown stoichiometry there is also evidence that Orco may build homomeres (Neuhaus et al., 2005; Benton et al., 2006; German et al., 2013). Reports of the purification of insect OR subunits suggest potential dimeric and

quaternary structure formation between Orco and Or22a (Carraher et al., 2013). In this study we engineered the minimal oligomeric structure of Orco and asked whether Orco di exhibits the same channel properties like Orco wt.

The calcium imaging experiments with Orco di expressing cells have demonstrated a Ca^{2+} influx in response to non-odor OR agonists such as VUAA1 (Jones et al., 2011; Chen and Luetje, 2012) (Figure 2). Heterologously expressed Orco proteins form Ca^{2+} permeable cation channels and show constitutive activity which leads to elevated intracellular [Ca^{2+}] resting levels (Sato et al., 2008; Wicher et al., 2008; Jones et al., 2011; Sargsyan et al., 2011). The basal $[Ca^{2+}]_i$ levels of Orco di expressing cells were also enhanced as compared to non-transfected CHO cells. This indicates also a background activity of Orco di channels (Figure 2F). The agonist stimulation produced Ca^{2+} signals similar to those observed for Orco wt that were depending on extracellular Ca^{2+}. Thus, Orco di shows functional expression and forms a Ca^{2+} permeable cation channel. Whole cell current measurements using patch clamp further confirm that Orco di displays ion channel activity and generates a transient inward current similar to Orco wt when activated by an appropriate ligand (Figure 3).

In a recent study we showed that CaM activity affects the function of Orco channels (Mukunda et al., 2014). Stimulation of Orco wt cells in presence of the CaM inhibitor W7 showed significantly reduced and prolonged $[Ca^{2+}]_i$ responses. The Orco protein contains a conserved putative CaM binding motif (^{336}SAIKYWER^{344}) in the second intracellular loop. A point mutation in this putative CaM site (K339N) affects the Ca^{2+} responses elicited by agonist stimulation. As the Orco di protein also contains the putative CaM binding motif it was expected that CaM would regulate this construct. Indeed, the responses obtained with Orco di were similar to those obtained with Orco wt in presence of W7 (Figure 4B, C), suggesting that Orco di is modulated by CaM as Orco wt.

A mutational study of *Bombyx* pheromone receptors suggests that both constituents of olfactory receptors, Orco and OrX proteins contribute to the ion channel pore (Nakagawa 2012). Also, expression of Orco alone leads to functional channels suggesting that they may dimerize which is supported by FRET experiments (German et al., 2013). Coexpression of Orco di and Or22a elicited Ca^{2+} transients in response to agonist application as seen in cells expressing Or22a/Orco wt. This suggests an interaction of OrX protein here represented by Or22a (Figure 5). The construction of concatameric GPCR dimers has raised the question whether they would form a functional dimer composed of the two coupled subunits or interconcatameric dimers, i.e. tetramers (Terpager et al., 2009). The first alternative was

expected for homomeric constructs such as the β2-adrenergic receptor, but not for a heteromeric couple of β2-adrenergic receptor and neurokinin receptor 1. A similar question arises concerning the composition of Or22a and Orco complex. There might be a tetrameric interaction between two Or22a units and the dimer.

In conclusion, our experiments demonstrate that the synthetic Orco di construct is functionally expressed and is forms a functional Ca^{2+}-permeable cation channel. Like Orco wt, it can be activated by synthetic agonists like VUAA1 and its derivatives. Furthermore, Orco di seems to be constitutively active leading to enhanced basal $[Ca^{2+}]_i$ levels in Orco di expressing cells. Finally, our results show that Orco di is modulated by CaM in similar way as Orco wt and it interacts with OrX proteins such as Or22a. Thus the functional properties of the Orco di construct are very similar to those of Orco wt. This result would be compatible with the assumption that Orco channels build dimeric assemblies. At presence, however, this view is requires more support, for example by resolving the crystal structure of Orco complexes.

Acknowledgements

This study was supported by the Max Planck Society. The authors thank Sabine Kaltofen for assistance.

References

Benton, R., Sachse, S., Michnick, S.W., and Vosshall, L.B. (2006). Atypical membrane topology and heteromeric function of *Drosophila* odorant receptors in vivo. *Plos Biology* 4**,** 240-257.

Carraher, C., Nazmi, A.R., Newcomb, R.D., and Kralicek, A. (2013). Recombinant expression, detergent solubilisation and purification of insect odorant receptor subunits. *Protein Expr Purif* 90**,** 160-169.

Chen, S., and Luetje, C.W. (2012). Identification of New Agonists and Antagonists of the Insect Odorant Receptor Co-Receptor Subunit. *Plos One* 7.

Deng, Y., Zhang, W., Farhat, K., Oberland, S., Gisselmann, G., and Neuhaus, E.M. (2011). The Stimulatory G alpha(s) Protein Is Involved in Olfactory Signal Transduction in *Drosophila*. *Plos One* 6.

German, P.F., Van Der Poel, S., Carraher, C., Kralicek, A.V., and Newcomb, R.D. (2013). Insights into subunit interactions within the insect olfactory receptor complex using FRET. *Insect Biochem Mol Biol* 43**,** 138-145.

Getahun, M.N., Olsson, S.B., Lavista-Llanos, S., Hansson, B.S., and Wicher, D. (2013). Insect Odorant Response Sensitivity Is Tuned by Metabotropically Autoregulated Olfactory Receptors. *Plos One* 8.

Ignatious Raja, J.S., Katanayeva, N., Katanaev, V.L., and Galizia, C.G. (2014). Role of Go/i subgroup of G proteins in olfactory signaling of *Drosophila melanogaster*. *Eur J Neurosci* 39**,** 1245-1255.

Jones, P.L., Pask, G.M., Rinker, D.C., and Zwiebel, L.J. (2011). Functional agonism of insect odorant receptor ion channels (vol 108, pg 8821, 2011). *Proc Natl Acad Sci U S A* 108**,** 11298-11298.

Kain, P., Chandrashekaran, S., Rodrigues, V., and Hasan, G. (2009). *Drosophila* Mutants in Phospholipid Signaling Have Reduced Olfactory Responses as Adults and Larvae. *J Neurogenet* 23**,** 303-312.

Kato, H.E., Zhang, F., Yizhar, O., Ramakrishnan, C., Nishizawa, T., Hirata, K., Ito, J., Aita, Y., Tsukazaki, T., Hayashi, S., Hegemann, P., Maturana, A.D., Ishitani, R., Deisseroth, K., and Nureki, O. (2012). Crystal structure of the channelrhodopsin light-gated cation channel. *Nature* 482**,** 369-374.

Larsson, M.C., Domingos, A.I., Jones, W.D., Chiappe, M.E., Amrein, H., and Vosshall, L.B. (2004). Or83b encodes a broadly expressed odorant receptor essential for *Drosophila* olfaction. *Neuron* 43**,** 703-714.

Lundin, C., Kall, L., Kreher, S.A., Kapp, K., Sonnhammer, E.L., Carlson, J.R., Von Heijne, G., and Nilsson, I. (2007). Membrane topology of the *Drosophila* OR83b odorant receptor. *Febs Letters* 581**,** 5601-5604.

Mukunda, L., Miazzi, F., Kaltofen, S., Hansson, B.S., and Wicher, D. (2014). Calmodulin modulates insect odorant receptor function, in *Cell Calcium*. 2014 Elsevier Ltd).

Mueller, M., Bamann, C., Bamberg, E., and Kuhlbrandt, W. (2011). Projection structure of channelrhodopsin-2 at 6 A resolution by electron crystallography. *J Mol Biol* 414**,** 86-95.

Nakagawa, T., Pellegrino, M., Sato, K., Vosshall, L.B., and Touhara, K. (2012). Amino Acid Residues Contributing to Function of the Heteromeric Insect Olfactory Receptor Complex. *Plos One* 7.

Nakagawa, T., Sakurai, T., Nishioka, T., and Touhara, K. (2005). Insect sex-pheromone signals mediated by specific combinations of olfactory receptors. *Science* 307**,** 1638-1642.

Neuhaus, E.M., Gisselmann, G., Zhang, W.Y., Dooley, R., Stortkuhl, K., and Hatt, H. (2005). Odorant receptor heterodimerization in the olfactory system of *Drosophila* melanogaster. *Nat Neurosci* 8**,** 15-17.

Nichols, A.S., Chen, S., and Luetje, C.W. (2011). Subunit Contributions to Insect Olfactory Receptor Function: Channel Block and Odorant Recognition. *Chem Senses* 36**,** 781-790.

Pask, G.M., Jones, P.L., Ruetzler, M., Rinker, D.C., and Zwiebel, L.J. (2011). Heteromeric Anopheline Odorant Receptors Exhibit Distinct Channel Properties. *Plos One* 6.

Penna, A., Demuro, A., Yeromin, A.V., Zhang, S.L., Safrina, O., Parker, I., and Cahalan, M.D. (2008). The CRAC channel consists of a tetramer formed by Stim-induced dimerization of Orai dimers. *Nature* 456**,** 116-120.

Sargsyan, V., Getahun, M.N., Llanos, S.L., Olsson, S.B., Hansson, B.S., and Wicher, D. (2011). Phosphorylation via PKC regulates the function of the *Drosophila* odorant co-receptor. *Front Cell Neurosci* 5.

Sato, K., Pellegrino, M., Nakagawa, T., Nakagawa, T., Vosshall, L.B., and Touhara, K. (2008). Insect olfactory receptors are heteromeric ligand-gated ion channels. *Nature* 452**,** 1002-U1009.

Smart, R., Kiely, A., Beale, M., Vargas, E., Carraher, C., Kralicek, A.V., Christie, D.L., Chen, C., Newcomb, R.D., and Warr, C.G. (2008). *Drosophila* odorant receptors are novel seven transmembrane domain proteins that can signal independently of heterotrimeric G proteins. *Insect Biochem Mol Biol* 38**,** 770-780.

Terpager, M., Scholl, D.J., Kubale, V., Martini, L., Elling, C.E., and Schwartz, T.W. (2009a). Construction of covalently coupled, concatameric dimers of 7TM receptors. *J Recept Signal Transduct Res* 29**,** 235-245.

Wicher, D. (2010). Design principles of sensory receptors. *Front Cell Neurosci* 4**,** 25.

Wicher, D., Schaefer, R., Bauernfeind, R., Stensmyr, M.C., Heller, R., Heinemann, S.H., and Hansson, B.S. (2008). *Drosophila* odorant receptors are both ligand-gated and cyclic-nucleotide-activated cation channels. *Nature* 452**,** 1007-U1010.

Figure legends

Figure 1| Scheme of the Orco di construct. Two Orco subunits are fused together and spaced by the 1-transmembrane protein SCN1B to grant for a correct orientation of both Orco subunits. The 3.6kb construct was cloned into a pcDNA3.1 (-) expression vector using Xho I and Hind III restriction sites.

Figure 2| Calcium responses to OR agonist in CHO cells expressing Orco wt and Orco di. (A) Free intracellular calcium concentration $[Ca^{2+}]_i$ in Orco wt and Orco di expressing cells in response to application of VUAA1 (100 μM) (wt, n = 37; di, n = 28) **(B, C)** Comparison of maximum $[Ca^{2+}]_i$ **(B)** and decay time constants **(C)** in cells expressing Orco **wt and Orco di as in (A). (D-E) [Ca2+]i in Orco di upon VUAA1 (100uM) stimulation in (D)** Ca^{2+} free bath solution and **(E)** in presence of Ruthenium red (0 Ca^{2+}, n = 27 ; Ru red, 100 μM, n = 26). **(F)** Comparison of basal $[Ca^{2+}]_i$ levels in non-transfected cells (n=40) and Orco wt or Orco di expressing cells as in (A). Data represent mean ± SEM; unpaired t-test, * $p < 0.05$, *** $p < 0.001$, ns, not significant.

Figure 3| Whole cell current responses in cells expressing Orco wt and Orco di. (A, B) Representative current recordings in Orco wt **(A)** and Orco di **(B)** expressing cells upon stimulation with OLC12 (100 μM, arrows) at a holding potential of -60mV. **(C, D)** Comparison of current maxima **(C)** and decay time constant **(D)** for Orco wt and Orco dimer expressing cells (wt, n = 12; di, n = 15). Data represent mean ± SEM; unpaired t-test, * $p < 0.05$, ns, not significant.

Figure 4| The calmodulin inhibitor W-7 modifies the Ca^{2+} response upon OR agonist stimulation in Orco di expressing cells. (A) $[Ca^{2+}]_i$ upon application of VUAA1 (100 μM) in the presence of W7 (10 μM)(n = 34). **(B, C)** Comparison of maximum $[Ca^{2+}]_i$ **(B)** and decay time constants **(C)** in cells expressing Orco di under control conditions and in presence of W7 (control, n =28). Data represent mean ± SEM; unpaired t-test, ** $p < 0.01$, *** $p < 0.001$.

Figure 5| Calcium responses in cells coexpressing Or22a and Orco wt or Orco di. (A) $[Ca^{2+}]_i$ upon application of VUAA1 (100 μM) for Or22a coexpressed with Orco wt (n = 19) and Orco di (n = 13). **(B, C)** Comparison of maximum $[Ca^{2+}]_i$ **(B)** and decay time constant **(C)** in cells coexpressing Or22a with Orco wt or Orco di as in (A). Data represent mean ± SEM; unpaired t-test, ** $p < 0.01$, ns, not significant.

Figure 1

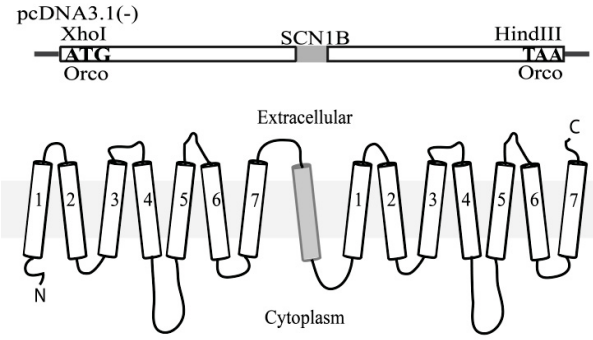

Figure 2

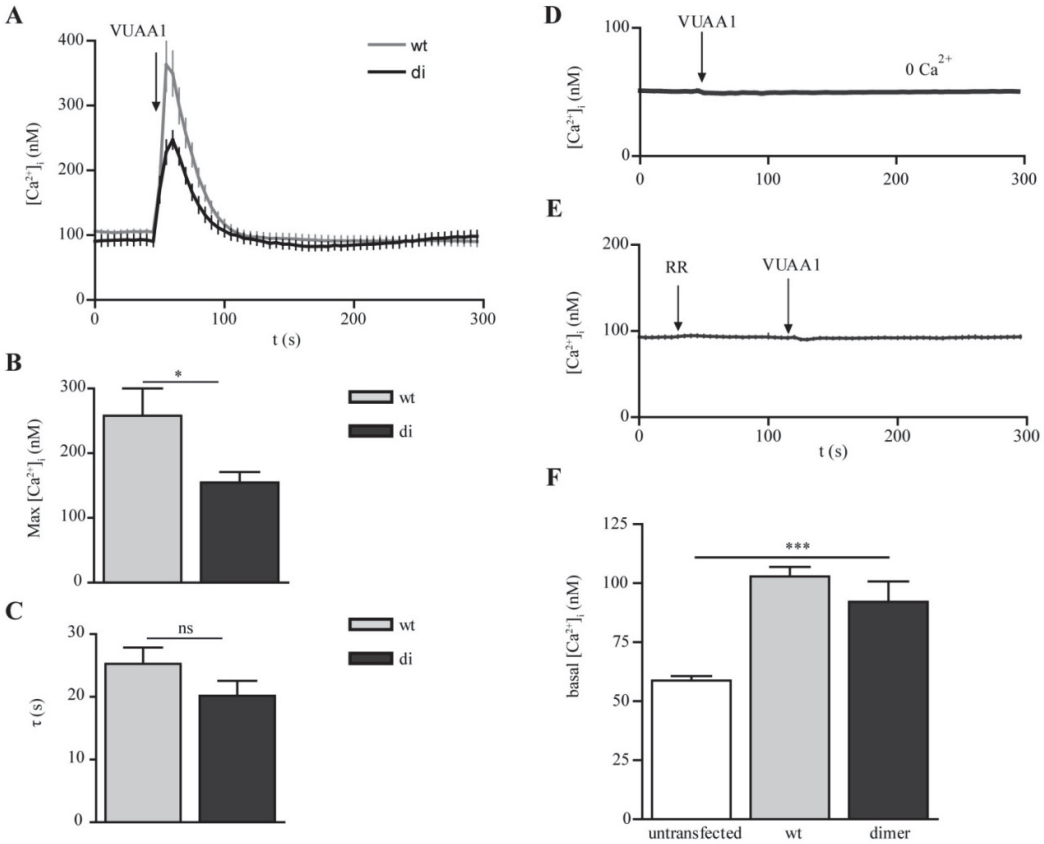

Figure 3

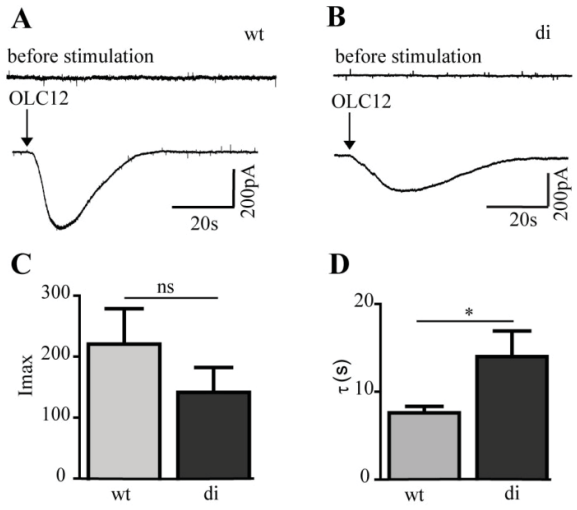

Figure 4

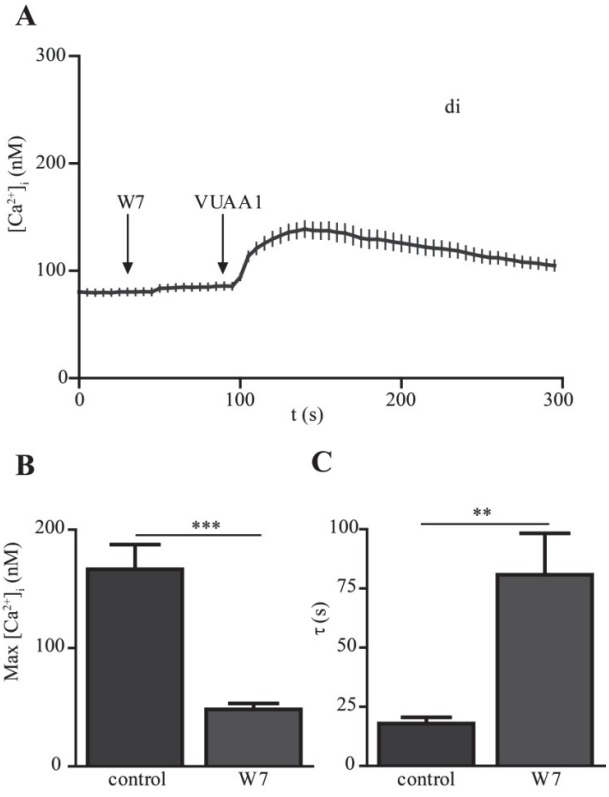

Figure 5

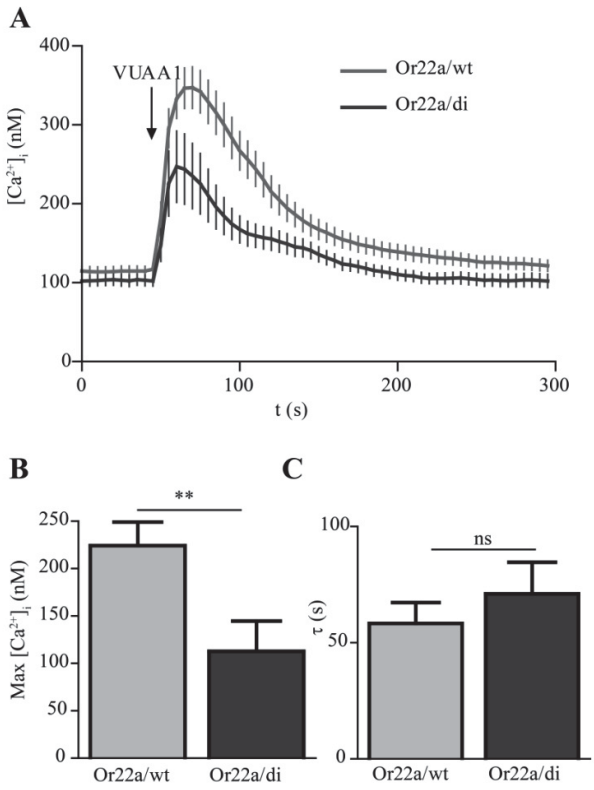
A
400
300
200
100
0
[Ca2+]i (nM)
VUAA1
Or22a/wt
Or22a/di
0
100
200
300
t (s)
B
**
250
200
150
100
50
0
Max [Ca2+]i (nM)
Or22a/wt
Or22a/di
C
ns
100
50
0
τ (s)
Or22a/wt
Or22a/di

Manuscript II

A conserved dedicated olfactory circuit for detecting harmful microbes in *Drosophila*

Cell

A Conserved Dedicated Olfactory Circuit for Detecting Harmful Microbes in *Drosophila*

Marcus C. Stensmyr,[1,3,*] Hany K.M. Dweck,[1,3] Abu Farhan,[1,3] Irene Ibba,[1,3] Antonia Strutz,[1] Latha Mukunda,[1] Jeanine Linz,[1] Veit Grabe,[1] Kathrin Steck,[1,4] Sofia Lavista-Llanos,[1] Dieter Wicher,[1] Silke Sachse,[1] Markus Knaden,[1] Paul G. Becher,[2] Yoichi Seki,[1,5] and Bill S. Hansson[1,*]

[1]Department of Evolutionary Neuroethology, Max Planck Institute for Chemical Ecology, Hans-Knöll-Strasse 8, 07745 Jena, Germany
[2]Division of Chemical Ecology, Swedish University of Agricultural Sciences, Box 102, 23053 Alnarp, Sweden
[3]These authors contributed equally to this work
[4]Present address: Behavior and Metabolism Laboratory, Centro Champalimaud Programa de Neurociências, Av. Brasília, Doca de Pedrouços, 1400-038 Lisbon, Portugal
[5]Present address: Laboratory of Cellular Neurobiology, School of Life Science, Tokyo University of Pharmacy and Life Sciences, 1432-1 Horinouchi, Hachioji, Tokyo 192-0392, Japan
*Correspondence: mstensmyr@ice.mpg.de (M.C.S.), hansson@ice.mpg.de (B.S.H.)
http://dx.doi.org/10.1016/j.cell.2012.09.046

SUMMARY

Flies, like all animals, need to find suitable and safe food. Because the principal food source for *Drosophila melanogaster* is yeast growing on fermenting fruit, flies need to distinguish fruit with safe yeast from yeast covered with toxic microbes. We identify a functionally segregated olfactory circuit in flies that is activated exclusively by geosmin. This microbial odorant constitutes an ecologically relevant stimulus that alerts flies to the presence of harmful microbes. Geosmin activates only a single class of sensory neurons expressing the olfactory receptor Or56a. These neurons target the DA2 glomerulus and connect to projection neurons that respond exclusively to geosmin. Activation of DA2 is sufficient and necessary for aversion, overrides input from other olfactory pathways, and inhibits positive chemotaxis, oviposition, and feeding. The geosmin detection system is a conserved feature in the genus *Drosophila* that provides flies with a sensitive, specific means of identifying unsuitable feeding and breeding sites.

INTRODUCTION

Animals respond with innate behaviors to certain stimuli in their environment. Innate behaviors, in contrast to learned behaviors, are hardwired; i.e., confronted with a specific stimulus, the animal will respond with a stereotyped behavior (Tinbergen, 1951). Many innate behaviors are triggered by odors. Prime examples are pheromones (Karlson and Lüscher, 1959), which have been particularly well studied in insects. In the vinegar fly *Drosophila melanogaster*, the male-produced pheromone *cis*-vaccenyl acetate (cVA) activates a single class of olfactory sensory neurons (OSN), which provides input to a single glomerulus (Kurtovic et al., 2007; van der Goes van Naters and Carlson, 2007) and a sexually dimorphic and functionally segregated circuit within the olfactory system (Datta et al., 2008; Ruta et al., 2010). In insects, odors associated with food or oviposition substrates can also elicit innate behaviors. The smell of vinegar confers obligate attraction in flies (Stökl et al., 2010). Although the vinegar odor activates a number of OSN classes, only a single glomerulus is sufficient and necessary for positive chemotaxis (Semmelhack and Wang, 2009). Pathways underlying hardwired attraction have thus been well characterized. Olfactory circuits mediating odorant-induced innate avoidance are, however, poorly understood. From an evolutionary perspective, being able to detect and respond quickly to harmful features in the environment should be an essential task for the olfactory system. In the fly, CO_2 elicits innate avoidance, which, like the attraction pathways, is mediated via a single glomerular circuit devoted exclusively to this stimulus (Suh et al., 2004). No dedicated avoidance circuit for an odorant sensu stricto (i.e., a volatile organic compound) has, however, been found in the fly or in any other insect. So far, all identified aversive odorants have activated multiple glomeruli (Knaden et al., 2012), and their identification depends on decoding of complex combinatorial glomerular activation patterns.

A volatile compound of interest in this context is geosmin (trans-1,10-dimethyl-trans-9-decalol) (Figure 1A). This substance is produced by a select number of fungi (Mattheis and Roberts, 1992), bacteria (Gerber and Lechevalier, 1965), and cyanobacteria (Jüttner and Watson, 2007) and to the human nose has a distinct and immediately recognizable earthy odor. A recent study found that addition of a small amount of geosmin reduced the attraction of flies to vinegar volatiles (Becher et al., 2010). Given its capacity to modulate innate attraction, this microbial volatile must be a very potent repellent and, as such, is possibly a candidate stimulus for a dedicated pathway for innate avoidance.

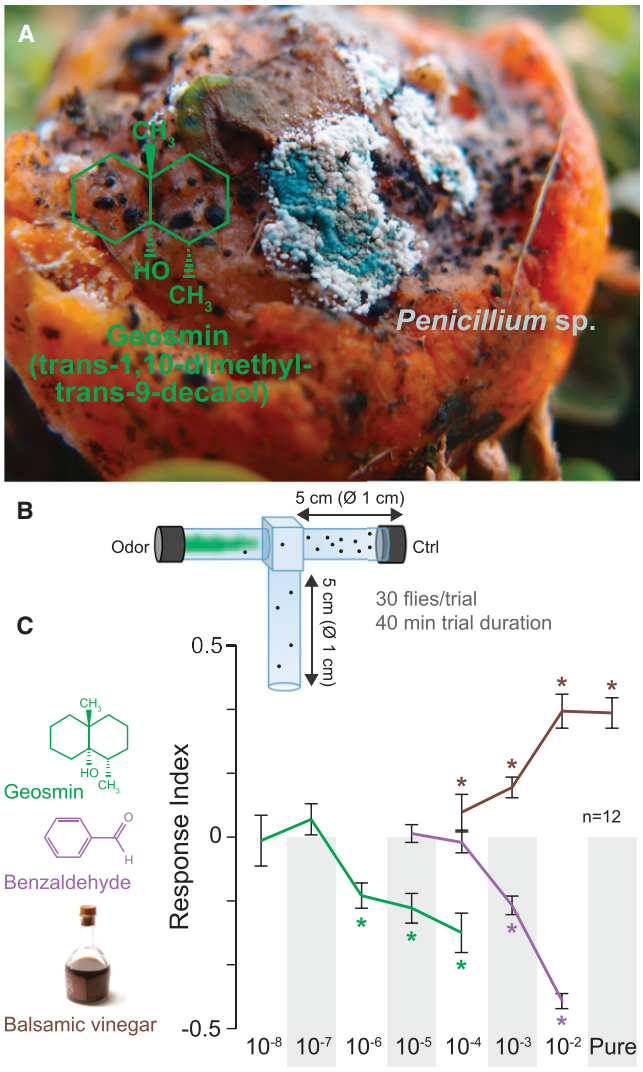

Figure 1. Geosmin—the Odor of Mold—Is Repellent to the Vinegar Fly

(A) Geosmin has a peculiar structure (left), which is distinct from odor ligands identified for *D. melanogaster*. Although a very common compound in nature, geosmin is produced only by a specific subset of microorganisms, including *Penicillium* sp. molds, shown here growing on an orange. Photo, MCS.

(B) Schematic drawing of the T-maze assay.

(C) Response indices of WT flies to geosmin, benzaldehyde, and balsamic vinegar in a T-maze assay. Deviation of the response index against zero was tested with a Student's t test ($p < 0.05$). Error bars represent SEM.

Here, we examine the functional significance of geosmin to the fly and show that geosmin activates only a single class of OSNs; these neurons express an odorant receptor that is exclusively tuned to this compound. Furthermore, we show that the geosmin-activated circuit constitutes a functionally segregated pathway, transferring the message arising from the periphery unaltered to central processing centers. We also demonstrate that this circuit alone is sufficient and necessary to trigger the avoidance behavior. Moreover, we show that, upon activation, the geosmin circuit overrides input from other circuits and inhibits positive chemotaxis. Additionally, we show that the peripheral part of the geosmin detection system is highly conserved across the genus *Drosophila*. Finally, we clearly demonstrate the ecological significance of this pathway, which is to detect toxic microbes.

RESULTS AND DISCUSSION

A Single Class of Olfactory Sensory Neurons Detects Geosmin

We first set out to determine the behavioral significance of geosmin by using a T-maze (Figure 1B). In this two-choice olfactory assay, geosmin on its own elicited avoidance at very low concentrations (10^{-6}) (Figure 1C). For comparison, benzaldehyde—a well-known repellant to flies—in the same assay required a 1,000-fold higher dose than geosmin to trigger repulsion (Figure 1C). The actual fold difference in flies' behavioral sensitivity toward these two compounds is greater once volatility is factored in. The vapor pressure of geosmin is 1,000-fold lower than for benzaldehyde (0.001 mmHg versus 1.27 mmHg at 25°C). Thus, at a given dose and temperature, the number of geosmin molecules in vapor phase is substantially lower than for benzaldehyde. Geosmin is accordingly not only repellent but is also repellent when present in exceedingly low amounts.

Flies are evidently equipped with a sensitive detection system for geosmin. To identify the population of OSNs that is activated by geosmin, we next turned to electrophysiology. Specifically, we performed single-sensillum recording (SSR) measurements, a method that allowed us to assess odor-induced OSN activity extracellularly. We aimed to obtain SSR measurements from all antennal olfactory sensillum types while stimulating the contacted OSNs with geosmin. The ~450 olfactory sensilla of the fly antennae (Shanbhag et al., 1999) can be divided into 17 functional types, which in total house 46 functionally distinct OSN classes (de Bruyne et al., 2001; Hallem et al., 2004; Couto et al., 2005; Yao et al., 2005; van der Goes van Naters and Carlson, 2007; Benton et al., 2009). In addition to these well-classified sensilla, morphological data indicate that the antennae also contain one more type, the so-called intermediate sensilla; these sensilla house an unknown number of functional OSN classes (Shanbhag et al., 1999). The second olfactory organ of the fly, the maxillary palp, houses an additional three types for a total of six distinct OSN classes (de Bruyne et al., 1999). By performing a considerable number of SSR measurements ($n > 1000$) using diagnostic odors and by comparing the response properties of contacted OSNs with previously published ligand affinities, we were able to locate and record from all sensillum types present on the antennae (including two types of intermediate sensilla), as well as from the three types found on the maxillary palps (Figure 2A).

Response to geosmin came from just a single class of antennal OSNs, namely, the ab4B OSNs (Figures 2B and 2C). These neurons express the odorant receptors (OR) *Or56a* and *Or33a* (Couto et al., 2005; Fishilevich and Vosshall, 2005), of which only the former is functional in the *Canton-S* strain we used here (Kreher et al., 2008). Although ab4B OSNs have been measured from previously (e.g., de Bruyne et al., 2001), geosmin is the first ligand reported for this neuron class. To confirm that

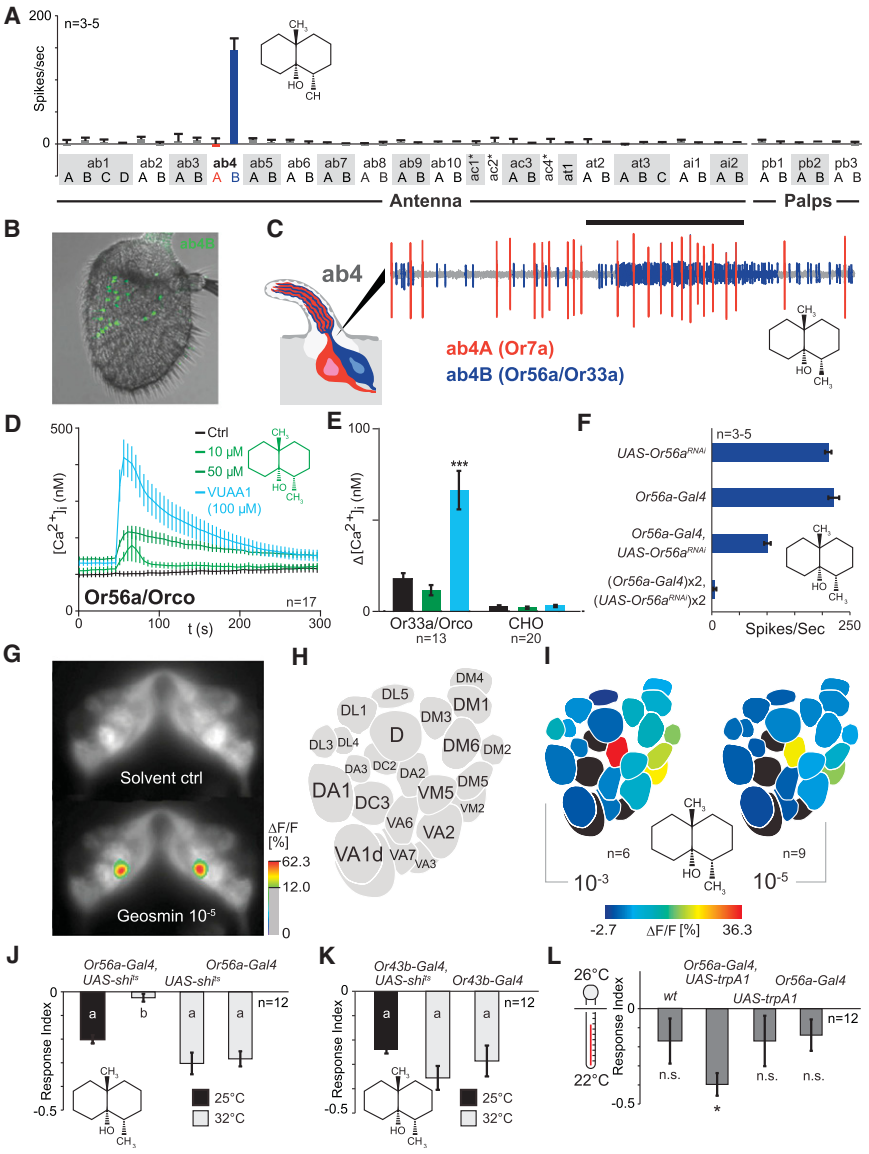

Figure 2. Geosmin Activates a Single Class of Antennal Olfactory Sensory Neurons

(A) SSR measurements from all olfactory sensilla with geosmin (10^{-3}) as a stimulus. ab, antennal basiconic sensilla (s.); ac, antennal coeloconic s.; at, antennal trichoid s.; ai, antennal intermediate s.; pb, palp basiconic s. Stars denote that activity from individual OSNs was not separated. Error bars represent SEM.

(B) Distribution of ab4B neurons on the antenna as visualized by the expression of GFP from the *Or56a* promoter.

(C) Representative SSR traces from an ab4 sensillum. The smaller amplitude spiking neuron, i.e., ab4B responds to geosmin (10^{-3}). The duration of the stimulus delivery (0.5 s) is marked by the black bar.

(D) The free intracellular Ca^{2+} concentration $[Ca^{2+}]_i$ in CHO cells expressing Or56a and Orco increases after the application of geosmin and VUAA1 (100 µM), but not of saline (control). Error bars represent SEM.

(E) Mean increase in free intracellular Ca^{2+} concentration $[Ca^{2+}]_i$ in CHO cells expressing Orco and Or33a or nontransfected CHO cells after the application of saline (control), geosmin (50 µM), and VUAA1 (100 µM). Star denotes response significantly different from control (Student's t test, $p < 0.05$). Color scale as in (D). Error bars represent SEM.

(F) Quantification of responses to geosmin (10^{-3}) from ab4B OSNs of flies expressing RNAi against Or56a in the ab4B OSNs and the corresponding parental lines. Error bars represent SEM.

(G) False color-coded images showing solvent-induced (top) and geosmin-induced (bottom) calcium-dependent fluorescence changes in the AL of a fly expressing the activity reporter GCaMP3.0 from the *Orco* promoter.

(H) Glomerular atlas of the AL.

(I) Odor-induced activity plotted on schematic ALs (average % $\Delta F/F$).

(J) RI to geosmin (10^{-5}) of flies expressing *Shibire^{ts}* from the *Or56a* promoter and corresponding parental lines in a T-maze assay. Significant differences are denoted by letters (analysis of variance [ANOVA] followed by Tukey's test; $p < 0.05$). Error bars represent SEM.

(K) RIs to geosmin (10^{-5}) of flies expressing *Shibire^{ts}* from the *Or43b* promoter and the corresponding parental lines in a T-maze assay. No significant differences (ANOVA followed by Tukey's test; $p > 0.05$). Error bars represent SEM.

(L) RIs of flies expressing *dTRPA1* from the *Or56a* promoter, the corresponding parental lines, and WT in a T-maze assay confronted with a choice between 22 and 26°C. Deviation of the RI against zero was tested with a Student's t test ($p < 0.05$). Error bars represent SEM.

See also Figure S1.

Or56a is indeed the geosmin receptor, we next expressed this protein in Chinese hamster ovary (CHO) cells that stably expressed the OR coreceptor *Orco* (Larsson et al., 2004). Because insect ORs are Ca^{2+}-permeable ionotropic receptors, OR activation can be monitored by measuring the free intracellular Ca^{2+} concentration $[Ca^{2+}]_i$. The application of geosmin transiently increased $[Ca^{2+}]_i$ in a concentration-dependent manner (Figure 2D). The cells responding to geosmin were seen to respond to the Orco agonist VUAA1 (Jones et al., 2011), although there was no response to control application of saline (Figure 2D and Figure S1A available online). We then expressed *Or33a* in the same CHO cell line. Although the cells responded to VUAA1, we found no responses to geosmin (Figure 2E). CHO cells not expressing *Orco* or either of the two tuning ORs produced no Ca^{2+} signals in response to the application of geosmin or VUAA1 (Figure 2E). Loss of function of *Or56a* should render ab4B OSNs insensitive to geosmin. We next used SSR to examine the function of ab4B OSNs expressing a *UAS*-RNA interference (RNAi) construct against *Or56a*. The expression of *UAS-Or56a^{RNAi}* reduced the response to geosmin in a dose-dependent manner (Figures 2F and S1B). In flies carrying one copy each of *Or56a-Gal4* and *UAS-Or56a^{RNAi}*, the response to

geosmin was reduced by ~50% compared to the response displayed by the parental lineages. With two copies of each, the response was essentially abolished (~98% reduction) (Figure 2F). Thus, we conclude that *Or56a* alone underlies the ability of the ab4B cells to detect geosmin.

To further verify that geosmin is detected only by a single class of OSNs, we next employed functional imaging to examine the activity pattern in the antennal lobe (AL) evoked by geosmin (Figures 2G and S1C). We used the *Gal4-UAS* system to express the Ca^{2+}-sensitive reporter gene GCaMP3.0 (Tian et al., 2009) from the *Orco* promoter, thereby labeling all OSNs except those relying on ionotropic receptors (Benton et al., 2009) for odorant detection. Activated glomeruli were then identified by comparing the activation pattern with the map of the fly AL (Couto et al., 2005; Fishilevich and Vosshall, 2005) (Figure 2H). We stimulated flies with diagnostic odors to assist glomerular identification (data not shown) and with geosmin at 10^{-3} and 10^{-5} dilutions (Figures 2G and 2I). At 10^{-5}, geosmin elicited repeatable signals from only a single locus in the AL—the DA2 glomerulus, which receives input from ab4B neurons (Couto et al., 2005; Fishilevich and Vosshall, 2005). We note that DA2 is also situated in the same lateral part of the AL that has previously been implicated in handling aversive odors (Knaden et al., 2012). In a number of recordings, we also noted activity from VM2; however, these signals were not consistently reproducible. In the SSR screen, we never observed any activity in response to geosmin from OSNs innervating VM2; these OSNs are housed in the ab8 sensillum (Figure 2A). Hence, the activity noted from VM2 most likely does not reflect actual peripheral input but, rather, may stem from intrinsic AL processes. We therefore conclude that geosmin is indeed detected by a single class of OSNs. It should be stressed that the level of specificity shown here toward a nonpheromonal odor is most unusual, if not unique, among the olfactory systems investigated to date.

Activation of the ab4B Neurons Is Necessary and Sufficient for the Aversive Behavior

If the behavior triggered by geosmin is solely derived from the activity of ab4B neurons, silencing this OSN subpopulation should also abolish the aversive behavior. To silence these neurons, we expressed the temperature-sensitive mutant dynamin *Shibire^{ts}* (Kitamoto, 2001) from the *Or56a* promoter. At the restrictive temperature (32°C), flies carrying this construct displayed no aversive behavior toward geosmin (Figure 2J). The same flies, tested at a permissive temperature (25°C), showed a strong aversion to geosmin. Parental lines tested at the nonpermissive temperature showed a somewhat increased repellency, which was likely caused by the increased volatility of geosmin at the higher temperature. Silencing the ab4B neurons had no effect on flies' behavior in response to benzaldehyde (Figure S1D). In line with the SSR experiments, silencing input to VM2—via the expression of *Shibire^{ts}* from the *Or43b* promoter—did not affect flies' behavior in response to geosmin (Figure 2K). The ab4B OSNs are evidently necessary for the aversive behavior.

We next asked whether selectively activating these neurons is sufficient to cause aversion. We expressed the temperature-sensitive cation channel *dTRPA1* in the ab4B neurons, a procedure that allowed us to conditionally activate these OSNs at temperatures >26°C (Hamada et al., 2008). As a control, we first examined the temperature preference (26°C versus 22°C) of wild-type (WT) flies in a T-maze assay. WT flies showed a tendency toward aversion against the higher temperature (Figure 2L). Having established baseline behavior in the assay, we next asked whether flies bearing the *Or56a-Gal4*, *UAS-dTRPA1* construct displayed a stronger aversion toward the higher temperature. In fact, flies expressing *dTRPA1* in ab4B OSNs showed significant avoidance toward the warm side, whereas parental control flies showed moderate (but insignificant) aversion (Figure 2L). Thus, specifically activating these neurons induces aversion in flies. In summary, these experiments demonstrate that the aversive behavior caused by geosmin is mediated solely through a single class of OSNs.

The ab4B Neurons Respond Exclusively to Geosmin

As seen, geosmin is detected by a single class of OSNs, ab4B. We next asked whether or not these neurons are exclusively tuned to geosmin. We again used SSR but now screened with 103 structurally diverse odorants (tested at 10^{-2} dilution) (Figure S2A). The larger spiking neuron in the ab4 sensillum responded to a range of compounds (Figure S2B). Interestingly, we note that the most potent ligands for these OSNs are all known repellants. The functional significance, if any, of having two neurons both responding to aversive odorants that are cocompartmentalized is unclear. The ab4B neurons, in contrast, displayed a striking degree of selectivity, as none of the screened odorants—apart from geosmin—elicited any increased spike firing (Figure 3A). Showing specificity in the context of the olfactory system is, however, difficult, as there are thousands of volatile chemicals in nature. Our tested set thus represents only a fraction of the volatile chemicals potentially present in the natural habitat of *D. melanogaster*.

To address this issue and to more firmly examine the specificity of these neurons, we next expanded our SSR investigation by using a gas chromatograph (GC) for stimulus delivery. GC-linked SSR enables the screening of headspace collections from complex odor sources and, consequently, enables the probing of large numbers of volatiles. We first sampled odors from a wide range of sources present in the natural habitat of *D. melanogaster* in native Africa as well as in the "Diaspora." We collected odors from 14 sources, including avoided ones, such as feces (from African mammals) and rotting meat, as well as attractive ones, such as fruits and vinegar. The total number of volatiles present in these samples is difficult to firmly establish, but the number of distinguishable flame ionization detection (FID) peaks amounts to ~2,900 in total. The actual number of compounds present is, however, likely considerably higher. The headspace of many fruits typically contains >400 volatiles (e.g., Petro-Turza, 1987); hence, in our samples, many more compounds were presumably present but only in amounts below the FID limit. These compounds were nevertheless effectively screened, as insects, including *Drosophila*, are capable of detecting compounds present well below the FID limit.

Having collected and verified the odor samples, we then proceeded to perform GC-SSR measurements from ab4B neurons.

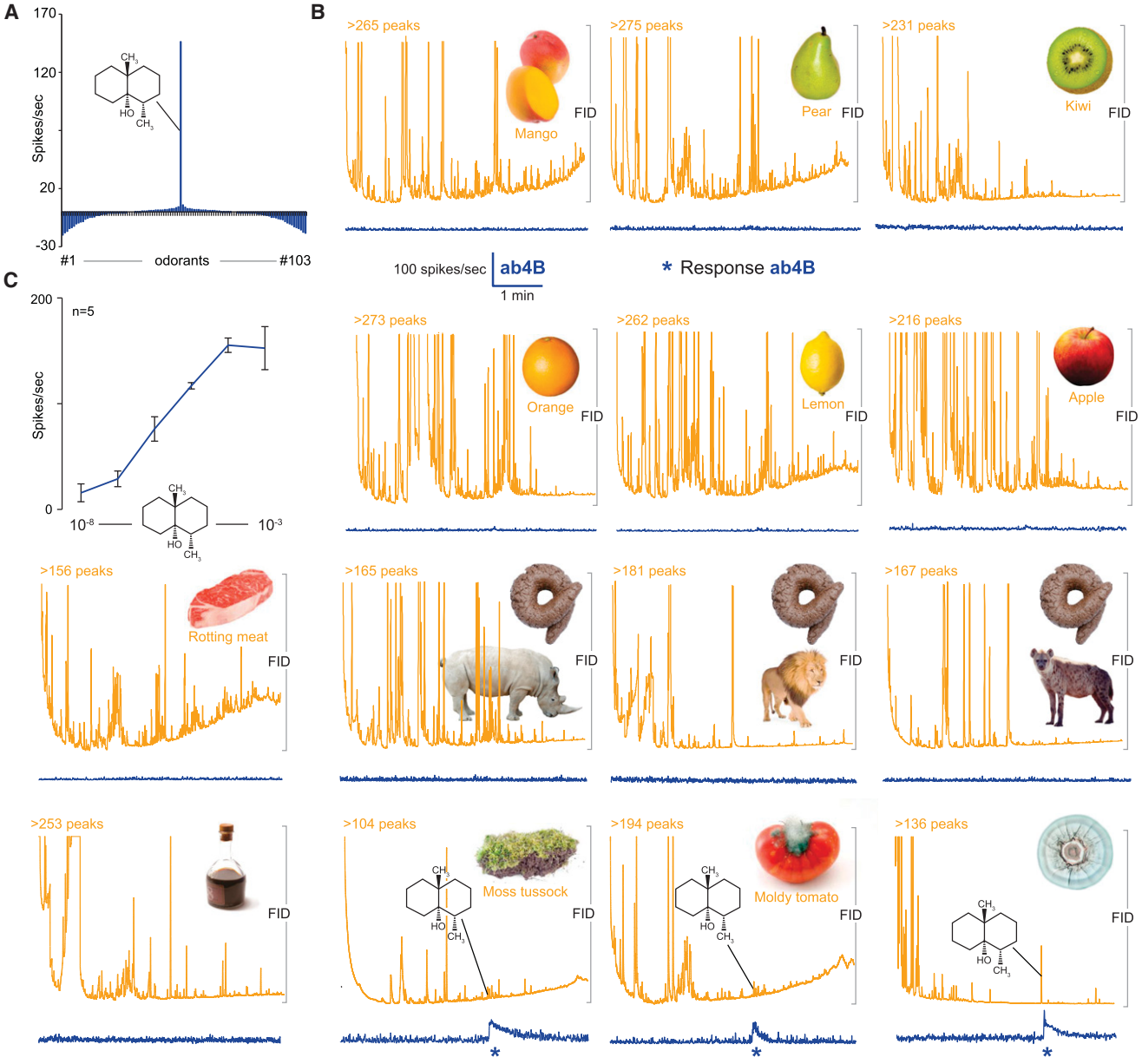

Figure 3. The ab4B Neurons Respond Exclusively to Geosmin

(A) Tuning curve for the ab4B neuron type based on a screen of 103 synthetic substances (10^{-2} dilution). Error bars represent SEM.

(B) Gas-chromatography-linked SSR measurements from ab4B neurons. The orange trace represents the FID, photos depict the screened odor sources, and the blue trace depicts the simultaneously recorded neural activity of ab4B neurons. Stars denote response. n = 1–3.

(C) Dose response curve from ab4B neurons toward geosmin. Error bars represent SEM.

See also Figure S2.

Out of the 14 odor samples we screened, only three evoked responses (Figure 3B), namely the headspace of a moldy tomato, a moss tussock, and isolated cultures of the common soil bacterium *Streptomyces coelicolor*. In each of the active samples, only a single FID peak elicited a response. We next used GC-linked mass spectroscopy (GC-MS) combined with synthetic standards to identify the functionally relevant peaks in these three samples; in all cases, these turned out to be geosmin. Thus, the ab4B neurons are indeed extremely specific, and it is reasonable to conclude that the sole function of these neurons is to detect geosmin.

How sensitive are the ab4B neurons toward geosmin? Our T-maze experiments (Figure 1C) had already shown that the flies respond behaviorally at very low concentrations. Indeed, the ab4B neurons respond to geosmin at 10^{-8} dilution (corresponding to 100 pg of substance in the stimulus pipette)

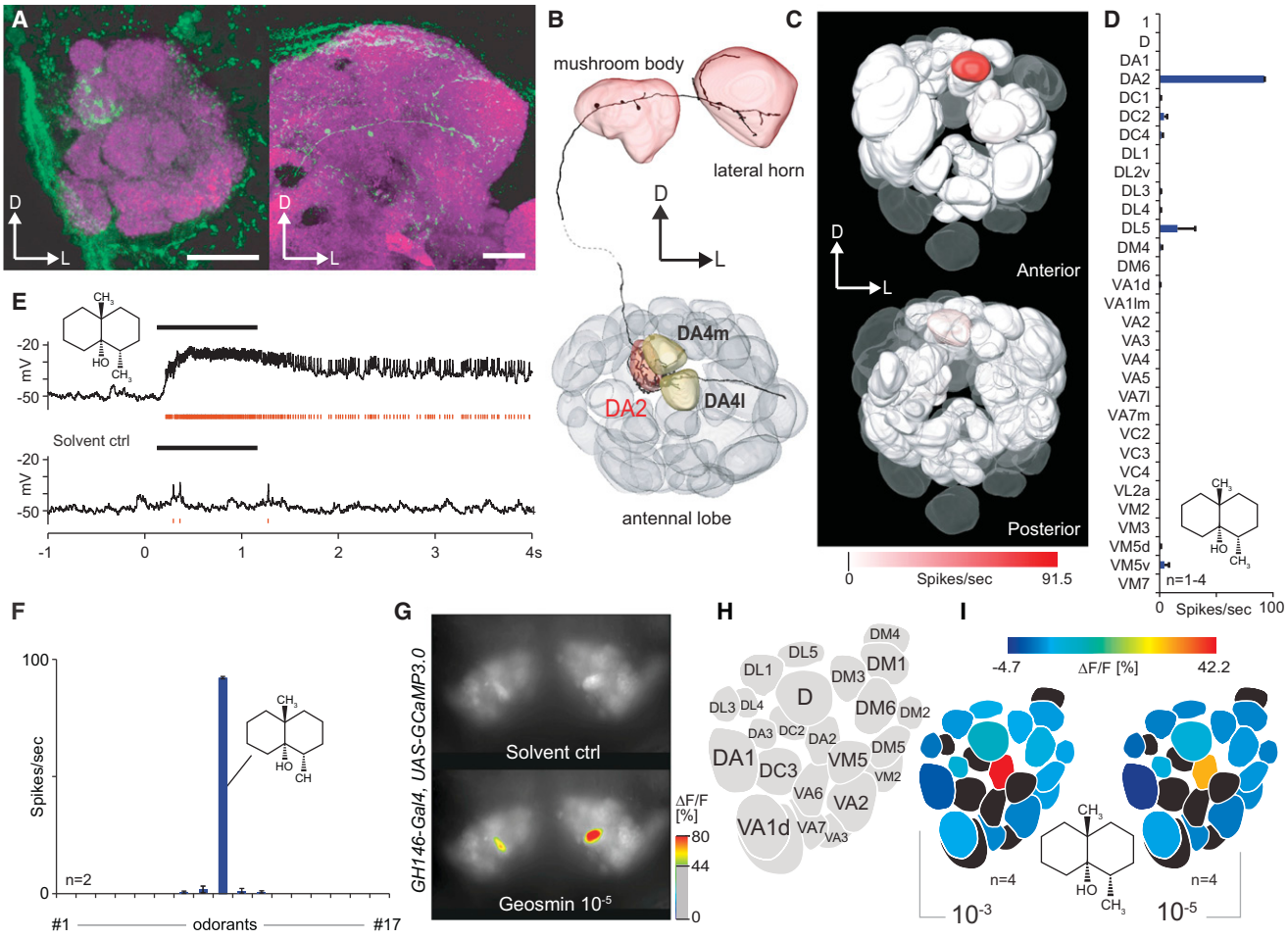

Figure 4. Geosmin Activates a Functionally Segregated Pathway

(A) A PN innervating the DA2 glomerulus (left) and sending its axon to the calyx of the mushroom body and terminating in the lateral horn (right). PN, green; nc82, magenta. D denotes dorsal, and L denotes lateral.

(B) Reconstruction of the neuron in (A).

(C) Glomeruli from which PN recordings were obtained (in solid), with the response to geosmin (10^{-3}) false color coded. Transparent glomeruli were not investigated.

(D) The net change in spike frequency in response to geosmin (10^{-3}) stimulation from PNs innervating 31 glomeruli. Error bars represent SEM.

(E) Example spike trace from a DA2 PN responding to geosmin (10^{-3}). Black bar marks the 1 s odor stimulus. Red trace represents extracted spikes.

(F) Tuning curve for DA2 PNs based on 17 synthetic substances (10^{-2} dilution, except geosmin, which was used at 10^{-3}). Error bars represent SEM.

(G) False color-coded images showing solvent-induced (top) and geosmin-induced (bottom) calcium-dependent fluorescence changes in AL PNs of a fly bearing the *GH146-Gal4*, *UAS-GCaMP3.0* constructs.

(H) Glomerular atlas of the AL.

(I) Odor-induced activity plotted on schematic ALs (average % Δ*F*/*F*).

See also Figure S3.

(Figure 3C), which is in good agreement with the dilution of geosmin (1.74×10^{-7}) causing reduced upwind flight attraction to vinegar headspace when vaporized in the wind tunnel (Becher et al., 2010).

Geosmin Triggers a Segregated Pathway through the Antennal Lobe to Higher Brain Centers

How is the specific tuning in flies to geosmin seen in the peripheral sensory neurons transferred to higher brain centers? In *Drosophila*, the OSNs form synapses with projection neurons (PNs) and local interneurons within the AL. Most PNs innervate only a single glomerulus (Figures 4A and 4B), whereas local interneurons typically show broad innervation throughout the AL. The PNs send their axons to the mushroom body and lateral horn (Figures 4A and 4B) (Vosshall and Stocker, 2007). PNs tend to respond to a somewhat broader range of odors than do their corresponding OSNs (Wilson et al., 2004; Bhandawat et al., 2007). For instance, the PNs connected to OSNs that respond only to geranyl acetate respond to additional odors as well. However, PNs connected to OSNs that respond to the sex

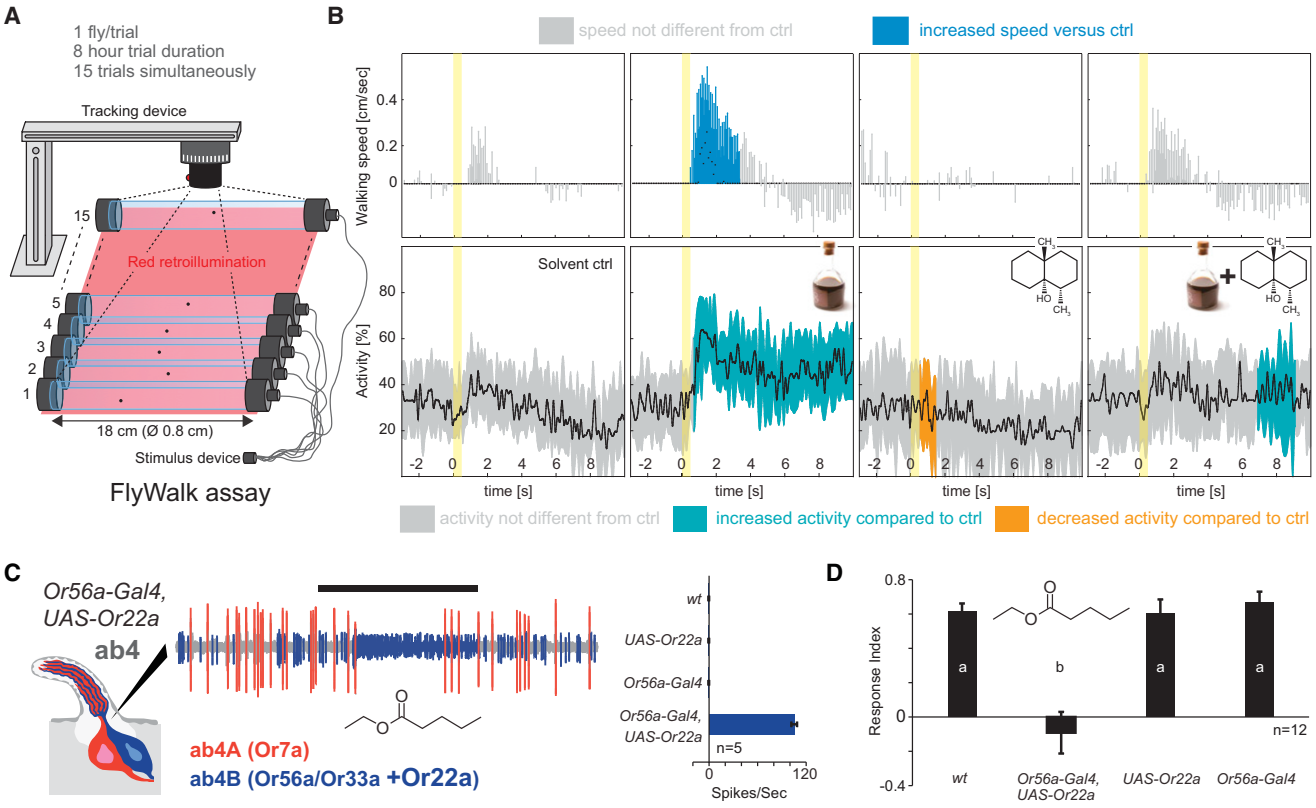

Figure 5. Activation of the Geosmin Pathway Reduces Attraction

(A) Schematic drawing of the Flywalk assay used in (B). For details, see Steck et al. (2012).

(B) Quantified behavior from individual flies stimulated with balsamic vinegar, geosmin (10^{-3}), and a mix of the two in the Flywalk assay. Top graphs, box plot representations of odor-induced changes in upwind speed of flies (n = 30); black line represents median upwind speed; box, interquartile range; whiskers, 90th and 10th percentiles. Lower graphs, undirected activity of flies (n = 30); black line, median activity; shaded area, interquartile range. Yellow area marks the 500 ms odor stimulus. Statistical analysis per Steck et al. (2012).

(C) Left, representative SSR trace from an ab4 sensillum, stimulated with ethyl butyrate (10^{-5}) in which the B neuron expresses Or22a. Right, quantification of mean responses to ethyl butyrate from control ab4B OSNs and ab4B OSNs misexpressing Or22a.

(D) Response indices of flies expressing Or22a in the ab4B OSNs, corresponding parental lines and WT flies to ethyl butyrate (10^{-5}) in a T-maze assay. Significant differences are denoted by letters (ANOVA followed by Tukey's test; $p < 0.05$). Error bars represent SEM.

See also Figure S4.

pheromone cVA do not show a broad response pattern and are just as specific as their cognate OSNs (Schlief and Wilson, 2007). We thus asked: how specific is the response of PNs that respond to geosmin?

We carried out whole-cell patch-clamp recordings from a large number of randomly selected uniglomerular PNs, stimulating with 17 chemicals, including geosmin (Figure S3). We obtained recordings and fills from 66 PNs (from 66 individual flies), which covered 31 different glomeruli. Geosmin elicited significant responses only from two PNs, both of which innervated the DA2 glomerulus (Figures 4A–4E). Although not all glomeruli were covered, this result strongly suggests that geosmin information does not diffuse broadly across the AL to other glomeruli. Moreover, DA2 PNs appear to be as selective as the input OSNs because these PNs responded exclusively to geosmin and not to any of the other screened compounds (Figures 4F and S3). To further examine the specificity of the AL output, we next imaged flies carrying the *GH146-Gal4* and *UAS-GCaMP3.0* constructs in which ~1/2 of the PNs express the GCaMP3.0 activity reporter (Stocker et al., 1997; Jefferis et al., 2001). Stimulation with geosmin again exclusively activated the DA2 glomerulus (Figures 4G–4I). Thus, we conclude that, like the labeled line pheromone pathway, the geosmin circuit forms a dedicated functionally segregated pathway, at least to the point of the calyx and lateral horn. The fate of the signal past this point remains to be elucidated.

The Geosmin Circuitry Can Modulate and Override Innate Attraction

As mentioned before, the addition of geosmin to vinegar significantly reduced positive chemotaxis in flies' response to this innately attractive odor. To verify that geosmin indeed has the capacity to reduce flies' attraction to vinegar, we next repeated the wind tunnel experiments with an alternative bioassay, the Flywalk (Steck et al., 2012) (Figure 5A). This assay enables high-resolution quantification of behavior from individual flies in

response to short pulses of an odor stimulus repeated during an extended period of time. Our Flywalk results parallel the findings from the wind tunnel (Figure 5B). Exposing flies to pulses of balsamic vinegar induced bursts of positive chemotaxis, which were significantly reduced when geosmin was added to the vinegar volatiles. Geosmin alone induced a "freezing" behavior, i.e., a decrease of the flies' activity, which, in this assay, reflects aversion (Steck et al., 2012). The ability of geosmin to reduce the attractiveness of vinegar is robust and can be repeated with both the trap assay (Larsson et al., 2004) (Figures S4A and S4B) and the T-maze (Figure S4C).

In light of the physiology findings, the cause of the reduced attractiveness of the geosmin-vinegar mix should stem from activation of the DA2 pathway. This circuit should consequently have the capacity to override and modulate an innate behavior. To test this notion, we used the *Or56a-Gal4* line to drive the expression of an additional odorant receptor (*Or22a* targeting glomerulus DM2) in ab4B OSNs (Figure 5C), enabling us to manipulate the activity of the DA2 circuit in the absence of geosmin and thereby to separate the chemical from the actual effect. In flies expressing Or22a under the *Or56a* promoter, stimulation with ethyl butyrate, a potent ligand for Or22a that is highly attractive to flies (Figure 5D), should result in the activation of both DM2 and DA2, in turn reducing the flies' attraction to ethyl butyrate. Through SSR, we first verified that the misexpression of Or22a conferred sensitivity toward ethyl butyrate in ab4B neurons (Figure 5C). Having established physiological function, we then tested the flies' behavioral response toward ethyl butyrate by using a T-maze. The parental control lines showed the expected strong positive response of WT flies toward this fruit ester. On the other hand, flies additionally expressing Or22a in the ab4B OSNs showed no attraction toward ethyl butyrate (Figure 5D). Thus, activating DA2 and the associated pathway can modulate and override innate attractive behavior.

Geosmin Is Used by the Fly to Detect Toxic Molds and Bacteria

We next asked what the possible evolutionary and ecological reason might be for the strong and hard-wired chemosensory avoidance of geosmin. Because geosmin itself is nontoxic to invertebrates as well as mammals (Young et al., 1996), the function of the circuit is not just to alert *D. melanogaster* to the presence of this compound. With some exceptions, the majority of volatiles flies detect are widely produced in nature and, thus, are difficult to firmly associate with a specific source. Geosmin—although very abundant in nature—is solely produced by a narrow range of microbes, in particular *Penicillium* fungal molds (Mattheis and Roberts, 1992) and *Streptomyces* soil bacteria (Gerber and Lechevalier, 1965). Has the system for detecting geosmin evolved to identify these specific microorganisms? We first examined whether flies could survive on these types of microbes. We transferred newly eclosed flies to vials with a yeast-containing medium or to vials additionally containing cultures of either *Streptomyces coelicolor* or *Penicillium expansum*. Flies were unable to survive in the presence of either of these microbes (Figure 6A), presumably due to the accumulation of toxins. Many fungal molds, including *P. expansum*, produce a range of toxic secondary metabolites, several of which have been shown to have strong insecticidal activity (Castillo et al., 1999). Many geosmin-producing microbes are not only toxic but are also known to outcompete or even kill the yeasts flies graze on (Arndt et al., 1999). Thus, for the fly, being able to detect and avoid fruit colonized by harmful molds and bacteria should be an essential skill.

Because many geosmin-producing microbes are detrimental to flies, we suspected that substrates colonized by this type of microbe are avoided for oviposition. Thus, we next looked for an olfactory-based oviposition preference in flies by using a two-choice assay (Figure 6B) in which flies were given the option of laying eggs on plates containing either standard *Drosophila* yeast medium or on plates additionally inoculated with *S. coelicolor*. Indeed, flies avoided laying eggs on plates containing *S. coelicolor* (Figure 6C). Is the avoidance of the bacterial plates mediated via geosmin? To address this question, we subsequently repeated the oviposition experiments. We inoculated one of the plates with a gene-targeted *S. coelicolor* strain (J3001), which carries a deletion in a key gene involved in the geosmin synthesis pathway (Gust et al., 2003). The J3001 strain is thus identical to WT *S. coelicolor* except for its inability to produce geosmin, the lack of which we also confirmed via GC-MS and GC-SSR (Figure 6D). Abolishing the production of geosmin completely eliminated the avoidance in response to *S. coelicolor* (Figure 6C). In the absence of geosmin, flies readily oviposited on the harmful media. Eggs deposited onto *S. coelicolor* did not develop into adult flies (data not shown), and survival on the J3001 strain did not differ from survival on WT *S. coelicolor* (log rank test; $p = 0.22$). In a pure olfactory choice assay, the trap assay (Figure S4A), flies also discriminated between the two strains, preferring J3001 over WT (Figure S5).

We next wondered whether the reluctance to oviposit in the presence of (WT) *S. coelicolor* is dependent on the DA2 circuit. To address this question, we examined the oviposition preference of flies carrying the previously used *Or56a-Gal4*, *UAS-Shibire^{ts}* construct. At permissive temperatures, these flies strongly avoided plates containing *S. coelicolor*, whereas at restrictive temperatures, there was no avoidance, and the flies even showed a slight preference for the bacterial substrate (Figure 6E). In line with our hypothesis, the presence of geosmin alone should also prevent egg laying, which it did. Plates containing geosmin (10^{-3}) were avoided as an oviposition substrate (Figure 6F). One could speculate that the presence of any strongly repellent odor would also prevent oviposition from occurring. However, benzaldehyde did not inhibit oviposition from occurring at 10^{-4} and 10^{-2} dilutions and barely did so even when tested as a pure substance (Figure 6F).

Are flies also hesitant to consume food contaminated with this type of microbe? We next examined feeding preference by using a capillary feeder assay (Figure 6G) (Ja et al., 2007); here, flies could choose between two 5% sucrose solutions, one of which was based on a wash from WT *S. coelicolor* colonies. Indeed, flies clearly preferred the pure sucrose solution (Figure 6H). We then repeated these experiments, replacing the WT *S. coelicolor* with the J3001 strain. The solution

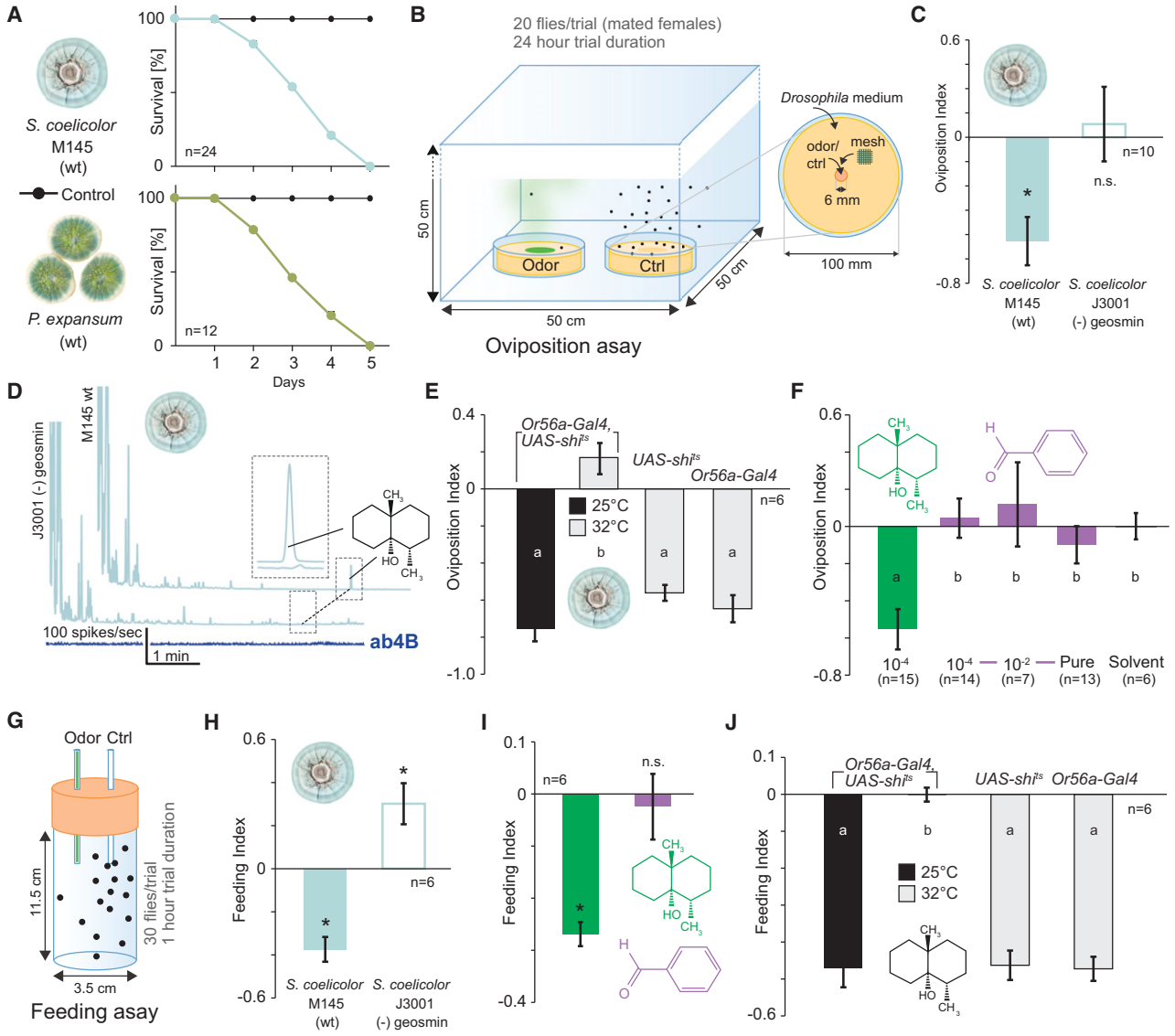

Figure 6. Geosmin Is Used by Flies to Detect Toxic Molds and Bacteria

(A) Survival rate of newly eclosed flies transferred to vials containing pure agar medium or medium with 1-week-old cultures of either of two geosmin-producing microbes.

(B) Schematic drawing of the oviposition choice assay used in (C), (E), and (F).

(C) Oviposition indices (OI) to WT (M145) and J3001 *S. coelicolor* of WT flies. The J3001 only differs from WT by its inability to produce geosmin. Deviation of the oviposition index against zero was tested with a Student's t test ($p < 0.05$). Error bars represent SEM.

(D) GC-MS and GC-SSR analysis of headspace from J3001 and M145. Pale blue represents flame ionization detection traces. The dark blue trace shows activity from an ab4B OSN being stimulated with J3001 headspace (no response).

(E) OIs to WT *S. coelicolor* of flies expressing *Shibire^{ts}* in the ab4B OSNs and corresponding parental lines at permissive (25°C) and restrictive (32°C) temperatures. Significant differences are denoted by letters (ANOVA followed by Tukey's test; $p < 0.05$). Error bars represent SEM.

(F) OIs to geosmin and benzaldehyde of WT flies. Significant differences are denoted by letters (ANOVA followed by Tukey's test; $p < 0.05$). Error bars represent SEM.

(G) Schematic drawing of the capillary feeding assay (modified from Ja et al. [2007]) used in (H)–(J).

(H) Feeding indices (FI) to 5% sucrose solutions containing traces of WT (M145) or J3001 *S. coelicolor* of WT flies. Deviation of the feeding index against zero was tested with a Student's t test ($p < 0.05$). Error bars represent SEM.

(I) FIs to 5% sucrose solutions containing geosmin (0.1%) or benzaldehyde (0.1%) of WT flies. Deviation of the feeding index against zero was tested with a Student's t test ($p < 0.05$). Error bars represent SEM.

(J) FIs to 5% sucrose solutions containing traces of WT (M145) *S. coelicolor* of flies expressing *Shibire^{ts}* from the *Or56a* promoter and corresponding parental lines at permissive (25°C) and restrictive (32°C) temperatures. Significant differences are denoted by letters (ANOVA followed by Tukey's test; $p < 0.05$). Error bars represent SEM.

See also Figure S5.

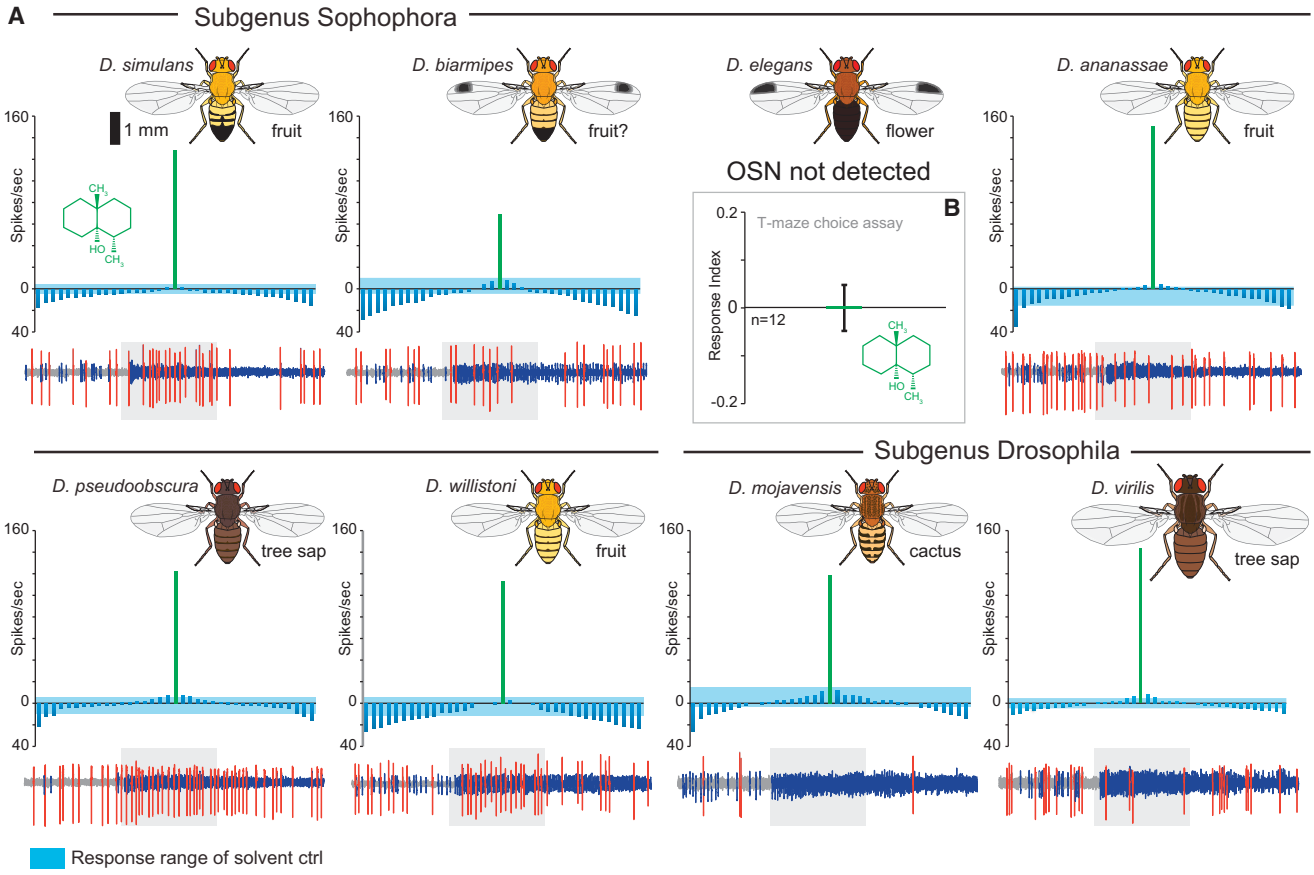

Figure 7. Responses to Geosmin in Drosophilids Are Deeply Conserved

(A) Tuning curves for neurons with similar response properties to the ab4B neurons of *D. melanogaster* from select members of the genus *Drosophila* (n = 3 for all species). The tuning curves are based on a screen with 37 compounds, tested at 10^{-2}. Below curves are representative SSR traces showing responses to geosmin (10^{-3}), with the gray box indicating the 0.5 s stimulus delivery period. The natural breeding substrates are indicated underneath the schematic drawings of the species. Error bars represent SEM.

(B) Response index to geosmin (10^{-5}) of *D. elegans* in a T-maze assay. Deviation of the response index against zero was tested with a Student's t test (not significant). Error bars represent SEM.

See also Figure S6.

containing J3001 did not reduce feeding but was slightly preferred over the sucrose-only solution (Figure 6H), suggesting that the aversion is due to the presence of geosmin. In line with this observation, adding geosmin (0.1%) also reduced feeding (Figure 6I). The addition of another aversive odor, benzaldehyde (0.1%), had no effect on feeding (Figure 6I). We next wondered whether the feeding aversion is due to olfactory input to the DA2 pathway. Indeed, the reduced feeding stems not from geosmin having an aversive taste but from the activation of ab4B OSNs because silencing input to this pathway—via *Shibire^{ts}*—also fully abolished the geosmin-induced feeding aversion (Figure 6J). Thus, geosmin also functions as an antifeedant, operating via the olfactory system.

Taken together, these findings strongly suggest that the ecological significance of geosmin is to alert flies to the presence of toxic molds and bacteria. The geosmin circuit performs a critical task, providing flies with a reliable and sensitive means of identifying unsuitable hosts.

The Geosmin Detection System Is Conserved across the Genus *Drosophila*

To shed light on the origin and evolution of the geosmin detection system circuit, we next turned to a comparative approach. We tested eight drosophilid species—chosen based on genome availability and phylogenetic and ecological considerations—for their capacity to detect geosmin (Figure S6A). We set out to identify neurons able to detect geosmin via SSR, stimulating with a set of 37 chemically diverse odorants (at 10^{-2} dilution) (Figure S3D). We located OSNs tuned to geosmin in all the screened species except *D. elegans* (Figure 7A). Electroantennogram recordings from this species also showed no response to geosmin (data not shown) and neither does this species respond behaviorally to geosmin in a T-maze assay (Figure 7B). As in *D. melanogaster*, in each of the species responding to geosmin, detection was noted only from a single class of OSNs, which also responded exclusively to geosmin (Figure 7A). The geosmin OSNs we found in the other species may well

serve the same function that they serve in *D. melanogaster*. The lack of a geosmin detection system in *D. elegans* may be a consequence of the low susceptibility to mold growth of this species' breeding substrate, namely, fresh flowers (Yoshida et al., 2000). Putatively functional orthologs of *Or56a* are also present across the species in which we have complete OR repertoires (Guo and Kim, 2007). We also located intact orthologs of *Or56a* in draft genome assemblies from an additional eight drosophilids (Figure S6B), including *D. biarmipes* and *D. elegans*. The function (if any) of the *Or56a* ortholog in the latter remains unknown. Analysis of selection pressure also showed that the *Or56a* genes are under overall purifying selection (Figure S6C). The response properties of the second neuron residing in these sensilla are much less conserved (Figure S6D). These neurons also do not express orthologous receptors across the examined species. In *D. melanogaster*, the ab4A neurons express Or7a (Hallem et al., 2004), orthologs of which are, however, found only in the subgenus *Sophophora* (Guo and Kim, 2007). Yet, also in species in which we can assume that Or7a underlies the response property, we did note variation in ligand affinity. The function of the ab4A OSNs hence likely reflects species-specific requirements. The striking specificity toward geosmin seen in the olfactory system of *D. melanogaster* is accordingly a basal feature of the genus *Drosophila*, conserved for at least ~40 million years (Russo et al., 1995).

Conclusions

The manner in which flies decode and rely upon geosmin has few, if any, direct parallels. Comparable circuits are essentially found only within the subset of the olfactory nervous system that relays pheromone information. However, also within this context, it is exceedingly rare for animals to rely on just a single chemical to identify a critical resource. Almost all pheromones characterized to date have been complex blends processed by multiple neuronal pathways. Moreover, the specificity toward geosmin shown here surpasses many pheromone-tuned neurons; if presented with enough odorants or with odorants in sufficient concentration, these neurons will also display responses to other substances (Hansson and Stensmyr, 2011).

The closest match to the geosmin pathway is found outside of the regular olfactory system, namely in the detection and processing machinery for the atmospheric trace gas CO_2. Although CO_2 is a fundamentally different chemical from geosmin, the similarity in which these two stimuli are decoded is striking. In flies, the CO_2 circuit forms a functionally segregated pathway that mediates innate avoidance. Input to the CO_2 circuit is likewise fed by sensory neurons exclusively tuned to a single stimulus (Suh et al., 2004). Although organized similarly, the ecological significance of these two circuits seems to differ. Geosmin is used by flies as a universal warning sign for the presence of toxic compounds that are comorbid with geosmin. The evolutionary significance of this circuit is clear: it provides flies with a sensitive and specific means to identify unsuitable hosts. The ecological meaning of CO_2 for *D. melanogaster* is, however, unclear. In fact, it is puzzling why flies would be repelled by CO_2 at all. *D. melanogaster* is highly adapted toward breeding (and feeding) on substrates with high ethanol content. Because CO_2 is a ubiquitous byproduct of alcoholic fermentation, it would make an ideal cue for flies to follow when searching for suitable hosts. Elucidating the role of CO_2 from the point of view of flies and using assays that better reflect the natural setting should be a focus of future studies.

Circuits analogous to the geosmin pathway are a likely feature in the olfactory systems of most, if not all, insects. Although these circuits are probably similar mechanistically and functionally (i.e., selective with regards to input, mediating innate aversion, and abolishing attraction), the identity of the eliciting stimulus will differ, reflecting the demands raised by the taxon-specific ecology.

EXPERIMENTAL PROCEDURES

Fly Stocks

All experiments with WT *D. melanogaster* were carried out with the Canton-S strain. Species other than *D. melanogaster* were obtained from the *Drosophila* species stock center (https://stockcenter.ucsd.edu/info/welcome.php). Transgenic lines were obtained from the Bloomington *Drosophila* stock center (http://flystocks.bio.indiana.edu/), except for *UAS-Or22a*, which was donated by L. Vosshall (The Rockefeller University, New York) and *UAS-Or56-a^{RNAi}*, which was obtained from the Vienna RNAi stock center (http://www.vdrc.at).

Stimuli and Chemical Analysis

All synthetic odorants tested were acquired from commercial sources (Sigma, http://www.sigma-aldrich.com and Bedoukian, http://www.bedoukian.com) and were of the highest purity available. (±)-Geosmin (of >97% purity) was obtained from Sigma. Stimuli preparation and delivery followed Stökl et al. (2010). The headspace collection of volatiles was carried out according to standard procedures. *S. coelicolor* M145 and J3001 strains were gifts from K. Flärdh (Lund University, Sweden) and K. Chater (John Innes Centre, UK), respectively. *P. expansum* was obtained from Centraalbureau voor Schimmelcultures (http://www.cbs.knaw.nl). Microorganisms were kept on strain-specific media (HiMedia, http://www.himedialabs.com), following standard protocols. Mammalian fecal samples were provided by the Leipzig Zoo. For GC stimulation, 1 μl of the odor sample was injected onto a DB5 column (Agilent Technologies, http://www.agilent.com), fitted in an Agilent 6890 GC, equipped with a four-arm effluent splitter (Gerstel, www.gerstel.com), and operated as previously described (Stökl et al., 2010) except for the temperature increase, which was set at 15°C min^{-1}. GC-separated components were introduced into a humidified airstream (200 ml min^{-1}) directed toward the antennae of a mounted fly. Signals from OSNs and FID were recorded simultaneously. GC-MS analysis was performed as previously described (Stökl et al., 2010).

Behavioral Assays

T-maze experiments were conducted as shown in Figure 1B, with flies starved for 4 hr prior to experiments with water provided ad libitum. The response index (RI) was calculated as (O-C)/T, where O is the number of flies in the baited arm, C is the number of flies in the control arm, and T is the total number of flies used in the trial. The resulting index ranges from −1 (complete avoidance) to 1 (complete attraction). Trap assay experiments (Figure S4A) were performed as described in Stökl et al. (2010) with RI calculated as above. The Flywalk experiments followed protocols outlined in Steck et al. (2012) (Figure 5A). Survival was measured for individual flies (males and females, except for tests with J3001, in which only females were examined), which were kept for 5 days (at 23°C) in glass tubes (16 × 100 mm) with metal caps containing 1-week-old cultures of *S. coelicolor* or *P. expansum* grown on yeast-containing media (HiMedia). Oviposition experiments were carried out as shown in Figure 6B. Oviposition index was calculated as (O-C)/(O+C), where O is the number of eggs on a baited plate, and C is the number of

eggs on a control plate. Feeding experiments were conducted as described in Figure 6G. A feeding index was calculated as (O-C)/(O+C), where O is the amount of food consumed from odorous solutions, and C is the amount from control sucrose-only solutions.

Physiology and Morphology

Electroantennogram (EAG) recordings were performed following standard procedures (e.g., Stökl et al., 2010). For SSR measurements, the recording electrode and the reference electrode (inserted into the eye) were positioned under a microscope (Olympus BX51W1; http://www.olympus.com). The recording electrode was positioned by using a motorized, piezo-translator-equipped micromanipulator (Märzhauser DC-3K/PM-10; http://www.marzhauser.com/de/). The signal was amplified (Syntech UN-06, http://www.syntech.nl), digitally converted (Syntech IDAC-4), and finally visualized and analyzed by using Syntech AutoSpike v3.2. CHO cells stably expressing dOrco (Trenzyme, http://www.trenzyme.com) were transiently transfected with dOr56a/pcDNA3.1(−) or dOr33a/pcDNA3.1(−) by using a Roti-Fect transfection kit (Carl Roth, http://www.carlroth.com) as described (Sargsyan et al., 2011). Ca^{2+} imaging of CHO cells was performed as described (Wicher et al., 2008). The functional imaging of odor-induced glomerular activity was conducted as outlined in Stökl et al. (2010). Patch-clamp recording was performed as previously described (Seki et al., 2010), except that in vivo preparation was used, and odor stimuli were given. Preparation followed Stökl et al. (2010), with the exception that the neurolemma was removed to allow the recording electrode access to the cell bodies of the PNs. Spike analysis, immunohistochemistry, laser scanning microscopy, and 3D reconstructions were performed as previously described (Seki et al., 2010).

Statistics and Bioinformatics

Estimates of the selection pressure were done by maximum likelihood as implemented in PAML (Yang, 1997). Additional orthologs of *Or56a* were identified via TBLASTN searches of draft genomes (courtesy of modENCODE/Baylor College of Medicine), downloaded from http://www.ncbi.nlm.nih.gov/bioproject/63477.

SUPPLEMENTAL INFORMATION

Supplemental Information includes six figures and can be found with this article online at http://dx.doi.org/10.1016/j.cell.2012.09.046.

ACKNOWLEDGMENTS

This work was supported by the Max Planck Society, the German Federal Ministry of Education and Research (A.S., V.G., and S.S.), and the Swedish research council Formas (P.G.B.). We wish to thank S. Caron and F. Maderspacher for valuable comments on the manuscript, E. Wheeler for editorial assistance, and R. Stieber, K. Weniger, and S. Kaltofen for technical support. We thank I. Urru for assisting with odor collections, S. Koczsan and J. Rybak for morphological analysis, and M. Thoma for providing help with the Flywalk experiments.

Received: June 7, 2012
Revised: August 28, 2012
Accepted: September 24, 2012
Published: December 6, 2012

REFERENCES

Arndt, C., Cruz, M.C., Cardenas, M.E., and Heitman, J. (1999). Secretion of FK506/FK520 and rapamycin by *Streptomyces* inhibits the growth of competing *Saccharomyces cerevisiae* and *Cryptococcus neoformans*. Microbiology *145*, 1989–2000.

Becher, P.G., Bengtsson, M., Hansson, B.S., and Witzgall, P. (2010). Flying the fly: long-range flight behavior of *Drosophila melanogaster* to attractive odors. J. Chem. Ecol. *36*, 599–607.

Benton, R., Vannice, K.S., Gomez-Diaz, C., and Vosshall, L.B. (2009). Variant ionotropic glutamate receptors as chemosensory receptors in *Drosophila*. Cell *136*, 149–162.

Bhandawat, V., Olsen, S.R., Gouwens, N.W., Schlief, M.L., and Wilson, R.I. (2007). Sensory processing in the *Drosophila* antennal lobe increases reliability and separability of ensemble odor representations. Nat. Neurosci. *10*, 1474–1482.

Castillo, M.-A., Moya, P., Cantín, A., Miranda, M.A., Primo, J., Hernández, E., and Primo-Yúfera, E. (1999). Insecticidal, anti-juvenile hormone, and fungicidal activities of organic extracts from different Penicillium species and their isolated active components. J. Agric. Food Chem. *47*, 2120–2124.

Couto, A., Alenius, M., and Dickson, B.J. (2005). Molecular, anatomical, and functional organization of the *Drosophila* olfactory system. Curr. Biol. *15*, 1535–1547.

Datta, S.R., Vasconcelos, M.L., Ruta, V., Luo, S., Wong, A., Demir, E., Flores, J., Balonze, K., Dickson, B.J., and Axel, R. (2008). The *Drosophila* pheromone cVA activates a sexually dimorphic neural circuit. Nature *452*, 473–477.

de Bruyne, M., Clyne, P.J., and Carlson, J.R. (1999). Odor coding in a model olfactory organ: the Drosophila maxillary palp. J. Neurosci. *19*, 4520–4532.

de Bruyne, M., Foster, K., and Carlson, J.R. (2001). Odor coding in the Drosophila antenna. Neuron *30*, 537–552.

Fishilevich, E., and Vosshall, L.B. (2005). Genetic and functional subdivision of the *Drosophila* antennal lobe. Curr. Biol. *15*, 1548–1553.

Gerber, N.N., and Lechevalier, H.A. (1965). Geosmin, an earthly-smelling substance isolated from actinomycetes. Appl. Microbiol. *13*, 935–938.

Guo, S., and Kim, J. (2007). Molecular evolution of *Drosophila* odorant receptor genes. Mol. Biol. Evol. *24*, 1198–1207.

Gust, B., Challis, G.L., Fowler, K., Kieser, T., and Chater, K.F. (2003). PCR-targeted *Streptomyces* gene replacement identifies a protein domain needed for biosynthesis of the sesquiterpene soil odor geosmin. Proc. Natl. Acad. Sci. USA *100*, 1541–1546.

Hallem, E.A., Ho, M.G., and Carlson, J.R. (2004). The molecular basis of odor coding in the *Drosophila* antenna. Cell *117*, 965–979.

Hamada, F.N., Rosenzweig, M., Kang, K., Pulver, S.R., Ghezzi, A., Jegla, T.J., and Garrity, P.A. (2008). An internal thermal sensor controlling temperature preference in Drosophila. Nature *454*, 217–220.

Hansson, B.S., and Stensmyr, M.C. (2011). Evolution of insect olfaction. Neuron *72*, 698–711.

Ja, W.W., Carvalho, G.B., Mak, E.M., de la Rosa, N.N., Fang, A.Y., Liong, J.C., Brummel, T., and Benzer, S. (2007). Prandiology of Drosophila and the CAFE assay. Proc. Natl. Acad. Sci. USA *104*, 8253–8256.

Jefferis, G.S.X.E., Marin, E.C., Stocker, R.F., and Luo, L. (2001). Target neuron prespecification in the olfactory map of *Drosophila*. Nature *414*, 204–208.

Jones, P.L., Pask, G.M., Rinker, D.C., and Zwiebel, L.J. (2011). Functional agonism of insect odorant receptor ion channels. Proc. Natl. Acad. Sci. USA *108*, 8821–8825.

Jüttner, F., and Watson, S.B. (2007). Biochemical and ecological control of geosmin and 2-methylisoborneol in source waters. Appl. Environ. Microbiol. *73*, 4395–4406.

Karlson, P., and Lüscher, M. (1959). Pheromones': a new term for a class of biologically active substances. Nature *183*, 55–56.

Kitamoto, T. (2001). Conditional modification of behavior in *Drosophila* by targeted expression of a temperature-sensitive shibire allele in defined neurons. J. Neurobiol. *47*, 81–92.

Knaden, M., Strutz, A., Ahsan, J., Sachse, S., and Hansson, B.S. (2012). Spatial representation of odorant valence in an insect brain. Cell Rep. *1*, 392–399.

Kreher, S.A., Mathew, D., Kim, J., and Carlson, J.R. (2008). Translation of sensory input into behavioral output via an olfactory system. Neuron *59*, 110–124.

Kurtovic, A., Widmer, A., and Dickson, B.J. (2007). A single class of olfactory neurons mediates behavioural responses to a *Drosophila* sex pheromone. Nature *446*, 542–546.

Larsson, M.C., Domingos, A.I., Jones, W.D., Chiappe, M.E., Amrein, H., and Vosshall, L.B. (2004). Or83b encodes a broadly expressed odorant receptor essential for *Drosophila* olfaction. Neuron *43*, 703–714.

Mattheis, J.P., and Roberts, R.G. (1992). Identification of geosmin as a volatile metabolite of *Penicillium expansum*. Appl. Environ. Microbiol. *58*, 3170–3172.

Petro-Turza, M. (1987). Flavor of tomato and tomato products. Food Rev. Int. *2*, 309–351.

Russo, C.A.M., Takezaki, N., and Nei, M. (1995). Molecular phylogeny and divergence times of drosophilid species. Mol. Biol. Evol. *12*, 391–404.

Ruta, V., Datta, S.R., Vasconcelos, M.L., Freeland, J., Looger, L.L., and Axel, R. (2010). A dimorphic pheromone circuit in *Drosophila* from sensory input to descending output. Nature *468*, 686–690.

Sargsyan, V., Getahun, M.N., Lavista Llanos, S., Olsson, S., Hansson, B., and Wicher, D. (2011). Phosphorylation via PKC regulates the function of the Drosophila odorant co-receptor. Front. Cell. Neurosci. Published online June 16, 2011. http://dx.doi.org/10.3389/fncel.2011.00005.

Schlief, M.L., and Wilson, R.I. (2007). Olfactory processing and behavior downstream from highly selective receptor neurons. Nat. Neurosci. *10*, 623–630.

Seki, Y., Rybak, J., Wicher, D., Sachse, S., and Hansson, B.S. (2010). Physiological and morphological characterization of local interneurons in the *Drosophila* antennal lobe. J. Neurophysiol. *104*, 1007–1019.

Semmelhack, J.L., and Wang, J.W. (2009). Select *Drosophila* glomeruli mediate innate olfactory attraction and aversion. Nature *459*, 218–223.

Shanbhag, S., Mueller, B., and Steinbrecht, R. (1999). Atlas of olfactory organ of *Drosophila melanogaster* 1. Types, external organization, innervation and distribution of olfactory sensilla. Int. J. Insect Morphol. Embryol. *28*, 377–397.

Steck, K., Veit, D., Grandy, R., Badia, S.B., Mathews, Z., Verschure, P., Hansson, B.S., and Knaden, M. (2012). A high-throughput behavioral paradigm for *Drosophila* olfaction - The Flywalk. Sci. Rep. *2*, 361.

Stocker, R.F., Heimbeck, G., Gendre, N., and de Belle, J.S. (1997). Neuroblast ablation in *Drosophila* P[GAL4] lines reveals origins of olfactory interneurons. J. Neurobiol. *32*, 443–456.

Stökl, J., Strutz, A., Dafni, A., Svatos, A., Doubsky, J., Knaden, M., Sachse, S., Hansson, B.S., and Stensmyr, M.C. (2010). A deceptive pollination system targeting drosophilids through olfactory mimicry of yeast. Curr. Biol. *20*, 1846–1852.

Suh, G.S., Wong, A.M., Hergarden, A.C., Wang, J.W., Simon, A.F., Benzer, S., Axel, R., and Anderson, D.J. (2004). A single population of olfactory sensory neurons mediates an innate avoidance behaviour in *Drosophila*. Nature *431*, 854–859.

Tian, L., Hires, S.A., Mao, T., Huber, D., Chiappe, M.E., Chalasani, S.H., Petreanu, L., Akerboom, J., McKinney, S.A., Schreiter, E.R., et al. (2009). Imaging neural activity in worms, flies and mice with improved GCaMP calcium indicators. Nat. Methods *6*, 875–881.

Tinbergen, N. (1951). The Study of Instinct (Oxford: Clarendon Press).

van der Goes van Naters, W., and Carlson, J.R. (2007). Receptors and neurons for fly odors in *Drosophila*. Curr. Biol. *17*, 606–612.

Vosshall, L.B., and Stocker, R.F. (2007). Molecular architecture of smell and taste in *Drosophila*. Annu. Rev. Neurosci. *30*, 505–533.

Wicher, D., Schäfer, R., Bauernfeind, R., Stensmyr, M.C., Heller, R., Heinemann, S.H., and Hansson, B.S. (2008). *Drosophila* odorant receptors are both ligand-gated and cyclic-nucleotide-activated cation channels. Nature *452*, 1007–1011.

Wilson, R.I., Turner, G.C., and Laurent, G. (2004). Transformation of olfactory representations in the *Drosophila* antennal lobe. Science *303*, 366–370.

Yang, Z.H. (1997). PAML: a program package for phylogenetic analysis by maximum likelihood. Comput. Appl. Biosci. *13*, 555–556.

Yao, C.A., Ignell, R., and Carlson, J.R. (2005). Chemosensory coding by neurons in the coeloconic sensilla of the *Drosophila* antenna. J. Neurosci. *25*, 8359–8367.

Yoshida, T., Chen, H.W., Toda, M.J., Kimura, M.T., and Davis, A.J. (2000). New host plants and host plant use for *Drosophila elegans* Bock and Wheeler, 1972. Drosoph. Inf. Serv. *83*, 18–21.

Young, W.F., Horth, H., Crane, R., Ogden, T., and Arnott, M. (1996). Taste and odour threshold concentrations of potential potable water contaminants. Water Res. *30*, 331–340.

Supplemental Information

Cell

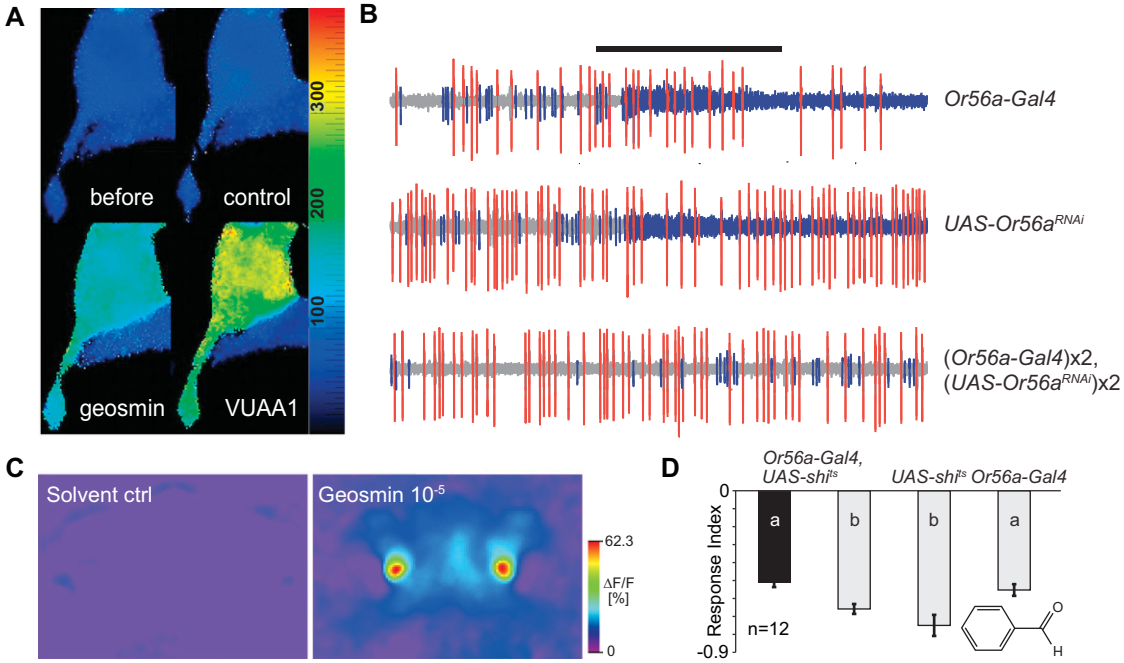

Figure S1. Molecular Function of Or56a, Related to Figure 2

(A) Color coded $[Ca^{2+}]_i$ (scaling bar, nM) in a CHO cell expressing *Or56a* and *Orco* before and 10 s after application of saline (control), geosmin (50 μM) and VUAA1 (100 μM).

(B) Representative SSR traces from control ab4 sensilla (top two traces) and from an ab4 sensillum with reduced levels of Or56a (bottom trace). Expression of RNAi directed against Or56a in ab4B OSNs (blue spikes) abolishes the response to geosmin (10^{-3}). Duration of the stimulus delivery (0.5 s) is marked by the black bar.

(C) Raw images from the same recording as in Figure 2G.

(D) Silencing ab4B neurons, via *Shibire^{ts}*, does not abolish aversion toward benzaldehyde (10^{-2} dilution). Significant differences are denoted by letters (ANOVA followed by Tukey's test; $p < 0.05$). Error bars represent SEM.

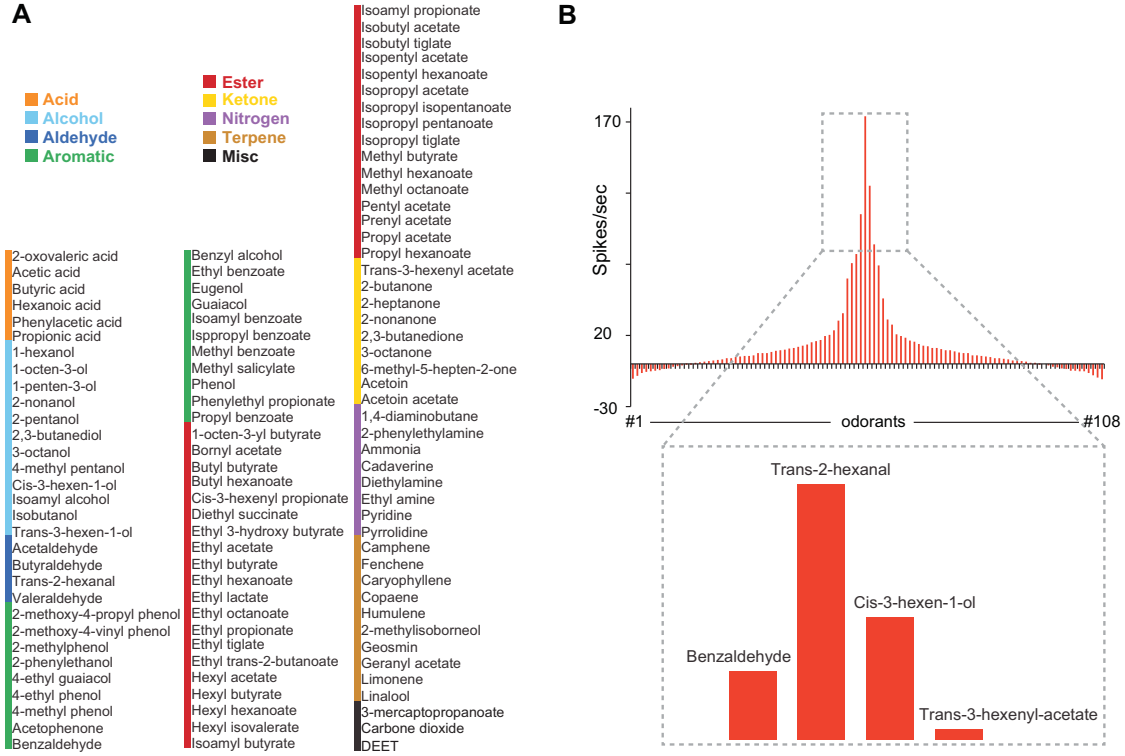

Figure S2. Screened Synthetic Volatiles and Properties of the ab4A Neuron, Related to Figure 3

(A) Screened odorants.

(B) Tuning curve for the ab4A neuron type based on a screen of 103 synthetic substances.

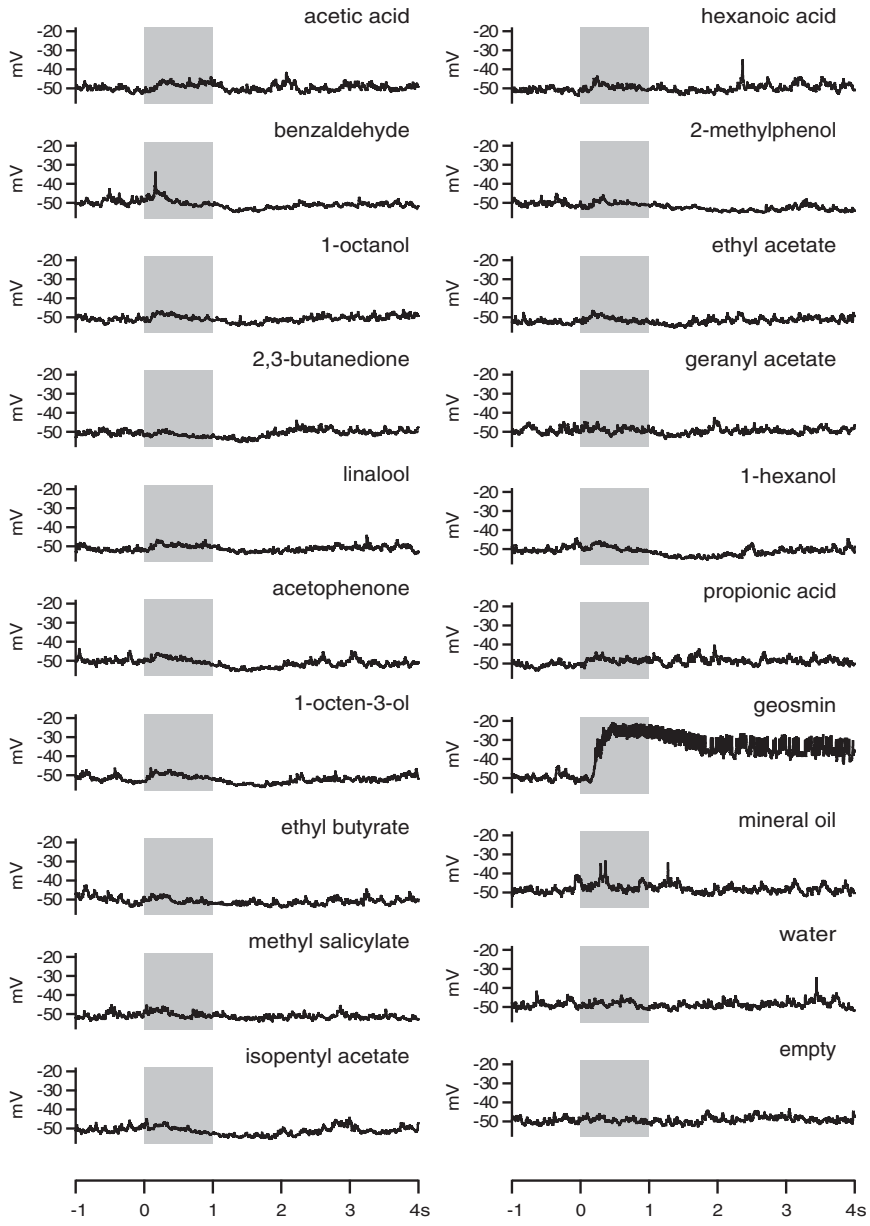

Figure S3. Spike Traces from a DA2 Projection Neuron, Related to Figure 4

Spike traces from a DA2 PN following odor stimulation. Only geosmin elicits any response.

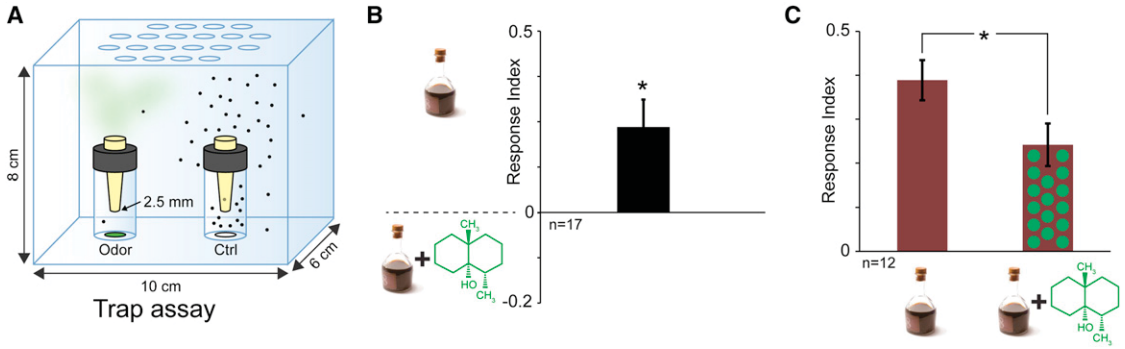

Figure S4. T-Maze and Trap Assay Choice Experiments with a Vinegar and Geosmin Mix, Related to Figure 5

(A) Schematic drawing of the trap assay (Larsson et al., 2004) used in panel (B). For each trial, ~50 flies were placed inside the test boxes. Number of flies in and outside traps was then counted after 24 hr (for further details, see Stökl et al. [2010] and Knaden et al. [2012]).

(B) Response index of wt flies given a choice between balsamic vinegar and balsamic vinegar additionally containing 10^{-3} geosmin in the trap assay. Deviation of the response index against zero was tested with a Student's t test ($p < 0.05$). Error bar represent SEM.

(C) Response indices of wt flies to balsamic vinegar and balsamic vinegar containing geosmin (10^{-3}) in the T-maze assay. Star denotes significant difference (Student's t test $p < 0.05$). Error bars represent SEM.

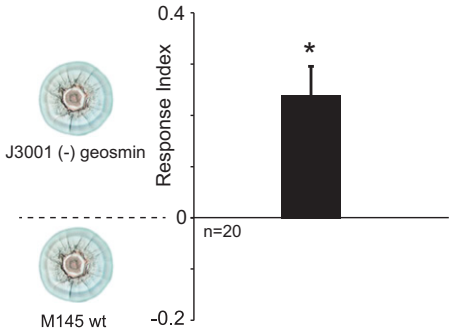

Figure S5. Trap Assay Two-Choice Experiment with WT and Mutant *S. coelicolor*, Related to Figure 6

Response index of flies given a choice between wt (M145) *S. coelicolor* and the J3001 strain in the olfactory choice trap assay (Figure S4A). Star denotes significant difference (Student's t test $p < 0.05$). Error bar represent SEM.

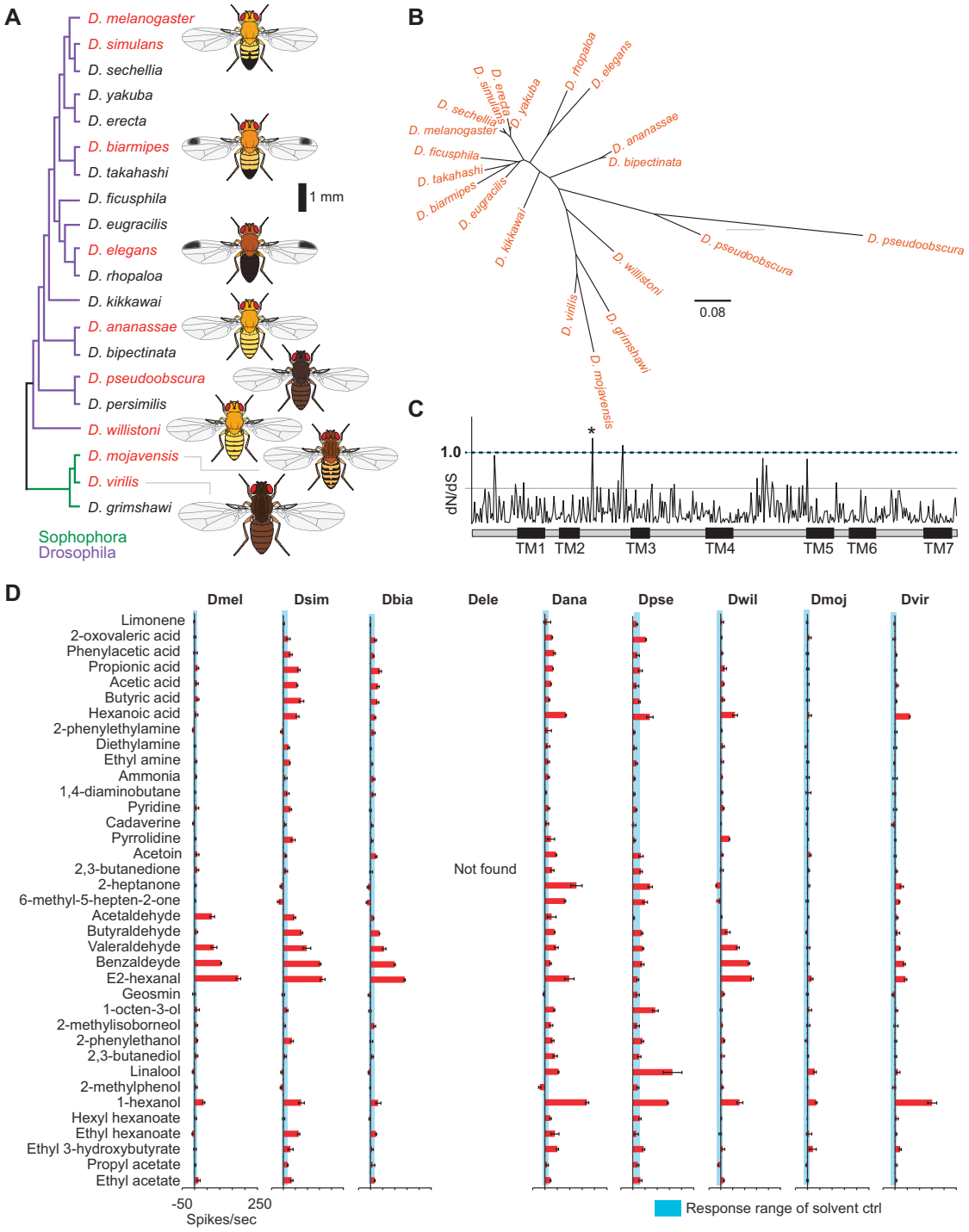

Figure S6. Molecular and Physiological Properties of the ab4 Type Sensillum across Related Drosophilids, Related to Figure 7

(A) Phylogenetic relationship of the examined species.

(B) Phylogenetic tree of *Or56a* orthologs from 19 species. The tree was constructed with RAxML from a Muscle alignment. Scale bar represents number of substitutions per site.

(C) Estimation of the selection pressure acting upon *Or56a*. Plot shows dN/dS ratios (obtained through PAML, model M8) for all codons, here plotted on the sequence of *D. melanogaster*. TM1-7 indicates putative locations of transmembrane domains (estimated with HMMTOP/TMHMM). Star denotes site under significant positive selection (Bayes Empirical Bayes).

(D) Response profile of neurons (n = 3) paired with the geosmin responsive neurons shown in Figure 6. Error bars represent SEM.

Manuscript III

In situ tip-recordings found no evidence for an Orco-based ionotropic mechanism of pheromone-transduction in *Manduca sexta.*

OPEN ACCESS Freely available online

PLOS ONE

In situ Tip-Recordings Found No Evidence for an Orco-Based Ionotropic Mechanism of Pheromone-Transduction in *Manduca sexta*

Andreas Nolte[1☯], Nico W. Funk[1☯], Latha Mukunda[2], Petra Gawalek[1], Achim Werckenthin[1], Bill S. Hansson[2], Dieter Wicher[2], Monika Stengl[2]*

1 Department of Animal Physiology, University of Kassel, Kassel, Germany, **2** Department Evolutionary Neuroethology, Max Planck Institute for Chemical Ecology, Jena, Germany

Abstract

The mechanisms of insect odor transduction are still controversial. Insect odorant receptors (ORs) are 7TM receptors with inverted membrane topology. They colocalize with a conserved coreceptor (Orco) with chaperone and ion channel function. Some studies suggest that insects employ exclusively ionotropic odor transduction via OR-Orco heteromers. Other studies provide evidence for different metabotropic odor transduction cascades, which employ second messenger-gated ion channel families for odor transduction. The hawkmoth *Manduca sexta* is an established model organism for studies of insect olfaction, also due to the availability of the hawkmoth-specific pheromone blend with its main component bombykal. Previous patch-clamp studies on primary cell cultures of *M. sexta* olfactory receptor neurons provided evidence for a pheromone-dependent activation of a phospholipase Cβ. Pheromone application elicited a sequence of one rapid, apparently IP_3-dependent, transient and two slower Ca^{2+}-dependent inward currents. It remains unknown whether additionally an ionotropic pheromone-transduction mechanism is employed. If indeed an OR-Orco ion channel complex underlies an ionotropic mechanism, then Orco agonist-dependent opening of the OR-Orco channel pore should add up to pheromone-dependent opening of the pore. Here, in tip-recordings from intact pheromone-sensitive sensilla, perfusion with the Orco agonist VUAA1 did not increase pheromone-responses within the first 1000 ms. However, VUAA1 increased spontaneous activity of olfactory receptor neurons Zeitgebertime- and dose-dependently. We conclude that we find no evidence for an Orco-dependent ionotropic pheromone transduction cascade in *M. sexta*. Instead, in *M. sexta* Orco appears to be a slower, second messenger-dependent pacemaker channel which affects kinetics and threshold of pheromone-detection via changes of intracellular Ca^{2+} baseline concentrations.

Citation: Nolte A, Funk NW, Mukunda L, Gawalek P, Werckenthin A, et al. (2013) *In situ* Tip-Recordings Found No Evidence for an Orco-Based Ionotropic Mechanism of Pheromone-Transduction in *Manduca sexta*. PLoS ONE 8(5): e62648. doi:10.1371/journal.pone.0062648

Editor: Alan Nighorn, University of Arizona, United States of America

Received December 6, 2012; **Accepted** March 25, 2013; **Published** May 3, 2013

Funding: This study was supported by the Max Planck Society (L.M., B.S.H., D.W.) and DFG grants STE 531/20-1, -2, HA 5871/2-1 and WI 1422/3-2. The funders had no role in study design, data collection and analysis, decision to publish, or preparation of the manuscript.

Competing Interests: The authors have declared that no competing interests exist.

* E-mail: stengl@uni-kassel.de

☯ These authors contributed equally to this work.

Introduction

In insects odorants are detected by olfactory receptors (ORs) which form a large receptor family of seven transmembrane domain (7 TM) proteins [1–5]. ORs are expressed in the dendrites of insect olfactory receptor neurons (ORNs) which innervate hair-like sensilla on the antenna [6,7]. ORs have an inverted membrane topology with an extracellular C-terminus in comparison to conventional G-protein coupled 7TM receptors [8–12]. Besides the diverse ORs binding various odor ligands, a highly conserved protein with weak homology to ORs, named Or83b in the fruitfly *Drosophila melanogaster*, is co-expressed in ORNs of different insect species [1,13–23]. In the fruitfly Or83b was suggested to be a coreceptor forming OR-Or83b heteromers [8,24] and was consequently renamed Orco [25]. Orco is a prerequisite for odor detection since it is a chaperone necessary for the localization of ORs to the ciliated dendrites of ORNs [8,26]. Additional functions of Orco are still under discussion. It was proposed that OR-Orco complexes constitute ligand-gated receptor ion channels promoting ionotropic odor transduction [27,28]. Both, OR and Orco, were predicted to contribute to the pore of the odor-gated receptor-ion channel complex [27,29–31]. In contrast, there is evidence for various metabotropic signal transduction cascades in different insect species [32–34]. While one study [27] suggested that all insect species employ solely ionotropic odor and pheromone transduction, another study [28] found evidence in *D. melanogaster* for both a less sensitive fast ionotropic pathway as well as a slower, more sensitive metabotropic transduction cascade coupled to adenylyl cyclase. In addition, the *D. melanogaster* Orco itself forms a leaky (spontaneously opening) cation channel activated by cGMP/cAMP, which relies on protein kinase C-dependent phosphorylation [28,35]. In contrast, patch-clamp studies on primary cell cultures of *M. sexta* ORNs as well as tip-recordings of pheromone-sensitive sensilla in intact moths suggested that moths employ different odor transduction cascades depending on stimulus concentration, behavioral

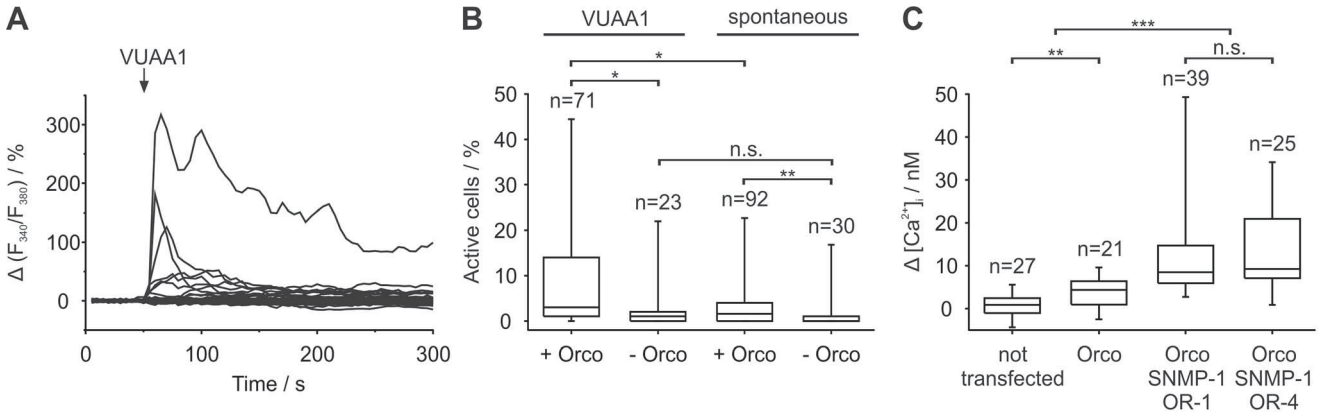

Figure 1. Heterologously expressed MsexOrco is activated by VUAA1 and increases spontaneous activity. Furthermore, MsexOrco appears to interact with MsexORs and/or SNMP-1 in heterologous expression systems. (A) Normalized calcium imaging data of HEK 293 cells transiently transfected with MsexOrco. Data for 100 cells are shown, where each line represents the percentage deviation of the fluorescence ratio ($\Delta(F_{340}/F_{380})$) for one cell. After VUAA1 application (100 µl of 100 µM, arrow) eight of 100 cells show an increase in the fluorescence ratio. (B) Percentages of active cells either transiently transfected with MsexOrco (+Orco) or not (-Orco) after VUAA1 application or without application (spontaneous) are compared (n = number of experiments; for each experiment the percentage of active cells was determined). (C) Box plots show the mean increase in the free intracellular Ca^{2+} concentration ($\Delta[Ca^{2+}]_i$) after VUAA1 application. HEK 293 cells were either not transfected or stably transfected with MsexOrco and optionally cotransfected with MsexSNMP-1 and MsexOR-1, or MsexOR-4 (n = number of cells). (B,C) Significant differences are indicated by asterisks (n.s. = not significant; *$P<0.05$, **$P<0.01$, ***$P<0.001$; Mann-Whitney test).
doi:10.1371/journal.pone.0062648.g001

context, and Zeitgebertime (ZT, with ZT 0 defined as the beginning of the light phase; see Materials and Methods) [33]. The main sex-pheromone component of *M. sexta*, bombykal (BAL), elicited a sequence of at least three consecutive pheromone-dependent inward currents, which were also triggered by IP_3 perfusion of ORNs [33,36–38]. The first, very rapid and transient pheromone-dependent Ca^{2+} inward current, which lasted less than 100 ms, triggered a sequence of Ca^{2+}-dependent ion channel openings. While Orco is present in *M. sexta* pheromone-dependent trichoid sensilla [22,39], it is not known whether additionally an Orco-dependent ionotropic pathway is responsible for the first pheromone-dependent trigger current in *M. sexta* ORNs, which resembled an IP_3-dependent Ca^{2+} current.

To investigate the function of Orco in pheromone transduction of *M. sexta*, we examined the effect of the Orco agonist VUAA1 [40]. If OR-Orco heteromers form BAL-gated ion channels, co-activation of Orco with VUAA1 during pheromone stimulation would mimic stimulation with higher pheromone doses. Thus, the Orco agonist would increase pheromone responses dose-dependently within the first ~25 ms (the first 6 action potentials) of the BAL response. In calcium imaging experiments on HEK 293 cells transiently or stably transfected with MsexOrco it was confirmed that VUAA1 is an MsexOrco agonist. However, in contrast to our expectations, VUAA1 perfusion of trichoid sensilla in intact *M. sexta* did not augment pheromone transduction within the first ~25 ms nor in the first 1000 ms of the pheromone response. Instead, Orco appears to be a spontaneously active ion channel, which affects spontaneous activity day-time-dependently on a slower time scale, possibly via sustained changes in the baseline Ca^{2+} concentration.

Results

It is not known if Orco is involved in the first rapid pheromone response in *M. sexta*. Consequently, we stimulated Orco *in situ* with its agonist VUAA1 during non-saturating BAL-stimulations [41]. First, we established whether VUAA1 is an MsexOrco agonist. Secondly, we tested whether MsexOrco forms a spontaneously active, Ca^{2+}-permeable cation channel as in *D. melanogaster* [27]. Finally, we challenged the hypothesis that insects in general employ solely ionotropic odor transduction [27] in tip-recordings from intact *M. sexta* pheromone specific sensilla. Different time windows of the pheromone response were evaluated separately to distinguish ionotropic or metabotropic signal transduction cascades. Since *M. sexta* responds with different sensitivity to pheromone stimulation in the sleep-wake cycle [42–44] the effects of VUAA1 infusion into pheromone-sensitive trichoid sensilla were compared at ZT 1–3 (activity phase) and ZT 9–11 (resting phase).

MsexOrco Forms a Spontaneously Active Cation Channel which is Activated by VUAA1 in a Heterologous Expression System

In Ca^{2+} imaging experiments stimulation with 100 µM VUAA1 increased intracellular Ca^{2+} concentrations in HEK 293 cells transiently transfected with MsexOrco (**Fig. 1A**). We confirmed that VUAA1 is an MsexOrco agonist since significantly more MsexOrco transfected cells (median: 3%) showed VUAA1-dependent intracellular Ca^{2+} concentration increases compared to controls not transfected with MsexOrco (median: 1%; **Fig. 1B**). Additionally the percentage of MsexOrco transfected cells showing VUAA1-dependent Ca^{2+} concentration increases was significantly higher than the percentage showing spontaneous Ca^{2+} concentration increases ($P = 0.024$; median: 1.78%). Moreover, MsexOrco transfected cells showed significantly more spontaneous Ca^{2+} concentration increases ($P = 0.003$) than non-Orco transfected cells (median: 0%). From these measurements we conclude that MsexOrco forms a leaky Ca^{2+}-permeable ion channel, whose open-probability can be increased by VUAA1.

Since the majority of transiently transfected cells did not respond to VUAA1 stimulation, apparently due to sparse membrane insertion of MsexOrco, we obtained a HEK 293 cell line with stably transfected MsexOrco. Similar to the transiently transfected cells less than 5% of the HEK cells responded to VUAA1 stimulation (n = 213). Ca^{2+} concentration increase after stimulation with 100 µM VUAA1 was small but significantly different from responses of non-transfected cells ($P = 0.003$,

Fig. 1C). Cotransfection with MsexSNMP-1 and pheromone receptor candidates MsexOR-1 or MsexOR-4 [39,45] did not change the percentage of responding cells, but significantly increased the VUAA1-dependent Ca^{2+} concentration increase compared to non-transfected and solely Orco transfected cells ($P<0.001$ for all, **Fig. 1C**). From these measurements we conclude that MsexOrco interacts with MsexORs and/or MsexSNMP-1.

VUAA1 does not Increase Pheromone Responses in *M. sexta*

In long-term tip-recordings infusion of VUAA1 did not affect pheromone-dependent sensillum potential amplitudes (SPA), neither during activity nor during resting phase (**Fig. 2A, S1; Tab. S2, S4**). Thus, Orco appears not to contribute to the rise of the BAL-dependent receptor potential. Also, analysis of the phasic action potential (AP) response did not provide evidence for a BAL-gated OR-Orco-dependent ion channel opening during the first ~25 ms of the pheromone response. In the beginning of the long-term tip-recordings the BAL-dependent AP frequency was not affected by VUAA1 during the activity phase (**Fig. 2B**). A significant decline only occurred with perfusion of 100 µM VUAA1 at rest. Both control and VUAA1 recordings showed a significant decline in AP frequency over the time course (**Fig. S2A–D; Tab. S2, S4**). This decline was significantly stronger in the presence of 100 µM VUAA1.

The latency of the first BAL-dependent AP remained unchanged in the beginning of the recordings during the activity phase (**Fig. 2C**). However, it was significantly prolonged for VUAA1 at rest (**Fig. S2A–D; Tab. S2, S4**). For both control and VUAA1 recordings the latency increased over the time course. This increase was significantly higher in the presence of 100 µM VUAA1 (**Fig. S2E,F; Tab. S2, S4**).

To determine further ion channel activation by VUAA1 within the first second of the pheromone response, post stimulus time histograms (PSTHs) were prepared (**Fig. 3**). The number of BAL-dependent APs was analyzed during the first 150 ms and 1000 ms after onset of the BAL-dependent sensillum potential (**Fig. S3, Tab. S2**, **S4**). In the beginning of the recordings neither VUAA1 concentration had any effect on the number of APs generated in the first 150 ms (**Fig. 3A,B; Tab S2, S4**). Neither was the number of APs during the first 1000 ms of the activity phase affected by VUAA1 (**Fig. S3C,D; Tab. S2, S4**), while at rest only 1 µM VUAA1 caused a significant decline (**Tab. S2, S4**). Comparison of the distribution (**Fig. 3**) and number of APs (**Fig. S3**) in controls over the course of the recordings indicates that the kinetics of the pheromone response shifted to a more tonic response pattern during rest. In addition, the decrease of the number of APs in the first 150 ms in control experiments indicated an increase in threshold at rest (**Fig. S3, Tab. S2, S4**). Application of the Orco agonist further enhanced this shift in kinetics and BAL-sensitivity during the course of the recording. This suggests that Orco activation affected the kinetics as well as the sensitivity of the BAL response on the time scale of minutes rather than milliseconds.

VUAA1 Increased Spontaneous and Background Activity

Next we examined whether Orco forms an ion channel involved in modulating spontaneous activity in the absence of pheromone. A significant VUAA1 dose-dependent increase in spontaneous activity without previous pheromone stimulation could be observed during activity and resting phase, with higher sensitivity to VUAA1 during activity phase (**Fig. 4B; Tab. S3, S4**). Also, the background activity between two pheromone stimulations was examined. Application of VUAA1 significantly increased back-

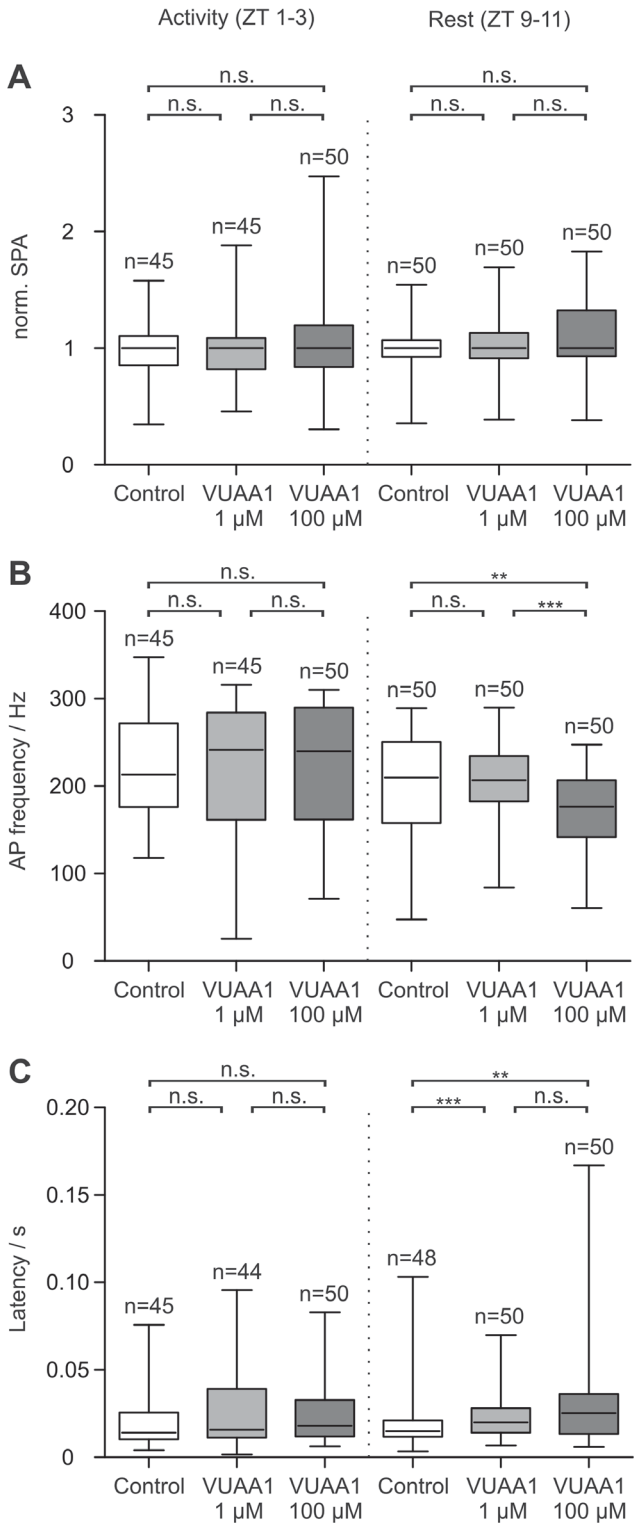

Figure 2. VUAA1-dependent MsexOrco activation does not increase the pheromone-dependent sensillum potential amplitude (SPA) nor the bombykal-dependent action potential (AP) frequency as it would be expected for an Orco-based ionotropic mechanism of pheromone transduction. (A–C) Box plots represent pheromone responses during the first 20 minutes (beginning) of the tip-recordings. (A) The pheromone-dependent SPA was never affected by VUAA1. (B) The pheromone-dependent AP response (first 5 APs) was not affected by VUAA1 during the activity phase, but was decreased at high agonist concentrations at rest. (C)

Only at rest the first pheromone-dependent AP was delayed by VUAA1. Significant differences are indicated by asterisks (n.s. = not significant; $^{**}P<0.01$, $^{***}P<0.001$; Mann-Whitney test).
doi:10.1371/journal.pone.0062648.g002

ground activity (**Fig. 4C,D; Tab. S2, S4**). However, no dose-dependent effect was found. While long-term control recordings showed a continuous decline over the time course, the decline was counteracted in 100 µM VUAA1 recordings during activity and resting phase (**Fig. S4**). Background activity was significantly higher than spontaneous activity in control and 1 µM VUAA1 recordings ($P<0.001$ for all). However, during the activity phase spontaneous activity was significantly higher than background activity under the influence of 100 µM VUAA1 ($P=0.006$).

Additionally, we analyzed whether VUAA1 affects the bursting pattern in the background activity of the BAL-sensitive ORN. The percentage of APs belonging to bursts and the number of APs per burst were calculated (**Fig. 5**). In the beginning of the recordings both VUAA1 concentrations decreased the number of APs per burst except for 100 µM VUAA1 at rest. The percentage of APs in bursts was always decreased by VUAA1. Addition of 100 µM VUAA1 significantly decreased the number of APs per bursts as well as the percentage of APs in bursts over the time course.

Discussion

Research in insect olfaction proposed controversial models of odor transduction [27,28,32,33]. Here, with long-term tip-recordings *in situ* from pheromone-sensitive trichoid sensilla of intact *M. sexta* we examined whether MsexOrco-dependent ionotropic pheromone transduction is employed. In heterologous expression systems we confirmed that VUAA1 [40] is an MsexOrco agonist and that MsexOrco forms a spontaneously opening Ca^{2+}-permeable cation channel, which appears to interact with co-transfected MsexORs/MsexSNMP-1 [46]. Unexpectedly, with *in situ* studies we found no evidence for the participation of an MsexOR-MsexOrco-dependent ionotropic transduction pathway during the first ~25, 150, or 1000 ms of the pheromone response during the first 20 min of the tip-recordings. Instead, MsexOrco affects pheromone response kinetics and sensitivity in pheromone- and ZT-dependent manner within the time period of minutes, possibly via its effects on spontaneous activity and pheromone-dependent background activity. We hypothesize that pheromone dependency results from pheromone-dependently activated metabotropic cascades, which changed open-probability and/or conductance of MsexOrco ion channels. We assume that ZT-dependency resulted from different Ca^{2+} baseline levels (which modulate MsexOrco) between rest and activity phase, possibly regulated via a circadian clock in ORNs [33,47,48]. Also differences in the pheromone response between beginning and end of long-term tip-recordings are most likely due to changes in Ca^{2+} baseline levels, possibly via the accumulation of DMSO. We suggest that MsexOrco forms a leaky second-messenger-dependent cation channel that controls membrane potential oscillations and intracellular Ca^{2+} baseline levels, and thereby kinetics and threshold of pheromone responses in *M. sexta*.

VUAA1 Activates MsexOrco

The discovery of different agonists and antagonists of the conserved coreceptor Orco has greatly facilitated the study of Orco function [31,40,49–54]. Since spontaneous Ca^{2+} signals occurred more frequently in HEK 293 cells expressing MsexOrco (**Fig. 1B**) it can also form functional leaky (spontaneously opening) ion channels as reported for *D. melanogaster* and *Anopheles gambiae* [27,28,35,40]. In addition, 100 µM VUAA1 activated MsexOrco as it does in different other species such as *A. gambiae, D. melanogaster, Culex quinquefasciatus, Harpegnatos saltator, Heliothis virescens* and *Ostrinia nubilalis* [31,40,49,50,52]. The small number of responding cells is very likely due to insufficient membrane

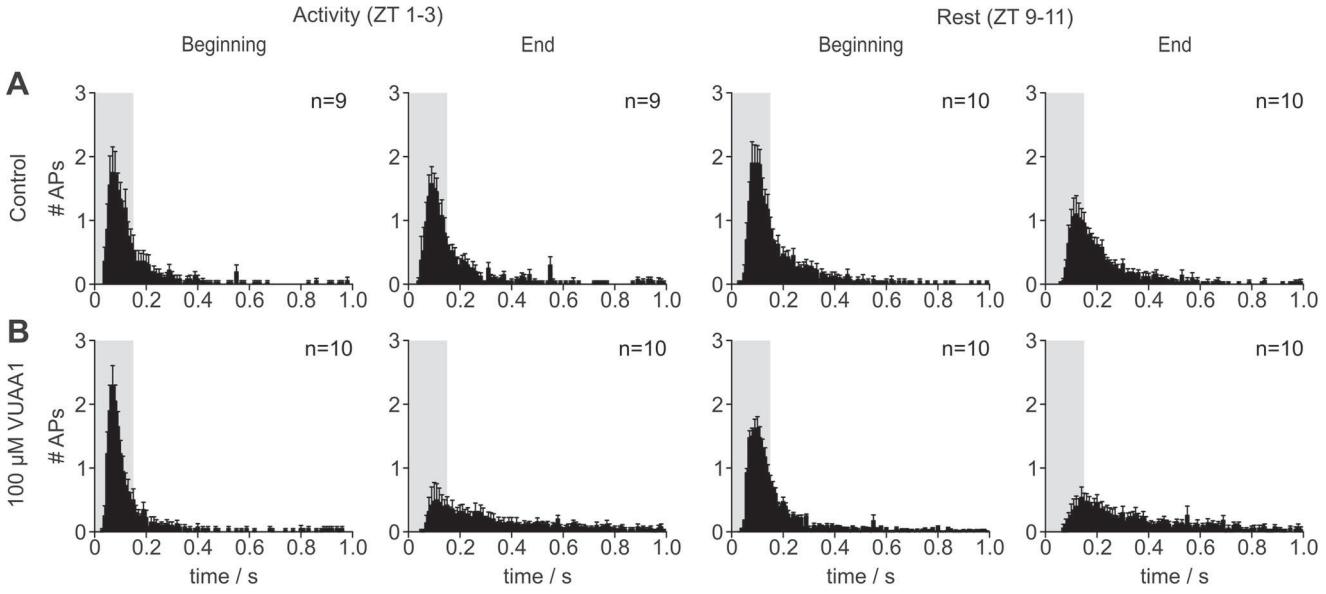

Figure 3. During the first 20 min of each recording VUAA1-dependent MsexOrco activation does not affect the first 150 ms or first 1000 ms of the pheromone response. Rather, MsexOrco-ion channel opening affects bombykal (BAL)-response kinetics at the time scale of minutes, at the last 20 min of the 2 h recording. (A,B) Post stimulus time histograms show the mean number of APs generated within the first 1000 ms after BAL stimulation (binsize = 10 ms). The number of APs within the first 150 ms (shaded area A,B) and the first 1000 ms did not change VUAA1-dependently during the first 20 minutes (beginning) of the recording. At the end of the tip-recordings (last 20 minutes) the pheromone responses shifted to a more tonic response pattern in the presence of 100 µM VUAA1 as compared to the beginning (see also Fig. S3).
doi:10.1371/journal.pone.0062648.g003

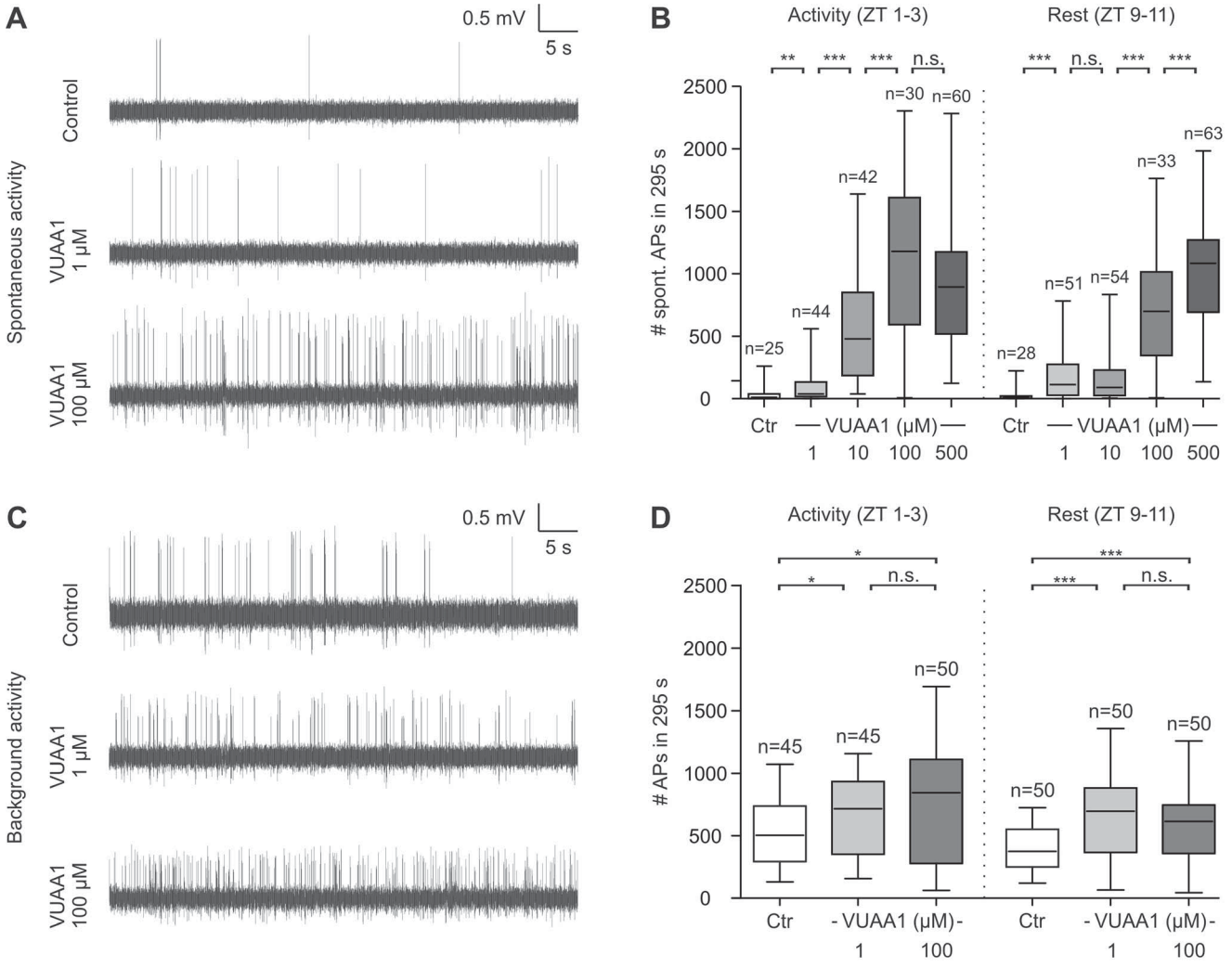

Figure 4. VUAA1- dependent MsexOrco activation increases spontaneous as well as background activity of olfactory receptor neurons (ORNs). Original recordings show spontaneous activity without previous BAL-stimulation (A) and background activity (C) after BAL-stimulation of bombykal- (BAL) sensitive ORNs (larger amplitude). Action potentials of smaller amplitude were generated by the second BAL-insensitive ORN. (B) Spontaneous activity was dose-dependently increased by VUAA1 stimulation, with lower VUAA1 concentrations required for saturation in the activity phase. (D) Lower VUAA1 concentrations increased the background activity already maximally during the first 20 min (beginning) of the recordings and more strongly than the spontaneous activity. Furthermore, MsexOrco appeared to express Zeitgebertime-dependent changes. Significant differences are indicated by asterisks (n.s. = not significant; *$P<0.05$, **$P<0.01$, ***$P<0.001$; Mann-Whitney test).
doi:10.1371/journal.pone.0062648.g004

insertion of MsexOrco in transiently as well as stably transfected cells. This indicates that in the heterologous vertebrate expression system important components necessary for efficient membrane targeting of MsexOrco are missing. It cannot be decided whether the increase in the VUAA1-dependent current after coexpression with MsexSNMP-1 and MsexOR-1, or MsexOR-4 (**Fig. 1C**) can be attributed to improved membrane insertion of MsexOrco, or to heteromultimerization and formation of ion channels with larger conductance. In summary, we conclude that VUAA1 is a suitable activator of MsexOrco ion channels.

MsexOrco does not Increase Bombykal Responses

Previous studies showed that Orco itself is not activated by odors in different species such as *D. melanogaster, A gambiae and C. quinquefasciatus* [24,27,28,31,40,50,55] and that VUAA1 binds to Orco directly increasing its ion channel open probability across species [31,40,49–52]. Therefore it was suggested that VUAA1 is an allosteric activator of possible OR-Orco heteromers, and that VUAA1 addition to the odor-sensitive sensillum should mimic an increase in odor concentration. Thus, VUAA1 and pheromone should act additively and non-competitively in opening the OR-Orco ion channel pore. If indeed MsexOR-MsexOrco heteromers form pheromone-gated ion channels responsible for the first pheromone-dependent inward current, infusion of VUAA1 should increase BAL-dependent receptor potentials and AP responses in *M. sexta*. Unexpectedly, this was not the case. Since neither the BAL-dependent SPA (**Fig. 2A, S1**), nor the phasic BAL-dependent AP response during the first ~25 (**Fig. 2B, S2A–D**), 150, and 1000 ms (**Fig. 3, S3**) during the first 20 min of the long-term tip-recordings increased VUAA1-dependently, it is very unlikely that MsexOR-MsexOrco heteromers form BAL-gated ion channels in *M. sexta*. This lack of a VUAA1 effect cannot be due to a saturation of the BAL response, since higher BAL concentrations employed previously resulted in dose-dependent increases of the pheromone response [41–44]. Since a 100-fold lower VUAA1

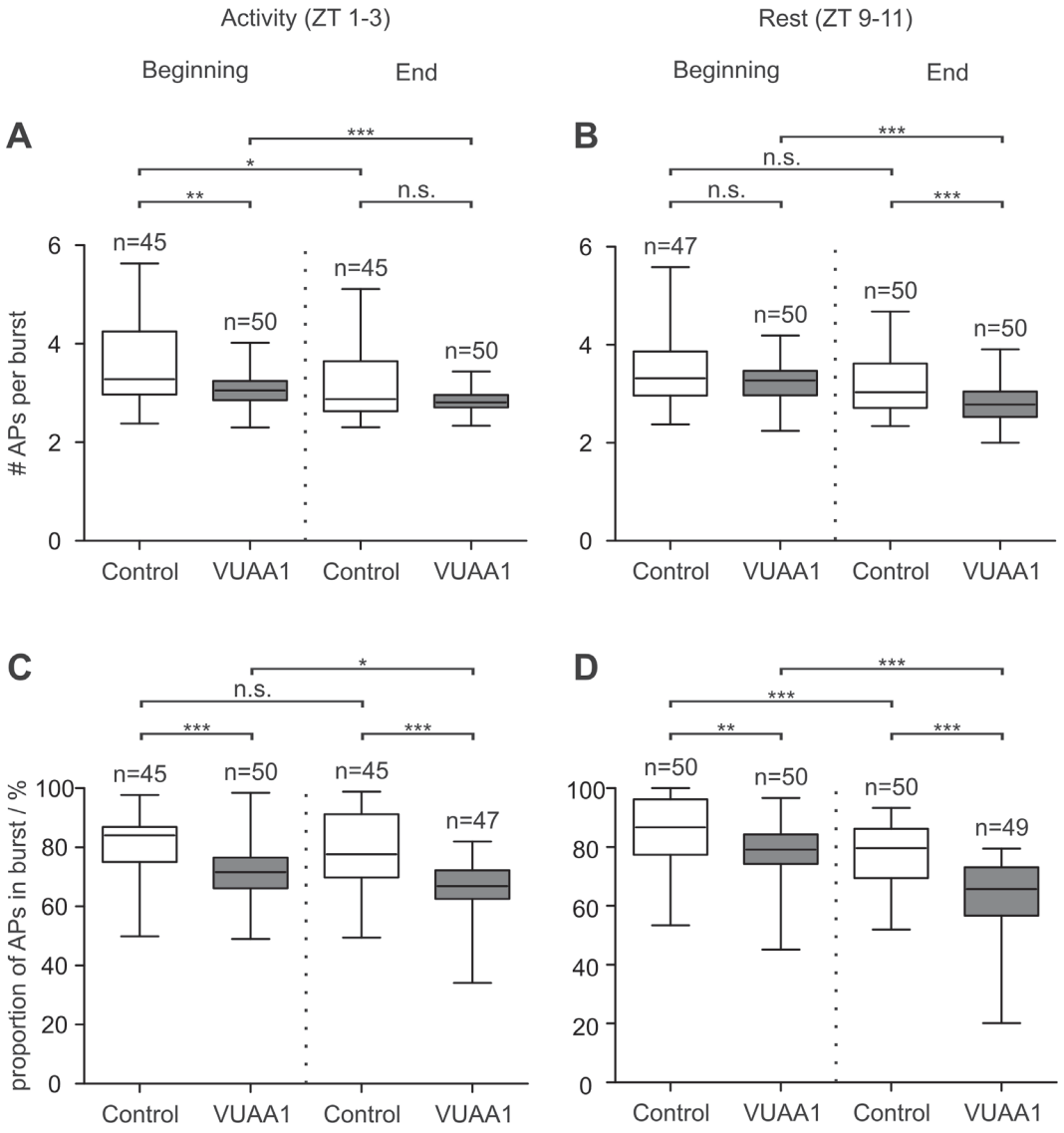

Figure 5. VUAA1-dependent MsexOrco activation affects bursting pattern of background activity. Comparison of the beginning (0–20 min) and end (100–120 min) of long term recordings showed a decrease of the number of action potentials (APs) per burst (**A,B**) as well as the percentage of APs in bursts (**C,D**) in the presence of 100 μM VUAA1. Furthermore, MsexOrco-dependent effects were mostly Zeitgebertime-dependent. Significant differences are indicated by asterisks (n.s. = not significant; *$P<0.05$, **$P<0.01$, ***$P<0.001$; Mann-Whitney test).
doi:10.1371/journal.pone.0062648.g005

concentration did not affect pheromone-dependent AP frequency (**Fig. 2B**) it is very unlikely that VUAA1 failed to activate MsexOR-MsexOrco due to adaptation. Furthermore, because VUAA1 dose-dependently increased the background and spontaneous activity of *M. sexta* ORNs (**Fig. 4, S4**) during the first 20 min of the tip-recordings, MsexOrco is sensitive to VUAA1 concentrations employed *in situ* as well as *in vitro* and the agonist successfully reached its target during this time window. Since VUAA1-dependent MsexOrco activation at all concentrations and at all ZTs tested never affected the SPA (**Fig. 2A, S1**) over the 2 h recording, MsexOrco does not appear to contribute to the BAL-dependent receptor potential. This assumption is consistent with the observation that Orco activation did not change the number of pheromone-dependent APs in the beginning of the tip-recordings (**Fig. 3, S3**). Nevertheless, MsexOrco activation significantly decreased the BAL-dependent phasic AP response during long-term tip-recordings with 100 μM VUAA1 (**Fig. S3**). This observation, together with a significant VUAA1-dependent latency increase (**Fig. 2C**) of the first BAL-dependent AP is reminiscent of cGMP-dependent adaptation observed previously [42]. This could indicate a sustained activation of a spontaneously opening ion channel in ORNs, which increases the intracellular cGMP levels Ca^{2+}-dependently and thus shifts the dose-response range of pheromone responsiveness to more adapted response ranges.

MsexOrco-activation by VUAA1 Affects Background Activity and Spontaneous Activity

As previously reported, Orco is involved in the generation of spontaneous activity in *D. melanogaster* and *A. gambiae in situ* [26,40,56,57]. Moreover, Orco was shown to form a leaky ion channel affecting spontaneous activity in different insect species such as in *D. melanogaster* and *A. gambiae* [27,28,35,40]. The same function could also be confirmed for MsexOrco *in situ* since VUAA1 significantly increased the spontaneous activity of the

non-stimulated BAL-sensitive ORNs (**Fig. 4A,B**). Furthermore, the VUAA1-dependent activation of spontaneous activity in ORNs, which never experienced pheromone stimulation before, was significantly different from VUAA1-dependent stimulation of background activity (**Fig. 4**). It is possible that pheromone-dependent metabotropic transduction cascades changed concentrations of intracellular messengers such as Ca^{2+} and cGMP, which then modified the open probability of MsexOrco as reported previously for Orco from *D. melanogaster* [28]. Furthermore, the VUAA1-dependent decrease in the percentage of APs belonging to bursts (**Fig. 5C, D**) correlated with the slowing of the response kinetics, which became more tonic with VUAA1 (**Fig. 3, S3**). This direct correlation between bursting behavior and pheromone response kinetics was also observed for octopamine application, which increased the number of APs in spontaneous bursts and sped up pheromone response kinetics as well as increased pheromone sensitivity [44]. Taken together, we believe these data indicate that in *M. sexta*, Orco is a spontaneously opening ion channel, which allows for spontaneous membrane potential oscillations in the absence of pheromone, rendering the cell sensitive to the timing of the input as prerequisite for temporal encoding. Pheromone then might increase the conductance of this possibly circadian clock-controlled Orco-pacemaker channel dose-dependently via pheromone-dependent metabotropic transduction cascades, which change intracellular second messenger levels. Thereby, response kinetics and sensitivity of pheromone responses might be modified Orco- and second messenger-dependently. Current experiments examine whether ZT-dependent differences in VUAA1 effects are due to circadian expression of MsexOrco and MsexOrco-dependent circadian changes of intracellular Ca^{2+} concentrations.

In summary, BAL transduction in *M. sexta* apparently involves a phospholipase Cβ-dependent metabotropic signal transduction cascade without evidence for the involvement of an additional MsexOrco-based ionotropic transduction cascade [33,36–38,41]. A multitude of different second messenger-gated ion channels, amongst them MsexOrco, regulates the pheromone response range and kinetics ZT- and dose-dependently allowing for gain control and differentiated behavioral responses [33]. More *in situ* studies are necessary to determine whether an Orco-based ionotropic mechanism plays a relevant role in odor transduction *in vivo* in other insects such as *D. melanogaster*.

Materials and Methods

Animals and Preparation

All experiments were performed on adult males of the hawkmoth *Manduca sexta* raised in breeding facilities at the University of Kassel as reported previously [43]. Animals were entrained to a 17 h:7 h light:dark cycle, where Zeitgebertime (ZT) 0 defines the beginning of the light phase and ZT 17 the beginning of the dark phase. Since *Manduca sexta* is a nocturnal insect species, mating behavior, male flight and oviposition occurs in the dark phase [58]. For further information regarding raising conditions and preparatory work see **SI Materials and Methods**.

Odorant Receptor Expression in Heterologous Systems

The odorant receptors (MsexOR-1, MsexOR-4), MsexOrco (= MsexOR-2) and sensory neuron membrane protein 1 (MsexSNMP-1) were identified previously [22,39,45]. The DNA was cloned into pcDNA3.1(-) expression vectors (Invitrogen) using standard molecular biology methods (**SI Materials and Methods; Tab. S1**). Human embryonic kidney cells (HEK 293, DSMZ) were grown on poly-L-lysine (0.01%, Sigma-Aldrich) coated coverslips. Further culture conditions and transient transfection were described by Wicher et al. [28]. Additionally, HEK 293 cells stably expressing MsexOrco were purchased from cytobox UG (Konstanz, Germany) and grown in cytobox^{TM} HEK select medium containing puromycin. Since the sensory neuron membrane protein 1 (SNMP-1) is coexpressed with pheromone receptors in moth ORNs [59–63] and SNMP-1 was shown to be required for pheromone detection in *D. melanogaster* [56,64] for some experiments, HEK 293 cells were transiently transfected with MsexSNMP-1 and MsexOR-1 or MsexOR-4.

Calcium Imaging

Calcium imaging experiments were performed on HEK 293 cells using Fura-2 [65] as calcium indicator. Cells were loaded by incubation in culture medium containing 2.5–5 μM of membrane permeable Fura-2 acetoxymethyl esters (Molecular Probes, Invitrogen) for 30–60 min at room temperature. Fura-2 was excited sequentially with wavelengths of 340 and 380 nm using a monochromator (Polychrom V, Till Photonics), coupled to an epifluorescence microscope (Axioskop FS, Zeiss, Jena, Germany) and controlled by an imaging control unit (ICU, Till Photonics). Cells were monitored using a 40× objective (LUMPlanFI/IR 40×/0,80W, Olympus) or a 10× objective (ACHROPLAN 10×/0,30W Ph1, Zeiss). Exposure times varied to achieve sufficient signal to background ratios for both excitation wavelengths. Emission for both excitation wavelengths was detected at 510 nm. Experiments lasted 5 min with a sampling interval of 5 s. VUAA1 (100 μl of 100 μM) was applied via pipette or via rapid solution changer (RSC, Bio-Logic, Claix, France) (**SI Materials and Methods**).

Tip-recordings

All recordings were performed at room temperature (19–22°C) in the end of the activity phase (ZT 1–3) and during the resting phase (ZT 9–11). A glass electrode filled with hemolymph Ringer was used as indifferent electrode and was inserted in the truncated end of the male's antenna. The recording electrode filled with sensillum lymph Ringer was slipped over the truncated sensillum [42]. The Orco agonist VUAA1 (1 μM or 100 μM) was applied passively via the sensillum lymph Ringer solution. Long-term tip-recordings lasted 2 h, recordings with 1 μM VUAA1 or spontaneous activity recordings lasted 20 min. Non-saturating, non-adapting pheromone stimulations of 50 ms duration with 1 μg BAL dissolved in 10 μl hexanol on filter paper were performed every 5 min [41,43]. Neuronal activity of the pheromone sensitive ORN between pheromone stimulations was recorded for 295 s (except the first 5 sec of the pheromone response) and was defined as background activity. Spontaneous activity of non-stimulated ORNs was measured in isolated moths not exposed to pheromone before. Spontaneous activity was recorded for the first 295 s under control conditions and if applicable subsequently from the same sensillum for another 3× 295 s in the presence of VUAA1 (1, 10, 100 or 500 μM). For further details see **SI Materials and Methods**.

Data Analysis and Statistics

Calcium imaging: Tillvision software (Version 4.5, Till Photonics) was employed to subtract background fluorescence, to define regions of interest (ROIs), and to calculate the ratio of fluorescence resulting from excitation at 340 nm and 380 nm (F_{340}/F_{380}). Only for the experiments with stably transfected HEK 293 cells the intracellular Ca^{2+} concentration was calculated on the basis of the measured fluorescence intensities as described before [28,65]. Mean change of the intracellular Ca^{2+} concentration ($\Delta[Ca^{2+}]_i$)

was determined from the area under the curve (AUC) over the time courses of the respective cells based on the Ca^{2+} concentration before VUAA1 application using Excel (2007, Microsoft Office). Matlab (Version R2012a, The MathWorks) was used to normalize imaging data and to determine the percentage of active cells (**Materials and Methods SI**).

All tip-recordings were analyzed using Spike2 software (version 7.01, Cambridge Electronic Design). The interval between two pheromone stimuli was divided into a direct stimulus response (5 s) and the following background activity (295 s). For statistics beginning (0–20 minutes) and end (100–120 minutes) of long-term tip-recordings were considered. The following parameters of the direct stimulus response were analyzed: The sensillum potential amplitude (SPA), defined as BAL-dependent negative deflection of the transepithelial potential, was evaluated as measure of the graded receptor potential. For statistical tests the SPA was normalized to the first data point of the recording. Since only the phasic component of the phasic-tonic BAL-response encodes stimulus quantity [41], the first 5 interspike intervals (~ the first 25 ms time window containing the first 6 APs) of the BAL response were analyzed as parameter for frequency encoding. To investigate temporal encoding the latency between the first AP after BAL stimulation and the onset of the SPA was determined. To examine encoding in the phasic-tonic response pattern the first 150 and 1000 ms after the onset of the BAL-dependent sensillum potential were analyzed and post stimulus time histograms (PSTHs, binwidth = 10 ms) were prepared for the beginning and the end of long-term tip-recordings. Analysis of the background activity was performed as follows: the number of APs was evaluated and the percentage of APs associated with bursts as well as the mean number of APs per burst was analyzed. A burst was defined as two or more APs with maximum interspike intervals of 50 ms.

All statistical tests were performed with Graphpad Prism (Version 5.01, Graphpad Software Inc.; **Tab. S2, S3, S4**). Shapiro-Wilk test was used to test for normality (not shown). Since the majority of data groups did not show a normal distribution all data groups were compared using Mann-Whitney test. The significance level $\alpha = 0.05$ was used for all tests. Compared data are presented as box plots, showing lower and upper quartile with median (box) and whiskers from minimum to maximum. Figures were generated with Graphpad Prism, Origin (Version 8.6) and Corel Draw (Version X3).

Supporting Information

Figure S1 VUAA1 does not increase sensillum potential amplitude (SPA).
(TIF)

Figure S2 VUAA1-dependent MsexOrco activation affects the threshold of pheromone-responses during the course of the 2 h-long recording, except during the first 20 min at the activity phase.
(TIF)

Figure S3 Orco agonist VUAA1 (100 μM) slows the kinetics of the bombykal (BAL) response.
(TIF)

Figure S4 VUAA1 increased background activity over the time course of the 2 h-long recordings.
(TIF)

Table S1 Primer sequences. Coding sequences are shown in capitals. If a restriction site was induced, the respective sequence and appropriate enzyme is indicated with fat letters. Abbreviations: for = forward primer, rev = reward primer.
(DOCX)

Table S2 Statistics for tip-recordings. Data groups were compared using Mann-Whitney-test ($\alpha = 0.05$). Corresponding *P*-values are shown.
(DOCX)

Table S3 Statistics for tip-recordings: Spontaneous activity. Data groups were compared using Mann-Whitney-test ($\alpha = 0.05$). Corresponding *P*-values are shown.
(DOCX)

Table S4 Medians of analyzed parameters in tip-recordings.
(DOCX)

Materials and Methods S1.
(DOCX)

Acknowledgements

We thank S. Kaltofen and S. Bucks for technical assistance, G. Kaschlaw and C. Sender for animal rearing as well as Dr. J. Weißflog and Dr. A. Svatoš for VUAA1 synthesis. Furthermore, we thank the reviewers (especially reviewer #1) for significant improvement of the manuscript.

Author Contributions

Commented on different stages of the manuscript: AN NWF BSH DW MS. Conceived and designed the experiments: AN NWF BSH DW MS. Performed the experiments: AN NWF LM PG. Analyzed the data: AN NWF LM AW DW. Wrote the paper: AN NWF MS.

References

1. Vosshall LB, Amrein H, Morozov PS, Rzhetsky A, Axel R (1999) A spatial map of olfactory receptor expression in the Drosophila antenna. Cell 96: 725–736.
2. Clyne PJ, Warr CG, Freeman MR, Lessing D, Kim J, et al. (1999) A novel family of divergent seven-transmembrane proteins: candidate odorant receptors in Drosophila. Neuron 22: 327–338.
3. Gao Q, Chess A (1999) Identification of candidate Drosophila olfactory receptors from genomic DNA sequence. Genomics 60: 31–39.
4. Stortkuhl KF, Kettler R (2001) Functional analysis of an olfactory receptor in Drosophila melanogaster. Proc Natl Acad Sci U S A 98: 9381–9385.
5. Hallem EA, Carlson JR (2006) Coding of Odors by a Receptor Repertoire. Cell 125: 143–160.
6. Altner H, Prillinger L (1980) Ultrastructure of invertebrate chemo-, thermo- and hygroreceptors and its functional significance. Int Rev Cytol 67: 69–139.
7. Stocker RF (2001) Drosophila as a focus in olfactory research: mapping of olfactory sensilla by fine structure, odor specificity, odorant receptor expression, and central connectivity. Microsc Res Tech 55: 284–296.
8. Benton R, Sachse S, Michnick SW, Vosshall LB (2006) Atypical membrane topology and heteromeric function of Drosophila odorant receptors in vivo. PLoS Biol 4: e20.
9. Wistrand M, Kall L, Sonnhammer EL (2006) A general model of G protein-coupled receptor sequences and its application to detect remote homologs. Protein Sci 15: 509–521.
10. Smart R, Kiely A, Beale M, Vargas E, Carraher C, et al. (2008) Drosophila odorant receptors are novel seven transmembrane domain proteins that can signal independently of heterotrimeric G proteins. Insect Biochem Mol Biol 38: 770–780.
11. Lundin C, Kall L, Kreher SA, Kapp K, Sonnhammer EL, et al. (2007) Membrane topology of the Drosophila OR83b odorant receptor. FEBS Lett 581: 5601–5604.
12. Tsitoura P, Andronopoulou E, Tsikou D, Agalou A, Papakonstantinou MP, et al. (2010) Expression and membrane topology of Anopheles gambiae odorant receptors in lepidopteran insect cells. PLoS ONE 5: e15428.
13. Vosshall LB, Wong AM, Axel R (2000) An olfactory sensory map in the fly brain. Cell 102: 147–159.

14. Hill CA, Fox AN, Pitts RJ, Kent LB, Tan PL, et al. (2002) G protein-coupled receptors in Anopheles gambiae. Science 298: 176–178.
15. Krieger J, Raming K, Dewer YM, Bette S, Conzelmann S, et al. (2002) A divergent gene family encoding candidate olfactory receptors of the moth Heliothis virescens. Eur J Neurosci 16: 619–628.
16. Krieger J, Klink O, Mohl C, Raming K, Breer H (2003) A candidate olfactory receptor subtype highly conserved across different insect orders. J Comp Physiol A Neuroethol Sens Neural Behav Physiol 189: 519–526.
17. Melo AC, Rutzler M, Pitts RJ, Zwiebel LJ (2004) Identification of a chemosensory receptor from the yellow fever mosquito, Aedes aegypti, that is highly conserved and expressed in olfactory and gustatory organs. Chem Senses 29: 403–410.
18. Pitts RJ, Fox AN, Zwiebel LJ (2004) A highly conserved candidate chemoreceptor expressed in both olfactory and gustatory tissues in the malaria vector Anopheles gambiae. Proc Natl Acad Sci U S A 101: 5058–5063.
19. Jones WD, Nguyen TA, Kloss B, Lee KJ, Vosshall LB (2005) Functional conservation of an insect odorant receptor gene across 250 million years of evolution. Curr Biol 15: R119–121.
20. Malpel S, Merlin C, Francois MC, Jacquin-Joly E (2008) Molecular identification and characterization of two new Lepidoptera chemoreceptors belonging to the Drosophila melanogaster OR83b family. Insect Mol Biol 17: 587–596.
21. Jordan MD, Anderson A, Begum D, Carraher C, Authier A, et al. (2009) Odorant receptors from the light brown apple moth (Epiphyas postvittana) recognize important volatile compounds produced by plants. Chem Senses 34: 383–394.
22. Patch HM, Velarde RA, Walden KK, Robertson HM (2009) A candidate pheromone receptor and two odorant receptors of the hawkmoth Manduca sexta. Chem Senses 34: 305–316.
23. Yang Y, Krieger J, Zhang L, Breer H (2012) The olfactory co-receptor Orco from the migratory locust (Locusta migratoria) and the desert locust (Schistocerca gregaria): identification and expression pattern. Int J Biol Sci 8: 159–170.
24. Neuhaus EM, Gisselmann G, Zhang W, Dooley R, Stortkuhl K, et al. (2005) Odorant receptor heterodimerization in the olfactory system of Drosophila melanogaster. Nat Neurosci 8: 15–17.
25. Vosshall LB, Hansson BS (2011) A unified nomenclature system for the insect olfactory coreceptor. Chem Senses 36: 497–498.
26. Larsson MC, Domingos AI, Jones WD, Chiappe ME, Amrein H, et al. (2004) Or83b encodes a broadly expressed odorant receptor essential for Drosophila olfaction. Neuron 43: 703–714.
27. Sato K, Pellegrino M, Nakagawa T, Vosshall LB, Touhara K (2008) Insect olfactory receptors are heteromeric ligand-gated ion channels. Nature 452: 1002–1006.
28. Wicher D, Schafer R, Bauernfeind R, Stensmyr MC, Heller R, et al. (2008) Drosophila odorant receptors are both ligand-gated and cyclic-nucleotide-activated cation channels. Nature 452: 1007–1011.
29. Nichols AS, Chen S, Luetje CW (2011) Subunit contributions to insect olfactory receptor function: channel block and odorant recognition. Chem Senses 36: 781–790.
30. Nakagawa T, Pellegrino M, Sato K, Vosshall LB, Touhara K (2012) Amino acid residues contributing to function of the heteromeric insect olfactory receptor complex. PLoS ONE 7: e32372.
31. Pask GM, Jones PL, Rutzler M, Rinker DC, Zwiebel LJ (2011) Heteromeric Anopheline odorant receptors exhibit distinct channel properties. PLoS ONE 6: e28774.
32. Nakagawa T, Vosshall LB (2009) Controversy and consensus: noncanonical signaling mechanisms in the insect olfactory system. Curr Opin Neurobiol 19: 284–292.
33. Stengl M (2010) Pheromone transduction in moths. Front Cell Neurosci 4: 133.
34. Deng Y, Zhang W, Farhat K, Oberland S, Gisselmann G, et al. (2011) The stimulatory Galpha(s) protein is involved in olfactory signal transduction in Drosophila. PLoS ONE 6: e18605.
35. Sargsyan V, Getahun MN, Llanos SL, Olsson SB, Hansson BS, et al. (2011) Phosphorylation via PKC Regulates the Function of the Drosophila Odorant Co-Receptor. Front Cell Neurosci 5: 5.
36. Stengl M (1994) Inositol-trisphosphate-dependent calcium currents precede cation currents in insect olfactory receptor neurons in vitro. J Comp Physiol A 174: 187–194.
37. Stengl M (1993) Intracellular-messenger-mediated cation channels in cultured olfactory receptor neurons. J Exp Biol 178: 125–147.
38. Stengl M, Hatt H, Breer H (1992) Peripheral processes in insect olfaction. Annu Rev Physiol 54: 665–681.
39. Grosse-Wilde E, Stieber R, Forstner M, Krieger J, Wicher D, et al. (2010) Sex-Specific Odorant Receptors of the Tobacco Hornworm Manduca Sexta. Front Cell Neurosci 4.
40. Jones PL, Pask GM, Rinker DC, Zwiebel LJ (2011) Functional agonism of insect odorant receptor ion channels. Proc Natl Acad Sci U S A 108: 8821–8825.
41. Dolzer J, Fischer K, Stengl M (2003) Adaptation in pheromone-sensitive trichoid sensilla of the hawkmoth Manduca sexta. J Exp Biol 206: 1575–1588.
42. Flecke C, Dolzer J, Krannich S, Stengl M (2006) Perfusion with cGMP analogue adapts the action potential response of pheromone-sensitive sensilla trichoidea of the hawkmoth Manduca sexta in a daytime-dependent manner. J Exp Biol 209: 3898–3912.
43. Flecke C, Nolte A, Stengl M (2010) Perfusion with cAMP analogue affects pheromone-sensitive trichoid sensilla of the hawkmoth Manduca sexta in a time-dependent manner. J Exp Biol 213: 842–852.
44. Flecke C, Stengl M (2009) Octopamine and tyramine modulate pheromone-sensitive olfactory sensilla of the hawkmoth Manduca sexta in a time-dependent manner. J Comp Physiol A Neuroethol Sens Neural Behav Physiol 195: 529–545.
45. Grosse-Wilde E, Kuebler LS, Bucks S, Vogel H, Wicher D, et al. (2011) Antennal transcriptome of Manduca sexta. Proc Natl Acad Sci U S A 108: 7449–7454.
46. German PF, van der Poel S, Carraher C, Kralicek AV, Newcomb RD (2013) Insights into subunit interactions within the insect olfactory receptor complex using FRET. Insect Biochem Mol Biol 43: 138–145.
47. Schuckel J, Siwicki KK, Stengl M (2007) Putative circadian pacemaker cells in the antenna of the hawkmoth Manduca sexta. Cell Tissue Res 330: 271–278.
48. Schendzielorz T, Peters W, Boekhoff I, Stengl M (2012) Time of day changes in cyclic nucleotides are modified via octopamine and pheromone in antennae of the Madeira cockroach. J Biol Rhythms 27: 388–397.
49. Jones PL, Pask GM, Romaine IM, Taylor RW, Reid PR, et al. (2012) Allosteric antagonism of insect odorant receptor ion channels. PLoS ONE 7: e30304.
50. Chen S, Luetje CW (2012) Identification of new agonists and antagonists of the insect odorant receptor co-receptor subunit. PLoS ONE 7: e36784.
51. Bohbot JD, Dickens JC (2012) Odorant receptor modulation: ternary paradigm for mode of action of insect repellents. Neuropharmacology 62: 2086–2095.
52. Taylor RW, Romaine IM, Liu C, Murthi P, Jones PL, et al. (2012) Structure-activity relationship of a broad-spectrum insect odorant receptor agonist. ACS Chem Biol 7: 1647–1652.
53. Pask GM, Bobkov YV, Corey EA, Ache BW, Zwiebel LJ (2013) Blockade of Insect Odorant Receptor Currents by Amiloride Derivatives. Chem Senses.
54. Röllecke K, Werner M, Hatt H, Gisselmann G. Characterization of Blockers and Modulators of Insect Odorant Receptors; 2011; Göttingen.
55. Elmore T, Ignell R, Carlson JR, Smith DP (2003) Targeted mutation of a Drosophila odor receptor defines receptor requirement in a novel class of sensillum. J Neurosci 23: 9906–9912.
56. Benton R, Vannice KS, Vosshall LB (2007) An essential role for a CD36-related receptor in pheromone detection in Drosophila. Nature 450: 289–293.
57. Su CY, Menuz K, Reisert J, Carlson JR (2012) Non-synaptic inhibition between grouped neurons in an olfactory circuit. Nature 492: 66–71.
58. Sasaki M, Riddiford LM (1984) Regulation of reproductive behaviour and egg maturation in the tobacco hawk moth, Manduca sexta Physiological Entomology 9: 315–327.
59. Rogers ME, Krieger J, Vogt RG (2001) Antennal SNMPs (sensory neuron membrane proteins) of Lepidoptera define a unique family of invertebrate CD36-like proteins. J Neurobiol 49: 47–61.
60. Forstner M, Gohl T, Gondesen I, Raming K, Breer H, et al. (2008) Differential expression of SNMP-1 and SNMP-2 proteins in pheromone-sensitive hairs of moths. Chem Senses 33: 291–299.
61. Rogers ME, Steinbrecht RA, Vogt RG (2001) Expression of SNMP-1 in olfactory neurons and sensilla of male and female antennae of the silkmoth Antheraea polyphemus. Cell Tissue Res 303: 433–446.
62. Vogt RG, Miller NE, Litvack R, Fandino RA, Sparks J, et al. (2009) The insect SNMP gene family. Insect Biochem Mol Biol 39: 448–456.
63. Rogers ME, Sun M, Lerner MR, Vogt RG (1997) Snmp-1, a novel membrane protein of olfactory neurons of the silk moth Antheraea polyphemus with homology to the CD36 family of membrane proteins. J Biol Chem 272: 14792–14799.
64. Jin X, Ha TS, Smith DP (2008) SNMP is a signaling component required for pheromone sensitivity in Drosophila. Proc Natl Acad Sci U S A 105: 10996–11001.
65. Grynkiewicz G, Poenie M, Tsien RY (1985) A new generation of Ca2+ indicators with greatly improved fluorescence properties. J Biol Chem 260: 3440–3450.

Supporting information

SI Materials and Methods

Animals

Hatched larvae were raised on artificial diet [modified after 1]. The adult stages were fed with a sugar solution offered in reaction vessels enclosed in pseudo-flowers made of filter paper treated with a synthetic blend of odors [modified after 2]. All *M. sexta* stages were kept at 24-27 °C and 40-60 % relative humidity in a 17h:7h light:dark cycle. Male pupae were isolated and used for experiments 1-2 days after eclosion. Experimental animals were fixated in a teflon holder with one antenna fixed with dental wax (Boxing wax, Sybron/Kerr, Romulus, MI, USA).

Odorant receptor expression in heterologous systems

Antennal mRNA was reverse transcribed using the Superscript II Mix (Invitrogen, Carlsbad, CA, USA). The resulting cDNA was used as template to amplify respective coding sequences for MsexOrco, MsexOR-1, MsexOR-4 and MsexSNMP-1 via PCR, adding suitable restriction sites outside the coding sequence (for primers see **Tab. S1**). PCR products were cloned into pCR®II-TOPO® vectors and transformed into *E. coli* (One Shot® Top10 competent cells, Invitrogen). Plasmids were isolated (QIAprep Spin MiniPrep Kit) and treated with suitable restriction enzymes (NEB, Ipswich, MA). Fragments were gel-purified and subcloned into the pcDNA3.1(-) expression vector (Invitrogen). After further replication in *E. coli* the vector was isolated (QIAGEN Plasmid Maxi Kit) and stored at -20 °C.

Solutions

Sensillum lymph Ringer (in mM: KCl, 6.4; $MgCl_2$, 12.0; $CaCl_2$, 1.0; NaCl, 12.0; HEPES, 10.0; D-glucose, 354.0) and hemolymph Ringer (in mM: KCl, 171.9; $MgCl_2$, 3.0; $CaCl_2$, 1.0; NaCl, 25.0; HEPES, 10.0; D-glucose, 22.5) were adjusted to pH 6.5. The osmolarity was adjusted with mannitol to 475 mOsmol/l for sensillum lymph Ringer and 450 mOsmol/l for hemolymph Ringer. Ringer solution for HEK 293 cells (in mM: NaCl, 135; KCl, 5; $MgCl_2$, 1; $CaCl_2$, 1; HEPES, 10; D-glucose, 10) was adjusted to pH 7.4.

The Orco agonist VUAA1 [3] N-(4-ethylphenyl)-2-((4-ethyl-5-(3-pyridinyl)-4H-1,2,4-triazol-3-yl)thio)acetamide was synthesized by the Research Group Mass Spectrometry/Proteomics (Max Planck Institute for Chemical Ecology, Jena,

Germany). The substance was dissolved in dimethyl sulfoxide (DMSO) at a concentration of 100 mM and stored at -20°C. For experiments VUAA1 was diluted in the respective Ringer solution. VUAA1 working solution, bath ringer solution for calcium imaging as well as the control hemolymph Ringer solution contained 0.1 % DMSO.

Stimulation with pheromone

Charcoal-filtered and moistened air streamed into a Clampex software-controlled solenoid valve (PA 202 004 P, Staiger, Erligheim, Germany) directing the air into one of two air branches. One branch of the perfusion system supplied the recording site with a continuous stream of clean, humidified air. The second branch passed a valve-controlled glass cartridge with a filter paper loaded with 1 µg bombykal (E,Z-10,12-hexadecadienal; BAL) dissolved in 10 µl *n*-hexan (Merck, Frankfurt, Germany). The BAL was generously provided by Dr. T. Christensen (University of Tucson, AZ, USA) and Dr. J. Krieger (University of Hohenheim, Germany). Pheromone stimuli (50 ms) were delivered every 5 min to avoid adaptation or depletion of pheromone. Released pheromone was removed quickly by a vacuum system installed directly below the mounted moth. One tip-recording encompassed 24 stimulations and lasted for 2 h.

Data Analysis

Calcium Imaging: Regions of interest (ROIs) were defined with Tillvision software by marking the profile of each cell. If the number of cells was far higher than 100, the ROIs were selected randomly and limited to 100. For each ROI the average ratio was calculated. Mean change of the intracellular Ca^{2+} concentration ($\Delta[Ca^{2+}]_i$) for the respective cells was determined from the area under the curve (AUC) over the time courses after normalization to $[Ca^{2+}]_i$ before VUAA1 application. Each AUC segment between two data points was calculated using the trapezoid method. AUC segments for the whole time course were summed and divided by the number of segments (n-1) multiplied by the framesize ($t_{j+1} - t_j$).

$$AUC = \frac{1}{2}\sum_{j=1}^{n-1}(([Ca^{2+}]_i)_j + ([Ca^{2+}]_i)_{j+1})(t_{j+1} - t_j)$$

$$mean\Delta([Ca^{2+}]_i) = \frac{AUC}{(n-1)(t_{j+1} - t_j)}$$

Further analysis was performed with Matlab (version R2012a, The MathWorks). First data (i.e. F_{340}/F_{380}-ratios for each cell) was normalized by calculating the mean of the first ten values of a measurement and the percentage deviation of the mean for each normalized value was calculated. Then the percentage of active cells for each experiment was determined. Cells were considered active, if the ratio exceeded the 20-fold standard deviation of the values measured before application. We

discriminated between Orco positive cells (i.e. transfected with Msex-Orco and optionally cotransfected with a pheromone receptor candidate (MsexOR-1 or MsexOR-4) and/or MsexSNMP-1) and Orco negative cells (optionally transfected with MsexOR-1, MsexOR-4 and/or MsexSNMP-1, but not with Msex-Orco).

Tip-recordings: The electrophysiological response of the olfactory receptor neuron to a stimulus was recorded continuously for 5 s with a sampling rate of 20 kHz (Clampex 8, Molecular Devices, Sunnyvale, CA, USA). To analyze the sensillum potential amplitude the signal was low-pass filtered (cutoff frequency: 50 Hz; with median filter: time constant = 0.05 ms; smooth process: time constant= 0.01). For evaluating the AP frequency a high-pass filter with a cutoff frequency of 150 Hz was used.

Background activity between two stimuli and spontaneous activity without stimulation were recorded discontinuously for 295 seconds (Clampex 8, fixed length events of 12.75 ms) with a sampling rate of 19.6 kHz (Clampex 8, fixed length events) for each trigger event. As shown by Dolzer et al. [4] in tip-recordings two types of APs could be distinguished according to their amplitude, with the larger amplitude cell being the BAL-sensitive cell and the smaller amplitude cell being sensitive for another component of the pheromone blend.

References

1. Bell RA, Joachim FG (1976) Techniques for rearing laboratory colonies of tobacco hornworms and pink bollworms. Ann entomol Coc Amer 69: 365-373.
2. Riffell JA, Lei H, Christensen TA, Hildebrand JG (2009) Characterization and coding of behaviorally significant odor mixtures. Curr Biol 19: 335-340.
3. Jones PL, Pask GM, Rinker DC, Zwiebel LJ (2011) Functional agonism of insect odorant receptor ion channels. Proc Natl Acad Sci U S A 108: 8821-8825.
4. Dolzer J, Krannich S, Fischer K, Stengl M (2001) Oscillations of the transepithelial potential of moth olfactory sensilla are influenced by octopamine and serotonin. J Exp Biol 204: 2781-2794.

SI Figures and Tables

Figure S1. VUAA1 does not increase sensillum potential amplitude (SPA). (A,B) The maximum SPA remained unchanged by VUAA1- dependent MsexOrco activation over the 2 h time course of recordings. **(C,D)** Comparison of the first and last 20 minutes (beginning and end; shaded areas in A,B) of the recordings revealed no significant change for the SPA in the presence of VUAA1 (100 µM) (n.s. = not significant, Mann-Whitney-Test).

Figure S2. VUAA1-dependent MsexOrco activation affects the threshold of pheromone-responses during the course of the 2 h-long recording, except during the first 20 min at the activity phase. (A,B) Time course of the AP frequency for recordings during activity and rest. Shaded areas show the first and last 20 minutes of the recordings (beginning and end). **(C,D)** VUAA1 infusion (100 µM) decreased bombykal (BAL)-dependent action potential frequency (first 6 APs) continuously during the 2 h recordings. **(E,F)** Also, the delay of the first AP of BAL responses increased with VUAA1. Significant differences are indicated by asterisks (n.s. = not significant; *P < 0.05, **P < 0.01, ***P < 0.001; Mann-Whitney test).

Figure S3. Orco agonist VUAA1 (100 µM) slows the kinetics of the bombykal (BAL) response. The BAL responses shift from a phasic to a more tonic response pattern. In the first 20 minutes (beginning) of all tip-recordings VUAA1 never affected BAL sensitivity during the first 150 ms **(A,B)** and 1000 ms **(C,D)**. In the last 20 minutes (end) of the tip-recordings the BAL responses shifted to a more tonic response pattern in the presence of VUAA1. Significant differences are indicated by asterisks (n.s. = not significant; *P < 0.05, **P < 0.01, ***P < 0.001; Mann-Whitney test).

Figure S4. VUAA1 increased background activity over the time course of the 2 h-long recordings. (A,B) Time course of the background activity for recordings during activity and rest. Shaded areas show beginning (first 20 minutes) and end (last 20 minutes) of the recordings. VUAA1-dependent MsexOrco activation affected background activity already within the first bin (295 s) of the recordings. **(C,D)** Decrease of the background activity in controls was counteracted by VUAA1. In the first as well as the last 20 minutes VUAA1 increased background activity significantly (n.s. = not significant; ***P < 0.001; Mann-Whitney test).

Table S1. Primer sequences. Coding sequences are shown in capitals. If a restriction site was induced, the respective sequence and appropriate enzyme is indicated with fat letters. Abbreviations: for=forward primer, rev=reward primer.

Table S2. Statistics for tip-recordings. Data groups were compared using Mann-Whitney-test (α=0.05). Corresponding *P*-values are shown.

Table S3. Statistics for tip-recordings: Spontaneous activity. Data groups were compared using Mann-Whitney-test (α=0.05). Corresponding *P*-values are shown.

161 **Table S4. Medians of analyzed parameters in tip-recordings.**

Figure_ S1

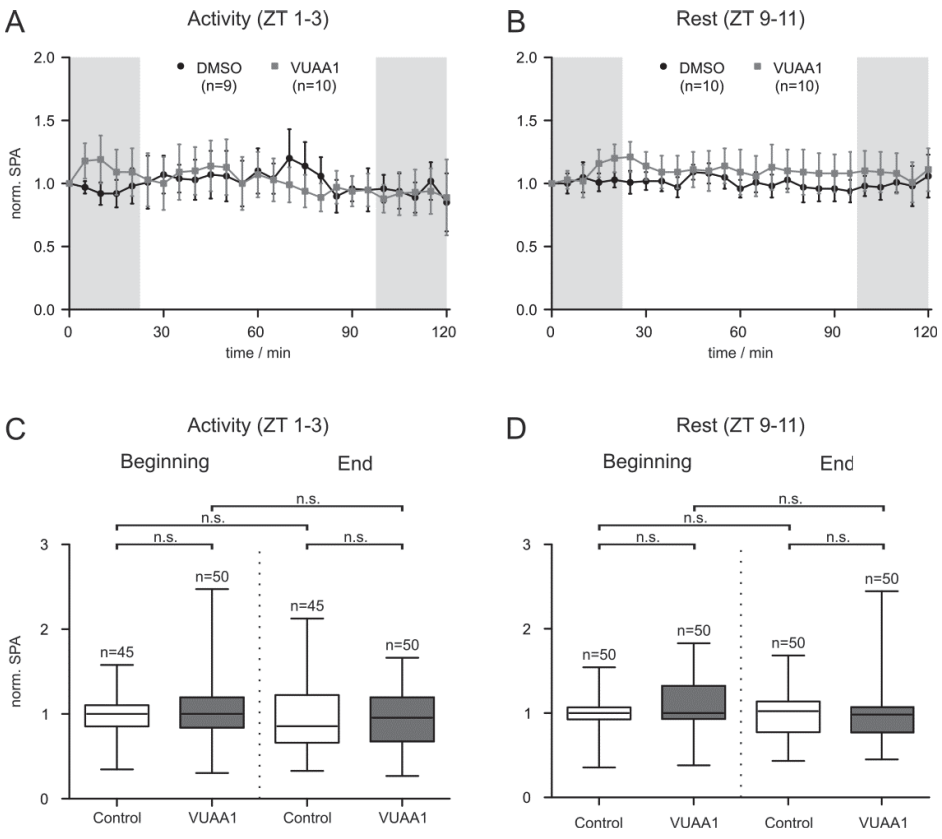
A
Activity (ZT 1-3)
DMSO (n=9)
VUAA1 (n=10)
norm. SPA
time / min
B
Rest (ZT 9-11)
DMSO (n=10)
VUAA1 (n=10)
time / min
C
Activity (ZT 1-3)
Beginning
End
n.s.
n=45
n=50
n=45
n=50
Control
VUAA1
Control
VUAA1
D
Rest (ZT 9-11)
Beginning
End
n=50
n=50
n=50
n=50

Figure_ S2

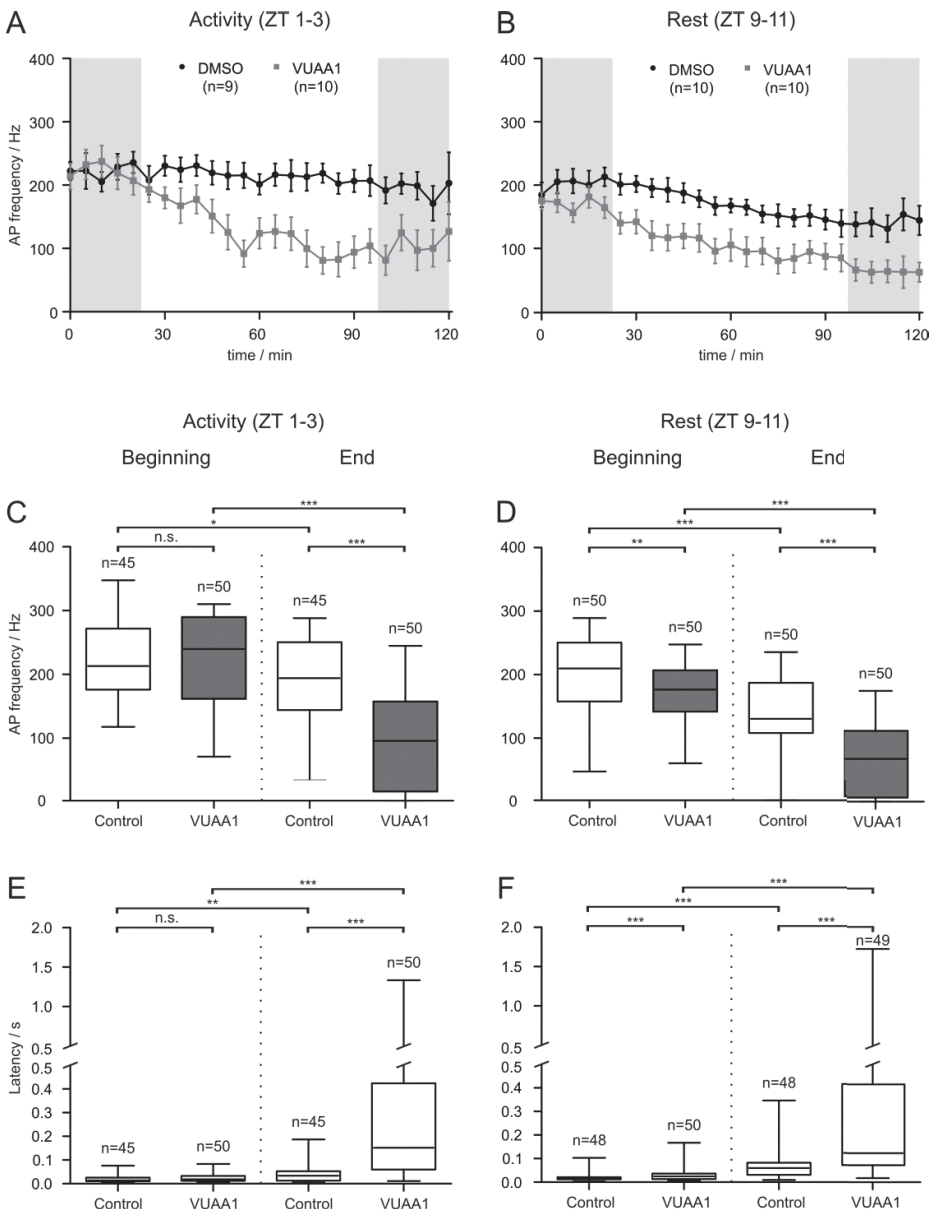
A
Activity (ZT 1-3)
DMSO (n=9)
VUAA1 (n=10)
AP frequency / Hz
time / min
B
Rest (ZT 9-11)
DMSO (n=10)
VUAA1 (n=10)
time / min
Activity (ZT 1-3)
Beginning
End
Rest (ZT 9-11)
Beginning
End
C
D
E
F
Latency / s
n.s.
Control
VUAA1

Figure_ S3

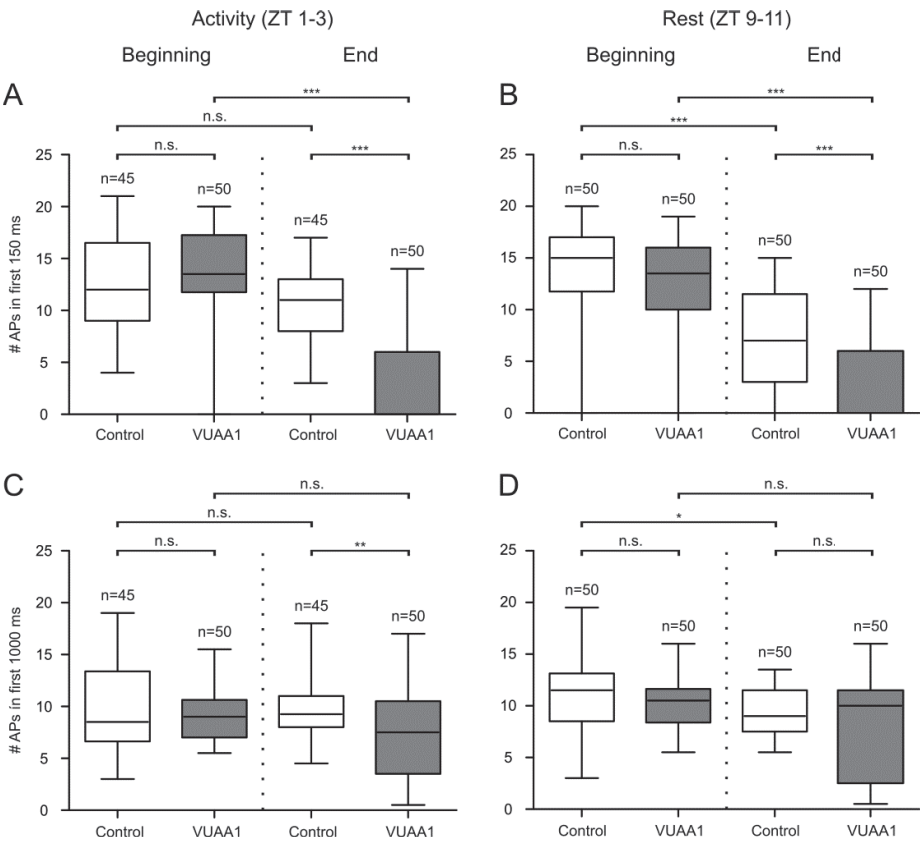
Activity (ZT 1-3)
Rest (ZT 9-11)
Beginning
End
A
B
C
D
APs in first 150 ms
APs in first 1000 ms
n.s.
***
**
*
n=45
n=50
Control
VUAA1

Figure_ S4

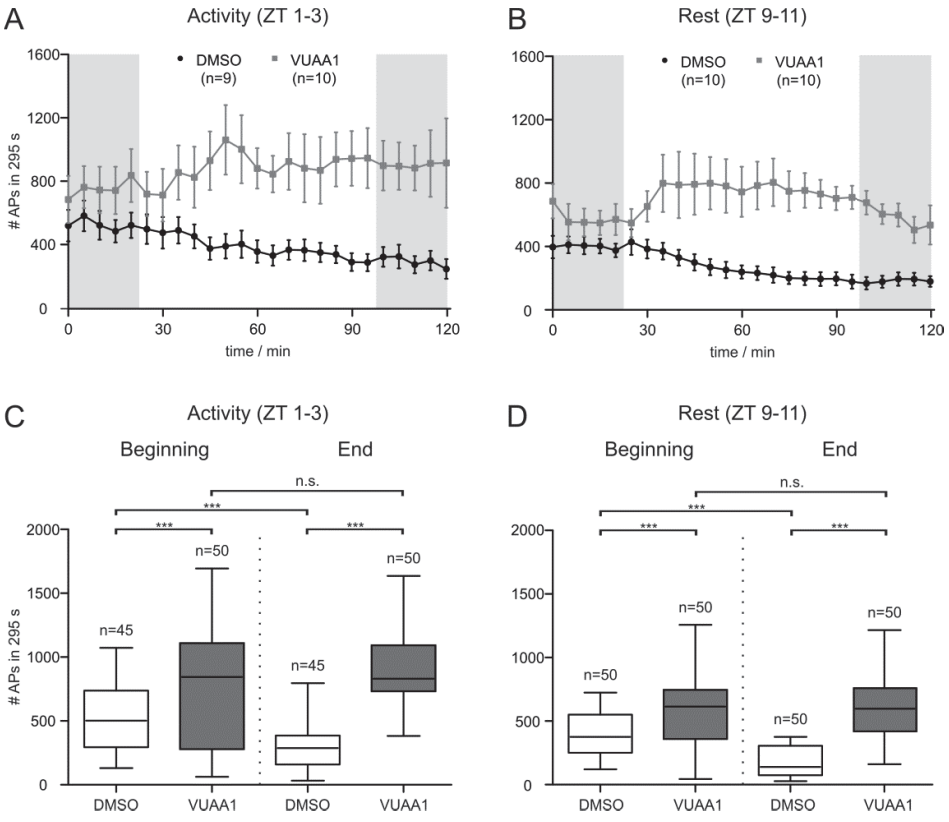
A
Activity (ZT 1-3)
DMSO (n=9)
VUAA1 (n=10)
APs in 295 s
time / min
B
Rest (ZT 9-11)
DMSO (n=10)
VUAA1 (n=10)
time / min
C
Activity (ZT 1-3)
Beginning
End
n.s.
***
n=45
n=50
DMSO
VUAA1
D
Rest (ZT 9-11)
Beginning
End

Table _S1

Primer name	Primer sequence
MsexOrco **BamHI** for	cgc **gga tcc** ATG ACC ATG CTT CTG CGG AA
MsexOrco **EcoRI** rev	ccg **gaa ttc** CTA TTT CAG CTG CAC CAA C
MsexOR-1 **KpnI** for	cc **ggt acc** ATG ATA TTT ATG GAC GAT CCT CTA TCA AAG
MsexOR-1 **XhoI** rev	ga **ctc gag** TTA GTT AGA AAC GGT GCG AAG AAA TG
MsexOR-4 **KpnI** for	cc **ggt acc** ATG AAG TTT TTT GTA GAC GGC AGC GAA ATA
MsexOR-4 **XhoI** rev	ga **ctc gag** TTA GCT CTC ATC TTT GGC GAT TGT TTG A
MsexSNMP-1 for	ATG CGG CTG GCA AGG GGA ATT AAG
MsexSNMP-1 rev	TTA CAT GTT GAT TTT TGG AGG CTC ATG AC

Table _S2

	Data groups		SPA	AP frequency	Latency	# APs 0-150	# APs 0-1000	Background activity	% of APs in bursts	# APs per burst
begin vs. begin	control ZT 1-3	1 µM VUAA ZT 1-3	0.855	0.572	0.191	0.898	0.124	0.040	0.001	0.044
	control ZT 1-3	100 µM VUAA ZT 1-3	0.340	0.694	0.052	0.146	0.484	0.012	< 0.001	0.002
	1 µM VUAA ZT 1-3	100 µM VUAA ZT 1-3	0.263	0.857	0.617	0.068	0.333	0.217	0.130	0.363
	control ZT 9-11	1 µM VUAA ZT 9-11	0.779	0.710	0.008	0.620	0.002	< 0.001	< 0.001	0.004
	control ZT 9-11	100 µM VUAA ZT 9-11	0.381	0.002	0.001	0.097	0.113	0.001	0.001	0.205
	1 µM VUAA ZT 9-11	100 µM VUAA ZT 9-11	0.474	0.001	0.136	0.124	0.059	0.331	0.001	0.010
	control ZT 1-3	control ZT 9-11	0.629	0.133	0.905	0.132	0.172	0.017	0.023	0.882
	1 µM VUAA ZT 1-3	1 µM VUAA ZT 9-11	0.383	0.013	0.342	0.035	0.173	0.704	0.398	0.137
	100 µM VUAA ZT 1-3	100 µM VUAA ZT 9-11	0.893	0.000	0.143	0.179	0.013	0.032	< 0.001	0.005
begin vs. end	control ZT 1-3	control ZT 1-3	0.796	0.039	0.002	0.134	0.693	< 0.001	0.693	0.014
	100 µM VUAA ZT 1-3	100 µM VUAA ZT 1-3	0.194	< 0.001	< 0.001	< 0.001	0.067	0.273	0.030	< 0.001
	control ZT 9-11	control ZT 9-11	0.904	< 0.001	< 0.001	< 0.001	0.015	< 0.001	0.000	0.050
	100 µM VUAA ZT 9-11	100 µM VUAA ZT 9-11	0.145	< 0.001	< 0.001	< 0.001	0.103	0.918	< 0.001	< 0.001
end vs. end	control ZT 1-3	100 µM VUAA ZT 1-3	0.979	< 0.001	< 0.001	< 0.001	0.007	< 0.001	< 0.001	0.387
	control ZT 9-11	100 µM VUAA ZT 9-11	0.657	< 0.001	< 0.001	< 0.001	0.344	< 0.001	< 0.001	0.001
	control ZT 1-3	control ZT 9-11	0.393	< 0.001	0.000	< 0.001	0.798	0.004	0.663	0.417
	100 µM VUAA ZT 1-3	100 µM VUAA ZT 9-11	0.459	0.055	0.953	0.943	0.382	< 0.001	0.348	0.387

Table_S3

Data groups		*P*-Value
control ZT 1-3	1 µM VUAA ZT 1-3	0.001
1 µM VUAA ZT 1-3	10 µM VUAA ZT 1-3	< 0.001
10 µM VUAA ZT 1-3	100 µM VUAA ZT 1-3	< 0.001
100 µM VUAA ZT 1-3	500 µM VUAA ZT 1-3	0.075
control ZT 9-11	1 µM VUAA ZT 9-11	< 0.001
1 µM VUAA ZT 9-11	10 µM VUAA ZT 9-11	0.780
10 µM VUAA ZT 9-11	100 µM VUAA ZT 9-11	< 0.001
100 µM VUAA ZT 9-11	500 µM VUAA ZT 9-11	< 0.001

Table _S4

	Data groups	norm. SPA	AP frequency / Hz	Latency / s	# APs 0-150	# APs 0-1000	Background activity / # APs in 295 s	% of APs in bursts	# APs per burst	Spont. Activity / # APs in 295 s
Begin	Control ZT 1-3	1.00	213.0	0.014	12.0	17.0	503.0	84.08	3.284	11
	1 µM VUAA1 ZT 1-3	1.00	241.4	0.016	13.0	16.0	715.0	74.17	3.103	38
	10 µM VUAA1 ZT 1-3	-	-	-	-	-	-	-	-	477.5
	100 µM VUAA ZT 1-3	1.00	239.9	0.018	13.5	18.0	844.5	71.64	3.052	1178
	500 µM VUAA ZT 1-3	-	-	-	-	-	-	-	-	894
	Control ZT 9-11	1.00	209.7	0.015	15.0	23.0	375.0	86.73	3.319	11
	1 µM VUAA1 ZT 9-11	1.00	206.8	0.020	15.0	18.5	696.0	70.95	2.908	113
	10 µM VUAA1 ZT 9-11	-	-	-	-	-	-	-	-	91
	100 µM VUAA1 ZT 9-11	1.00	176.6	0.025	13.5	21.0	614.0	79.11	3.273	698
	500 µM VUAA1 ZT 9-11	-	-	-	-	-	-	-	-	1083
End	Control ZT 1-3	0.86	194.3	0.034	11.0	18.5	288.0	77.63	2.879	-
	100 µM VUAA1 ZT 1-3	0.96	95.7	0.152	0.0	15.0	831.5	66.86	2.812	-
	Control ZT 9-11	1.02	130.4	0.060	7.0	18.0	139.5	79.60	3.034	-
	100 µM VUAA1 ZT 9-11	0.98	67.5	0.124	0.0	20.0	598.0	65.74	2.785	-

Manuscript IV

Calmodulin modulates insect odorant receptor function

Cell Calcium 55 (2014) 191–199

Contents lists available at ScienceDirect

Cell Calcium

journal homepage: www.elsevier.com/locate/ceca

Calmodulin modulates insect odorant receptor function

Latha Mukunda, Fabio Miazzi, Sabine Kaltofen, Bill S. Hansson, Dieter Wicher*

Max Planck Institute for Chemical Ecology, Department Evolutionary Neuroethology, Hans-Knöll-St. 8, D-07745 Jena, Germany

ARTICLE INFO

Article history:
Received 14 November 2013
Received in revised form 14 February 2014
Accepted 14 February 2014
Available online 23 February 2014

Keywords:
Drosophila
Odorant receptor
Orco
Olfactory sensory neuron
Calcium imaging

ABSTRACT

Insect odorant receptors (ORs) are heteromeric complexes of an odor-specific receptor protein (OrX) and a ubiquitous co-receptor protein (Orco). The ORs operate as non-selective cation channels, also conducting Ca^{2+} ions. The Orco protein contains a conserved putative calmodulin (CaM)-binding motif indicating a role of CaM in its function. Using Ca^{2+} imaging to monitor OR activity we investigated the effect of CaM inhibition on the function of OR proteins. Ca^{2+} responses elicited in *Drosophila* olfactory sensory neurons by stimulation with the synthetic OR agonist VUAA1 were reduced and prolonged by CaM inhibition with the potent antagonist W7 but not with the weak antagonist W5. A similar effect was observed for Orco proteins heterologously expressed in CHO cells when CaM was inhibited with W7, trifluoperazine or chlorpromazine, or upon overexpression of CaM-EF-hand mutants. With the Orco CaM mutant bearing a point mutation in the putative CaM site (K339N) the Ca^{2+} responses were akin to those obtained for wild type Orco in the presence of W7. There was no uniform effect of W7 on Ca^{2+} responses in CHO cells expressing complete ORs (Or22a/Orco, Or47a/Orco, Or33a/Orco, Or56a/Orco). For Or33a and Or47a we observed no significant effect of W7, while it caused a reduced response in cells expressing Or22a and a shortened response for Or56a.

1. Introduction

Functional properties of sensory receptors, such as sensitivity and response duration, have to be regulated according to the characteristics of the external signal transduced into intracellular information. To optimize temporal resolution the response to a given stimulus has to be terminated. The most straightforward mechanism of response cessation is a negative feedback control of receptor activation. Such mechanisms, as e.g. the Ca^{2+}-induced inhibition of cyclic nucleotide-gated channels in vertebrate olfactory sensory neurons (OSNs), inhibit further entry and terminate the odor signal [1].

Insect odorant receptors (ORs) represent ligand-gated non-selective cation channels that conduct also Ca^{2+} [2,3]. They are heterodimers composed of an odorant-specific OR protein (OrX) and an ubiquitous co-receptor protein (Orco) [4]. Besides the OrX/Orco heteromers also Orco homomers form Ca^{2+} conducting cation channels [3]. Activation of Orco channels plays an important role in the regulation of OR sensitivity to odorants [5]. Orco most probably contributes to the pore of the heteromeric OR channels [6]. While the heteromers are activated by odorants, both kinds of channels open upon binding of the synthetic ligand VUAA1 [7].

The Ca^{2+} import into cells through ion channels such as voltage-gated Ca^{2+} channels or cyclic nucleotide gated channels, and in consequence the free Ca^{2+} concentration, has to be tightly regulated [8–12]. Thus, termination of receptor response not only restores the capability to sense further stimuli but also protects the cell from Ca^{2+} overload that may damage or even kill it. One of the most important proteins that link Ca^{2+} concentration to regulation of Ca^{2+} influx or extrusion is calmodulin (CaM) [13]. CaM closes, for example, voltage-gated Ca^{2+} channels [14] and accelerates Ca^{2+} extrusion by the plasma membrane Ca^{2+} pump when activated by increased free Ca^{2+} level. In mammalian odorant receptors response termination includes CaM-mediated inactivation of CNG channels [15] and down regulation of intracellular free Ca^{2+} [16].

As insect OR activation is accompanied by Ca^{2+} influx into sensory cells, there is an obvious question whether CaM might play a role in regulating the function of insect ORs. To monitor OR activity, we observed the rise in intracellular Ca^{2+} concentration $[Ca^{2+}]_i$ as previously performed in vertebrate and invertebrate preparations [17,18]. We tested the effect of CaM inhibition on the agonist-induced rise in $[Ca^{2+}]_i$ in *Drosophila* OSNs and observed a reduced response. To specify the role of OR proteins in this regulation we proceeded to investigate the role of CaM in the

* Corresponding author. Tel.: +49 3641 571415.
E-mail address: dwicher@ice.mpg.de (D. Wicher).

http://dx.doi.org/10.1016/j.ceca.2014.02.013
0143-4160/

control of heterologously expressed Orco proteins and OrX/Orco combinations.

2. Materials and methods

2.1. Fly preparation and OR expression in cultured cells

Drosophila melanogaster flies with genotype *w;UAS-GCaMP3.0;Orco-Gal4* were maintained on conventional cornmeal agar medium under a 12 h light: 12 h dark cycle at 25 °C. Flies were anesthetized in ice; after decapitation antennae were excised, fixed in vertical position on a glass coverslip using a two component silicon and immersed in *Drosophila* Ringer solution (in mM HEPES, 5; NaCl, 130; KCl, 5; $MgCl_2$, 2; $CaCl_2$, 2; and sucrose, 36; pH = 7.3). Flagelli were cut below half of their length and incubated for 20 min to remove air bubbles.

The open reading frame of *Drosophila* Orco was PCR-amplified using gene specific primers with restriction sites for XhoI and HindIII and cloned into the pcrII TA-cloning vector (Invitrogen, Carlsbad, CA, USA). The identity of the insert was subcloned into the pcDNA3.1(−) expression vector via the integrated restriction sites. The sequences were confirmed by double strand DNA sequencing (Eurofins MWG Operon, Ebersberg, Germany). CHO cells stably expressing Orco were purchased from cytobox UG (Konstanz, Germany) and grown in cytobox™ CHO select medium containing puromycin. The cells were grown on poly-L-lysine (0.01%, Sigma–Aldrich, Steinheim, Germany) coated coverslips and cultured at a density of ~1×10^6 per 35 mm dish. The CaM mutants and Ors 22a, 47a, 33a and 56a were transfected with 0.3–0.5 μg/well using Rotifect transfection kit (Roth, Karlsruhe, Germany). For experiments cells were exposed to bath solution (in mM: NaCl, 135; KCl, 5; $MgCl_2$, 1; $CaCl_2$, 1; HEPES, 10; D-glucose, 10; pH = 7.4; osmolarity 295 mOsmol/l).

2.2. Site directed mutagenesis

Orco CaM K339N mutation was performed using site directed mutagenesis. Two overlapping mutagenic oligonucleotides were designed to introduce point mutation in position (Lysine) K 339 to Aspargine (N) residue. The PCR products were then used to run a full length PCR using Orco (full length) primers. The final product of 1.56 kb band was T:A cloned into Topo vector (invitrogen life technologies) and subsequently sub-cloned into XhoI and HindIII sites of pcDNA 3.1(−) expression vectors. The sequences were confirmed by double strand DNA sequencing (Eurofins MWG operon).

2.3. Calcium imaging in flies and cells

Excitation of cells and OSNs was performed with a monochromator (Polychrome V, TILL Photonics, Gräfelfing, Germany) coupled by means of an epifluorescence condenser into an Axioskop FS microscope (Carl Zeiss, Jena, Germany) with a water immersion objective (LUMPFL 40xW/IR/0.8; Olympus, Hamburg, Germany). Emitted light was separated by a 400-nm dichroic mirror and filtered with a 420-nm long-pass filter. Fluorescence images were acquired using a cooled CCD camera controlled by TILLVision 4.0 software (TILL Photonics). The resolution was 640 × 480 pixel in a frame of 175 μm × 130 μm.

GCaMP3.0 was excited with 475 nm light at a 0.2 Hz frequency with an exposition time of 50 ms. The response magnitude was calculated as the average $\Delta F/F$, expressed in percentage, for each frame, where F was estimated as the mean fluorescence level calculated for each neuronal body cell on 10 frames before each application of DMSO (control), W7 or W5 solution.

CHO cells were loaded with fura-2 by incubation in bath solution containing 5 μM fura-2/acetomethylester (Molecular Probes, Invitrogen) for 30 min. Free intracellular Ca^{2+} concentration ($[Ca^{2+}]_i$) was determined with the fluorescence ratio method and calculated according to $[Ca^{2+}]_i = K_{eff}(R - R_{min})/(R_{max} - R)$. Image pairs were obtained by excitation for 150 ms at 340 nm and 380 nm (ratio R); background fluorescence was subtracted. K_{eff}, R_{min}, and R_{max} were determined using permeabilized cells (Ca^{2+} free; 5 mM Ca^{2+}; 500 nM Ca^{2+}). The values of K_{eff}, R_{min}, and R_{max} were 1.95 μM, 0.2, and 5.3, respectively.

OSNs and CHO cells were stimulated using VUAA1 (application of 100 μl of 100 μM solution via pipette) after incubation in the presence of W7, W5 (application of 100 μl of 10 μM solution via pipette), or in the equivalent amount of DMSO (in which W7 or W5 were dissolved) as a control, for 50 s.

2.4. Chemicals

VUAA1 (N-(4-ethylphenyl)-2-((4-ethyl-5-(3-pyridinyl)-4H-1,2,4-triazol-3-yl)thio)acetamide) and VU0183254 (10-(((4-ethyl-5-(furyl)-4H-1,2,4-triazol-3-yl)thio)acetyl)-10H-phenothiazine) were synthesized by the group "Mass Spectrometry/Proteomics" of the Max-Planck Institute for Chemical Ecology (Jena, Germany). W-7 and W-5 hydrochloride were purchased from Tocris bioscience (Wiesbaden-Nordenstadt, Germany), and chlorpromazine (CPZ), trifluoperazine (TFP) and Ruthenium red (RR) from Sigma Aldrich (Steinheim, Germany).

2.5. Data analysis

The transmembrane domain prediction was performed by TTHMM server v.2.0. CaM motif prediction was done using CaM target database (http://calcium.uhnres.utoronto.ca/ctdb/ctdb/). The Orco sequences of various insect species were aligned using MUSCLE alignment tool (Geneios, Auckland, New Zealand). Statistical analysis was performed in Prism 4 software (GraphPad Software, Inc., La Jolla, CA, USA). Data were analyzed using paired or unpaired t-tests with Welch's correction in case heteroscedasticity of data occurred. Data are given as mean ± SEM (standard error of mean).

3. Results

As Orco is a ubiquitous constituent of insect ORs, a universal regulation of ORs via CaM would be expected to rely on the control of Orco function. Consequently, we first performed a screening for putative CaM binding sites in *Drosophila* Orco. We identified the candidate amino acid motif ^{336}SAIKYWVER^{344} within the second intracellular loop of the Orco protein (Fig. 1A). This motif is highly conserved in Orco proteins from other insect species, indicating an important functional role. For test purposes we produced an Orco mutant bearing a point mutation (K339N) in the putative CaM site.

We developed a fly antenna preparation expressing GCamp3 to perform Ca^{2+} imaging in olfactory sensory neurons (OSNs) under in situ conditions (Fig. 1). Removal of the proximal part of the third antenna segment allowed observation of OSN cell bodies localized within the antenna (Fig. 1). This preparation was then used to test a possible role of CaM in controlling OR function in OSNs. We asked whether inhibition of CaM had an effect on OR response upon stimulation with the agonist VUAA1. As ORs are Ca^{2+}-permeable channels the change in $[Ca^{2+}]_i$ could be used as a reporter for OR function. Application of VUAA1 caused a steep, transient increase in GCaMP3 fluorescence and thus in $[Ca^{2+}]_i$ (Fig. 2A and C). The peak of the response was reached within 10–15 s after stimulus onset, followed by a decay of fluorescence, the time course of which was described by an exponential function. The fluorescence level after response was lower than before indicating either bleaching or enhanced Ca^{2+} extrusion and/or buffering.

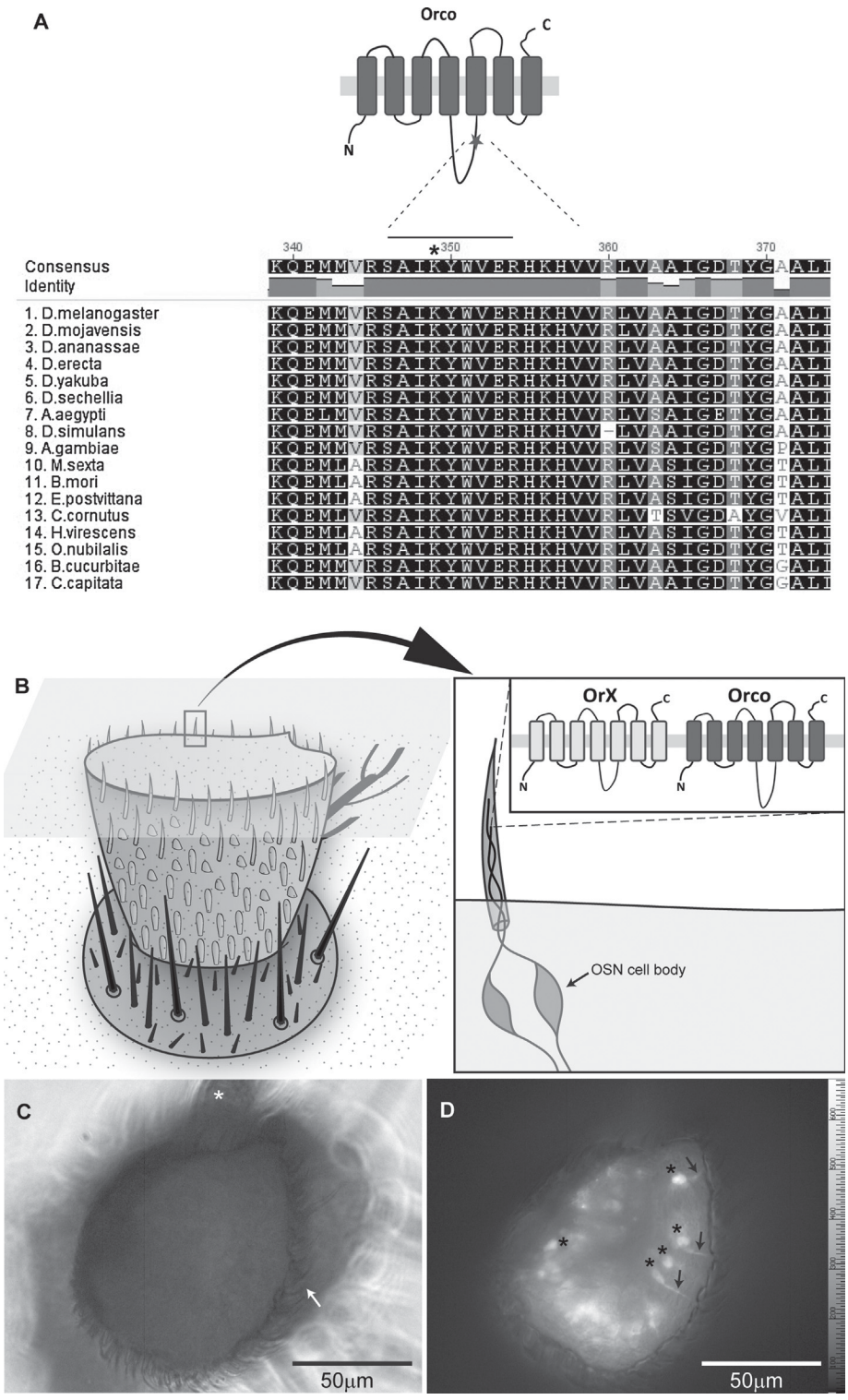

Fig. 1. Conservation of putative calmodulin (CaM) binding motifs in insect odorant coreceptor Orco and scheme of *Drosophila* antenna preparation. (A) Alignment of amino acids at the indicated position in the second intracellular loop of Orco. The amino acids ^{336}SAIKYWVER^{344} showing maximum score in CaM binding site search are highly conserved among various insect species (MUSCLE alignment, geneious software). Asterisk, position of the point mutation (K339N) introduced in the Orco CaM mutant. The NCBI accession number for Orco protein sequences are: *Drosophila melanogaster* NP 524235; *Drosophila mojavensis* BAJ23263.1; *Drosophila ananassae* XP 001959817.1; *Drosophila erecta* XP 001978924.1; *Drosophila yakuba* XP 002096053.1; *Drosophila sechellia* XP 002041712.1; *Aedes aegypti* AAT01220.1; *Drosophila simulans* XP 002080251.1; *Anopheles gambiae* AAR14939.1; *Manduca sexta* ACM18060.1; *Bombyx mori* NP 001037060.1; *Epiphyas postvittana* ACJ12928.1; *Ceratosolen cornutus* ACU31808.1; *Heliothis virescens* CAD31851.1; *Ostrinia nubilalis* BAJ23263.1; *Bactrocera cucurbitae* ADK97803.1; *Ceratitis capitata* NP 001266301.1. (B) *Drosophila* antenna preparation used for Ca^{2+} imaging experiments. Isolated antennae were embedded in a two-component silicon and rinsed with *Drosophila* ringer solution. The flagellum was cut below half of its length in order to get access to the olfactory sensory neurons (OSNs). The left insert shows a sensillum housing the OSN dendrites equipped with odorant receptors (ORs). ORs are composed of an odorant-specific receptor protein (OrX) and the Orco co-receptor. (B) Top view of the preparation in transmission light. Note the arista (asterisk) and the sensilla around the border of the cut (arrow). (C) Preparation as in (B) with GCaMP excitation by 475 nm light. Single neuronal cell bodies (asterisks) and processes toward the sensilla (arrows) become visible.

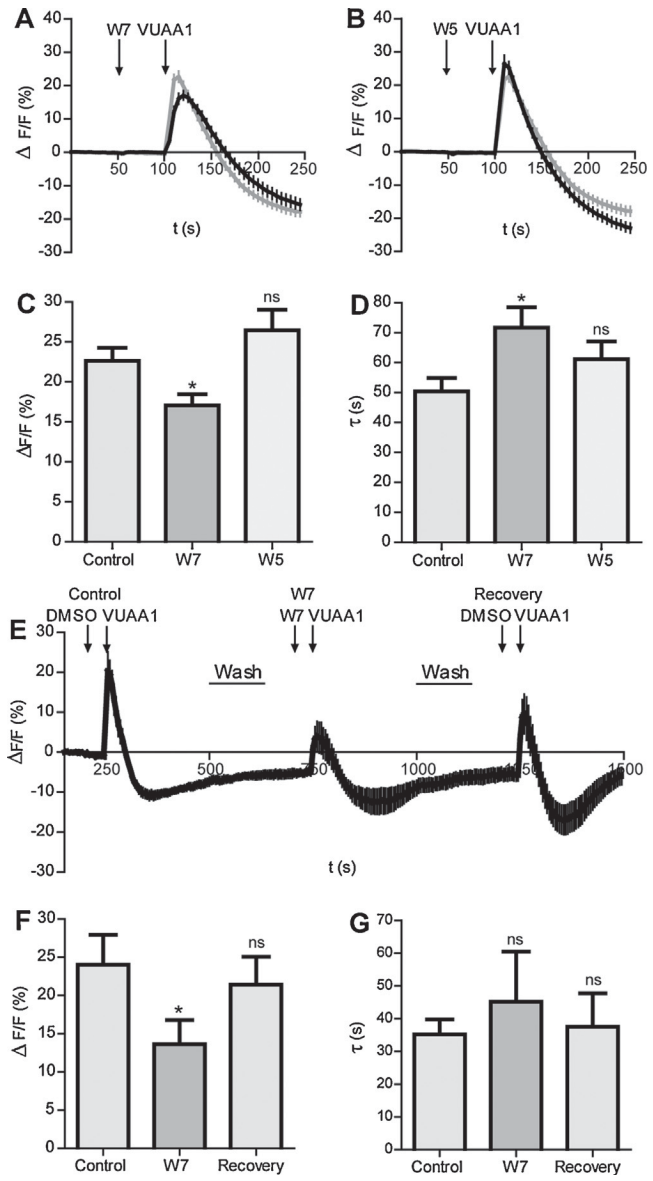

Fig. 2. Calmodulin inhibition affects maximum and time course of Ca^{2+} responses obtained upon OR activation by the agonist VUAA1 in *Drosophila* OSNs. (A and B) Fractional change in fluorescence responses following OR activation with VUAA1 (100 μM) in the presence of the potent CaM inhibitor W7 (10 μM, A) and the weak CaM inhibitor W5 (10 μM, B) (black traces), compared to control conditions with the solvent (DMSO) alone (gray traces). (C and D) Fluorescence peaks (C) and time constants of fluorescence decay (D) upon OR activation as in A and B. Two-tailed unpaired *t*-tests; $^{*}p < 0.05$; ns, not significant; $n = 50$. (E) Fluorescence responses upon OR activation using a washing protocol to test the recovery of the W7 effect in the same OSNs. (F and G) Fluorescence peaks (F) and time constants of fluorescence decay (G) as in (E). Two-tailed paired *t*-tests; $^{*}p < 0.05$; ns, not significant; $n = 6$.

Pretreatment with the potent CaM inhibitor W7 reduced the peak of the Ca^{2+} signal upon VUAA1 stimulation, while the weakly active analog W5 had no effect (Fig. 2A–C). Furthermore, W7 but not W5 prolonged the decay of the response (Fig. 2D). Using a washing protocol we asked whether the W7 effect on Ca^{2+} influx was reversible (Fig. 2E–G). W7 reduced the maximum of the response in a reversible manner (Fig. 2F) but with this approach we found no significant effect on the time course of the response, probably due to the variability produced by the washing protocol (Fig. 2G).

The results obtained in OSNs with CaM inhibition indicate a modulatory role of CaM on odor response. However, using these native cells does not allow to discriminate the contribution of Orco and/or the various odorant-specific OR proteins to this modulation. We thus continued the investigations using a heterologous expression system. First, *Drosophila* Orco was expressed in Chinese Hamster Ovary (CHO) cells. Ca^{2+} influx and subsequent increase $[Ca^{2+}]_i$ after VUAA1 application was visualized with fura 2. Receptor activation caused a steep increase in $[Ca^{2+}]_i$, followed by a decay of the signal to the basal level (Fig. 3A). The time course of the $[Ca^{2+}]_i$ decay was also well described by a single exponential with time constant τ. Cells not expressing Orco did not show any $[Ca^{2+}]_i$ signal upon VUAA1 application and were characterized by a lower Ca^{2+}resting level (Fig. 3A and B). The higher Ca^{2+}resting level in Orco expressing cells indicates a constitutive activity of Orco as observed in other heterologous expression systems [2,3]. To rule out a contribution of intracellular Ca^{2+} release we stimulated Orco expressing cells using Ca^{2+}-free bath solution and got no response (Fig. 3C). Ruthenium red (RR), which was previously shown to inhibit insect ORs [2,7,19,20], prevented the generation of a Ca^{2+} influx, thereby suggesting that ORs are the only source of the Ca^{2+} signal (Fig. 3D). Furthermore, in the presence of the OR-specific inhibitor VU0183254 [21], Orco stimulation with VUAA1 elicited only weak responses (Fig. 3E and F). The decay of the Ca^{2+} response reflects the closure of OR channels as well as Ca^{2+} buffering within and extrusion from the cytoplasm. It is presently unknown to which extent these mechanisms determine the time constant of the decay. Plotting the time constant versus the maximum Ca^{2+} response revealed a hyperbolic relationship (Fig. 3G). In cells with high Ca^{2+} responses the time course of $[Ca^{2+}]_i$ decay was faster compared with cells showing weak responses. To reduce the τ variation due to the size of the Ca^{2+} response we selected responses showing a minimum $[Ca^{2+}]_i$ rise of 220 nM under control conditions for further analysis (Fig. 3G, dotted line).

Preincubation of cells with the CaM inhibitor W7 strongly reduced and prolonged the response to VUAA1 while W5 had no significant effect (Fig. 4). With W7, the maximum increase in $[Ca^{2+}]_i$ was reduced to less than one third compared to control conditions (Fig. 4C), while the decay time constant τ increased by a factor of two (Fig. 4D). As determined from the area under curves, the average increase in $[Ca^{2+}]_i$ during the response decreased from 63 ± 7 nM (Control) to 34 ± 6 nM (W7; $n = 23$, $^{**}p < 0.01$). We also tested two other CaM inhibitors, trifluoperazine (TFP) and chlorpromazine (CPZ). For both compounds we observed a strongly reduced and prolonged response (Fig. 4E–H).

As CaM is known to regulate various proteins involved in controlling intracellular Ca^{2+} dynamics, among them the plasma membrane ATPase, the effect of CaM inhibition on size and shape of VUAA1-induced Ca^{2+} responses might be the sum of effects. To test whether Orco is specifically affected and if yes, to which amount, we expressed the Orco CaM mutant bearing a point mutation in the putative CaM site (K339N) and stimulated them with VUAA1. The Ca^{2+} responses were much weaker than observed for wt Orco (Fig. 4I and J), and did not differ from those obtained for wt Orco after W7 application, both for the maximum increase in $[Ca^{2+}]_i$ and for the decay time constant τ (Fig. 4K and L). Moreover, preincubation of Orco CaM expressing cells with W7 did not further reduce the response to VUAA1 (Fig. 4J). This rules out the possibility that the diminished Ca^{2+} response of Orco CaM is due to a weak expression level and not due to an impaired CaM effect. Taken together, our results demonstrate a significant contribution of Orco modulation by CaM. Furthermore, as stimulation of Orco CaM mimicks the effect of W7 on Orco wt, the CaM modulation of Orco dominates the observed effect on Ca^{2+} responses.

Additionally, we tested the effect of overexpression of CaM mutants vs. CaM WT in CHO cells stably expressing Orco. These CaM variants contained mutations in the EF-hand domains in the N-terminal part (CaM N), in the C-terminal part (CaM C) and in

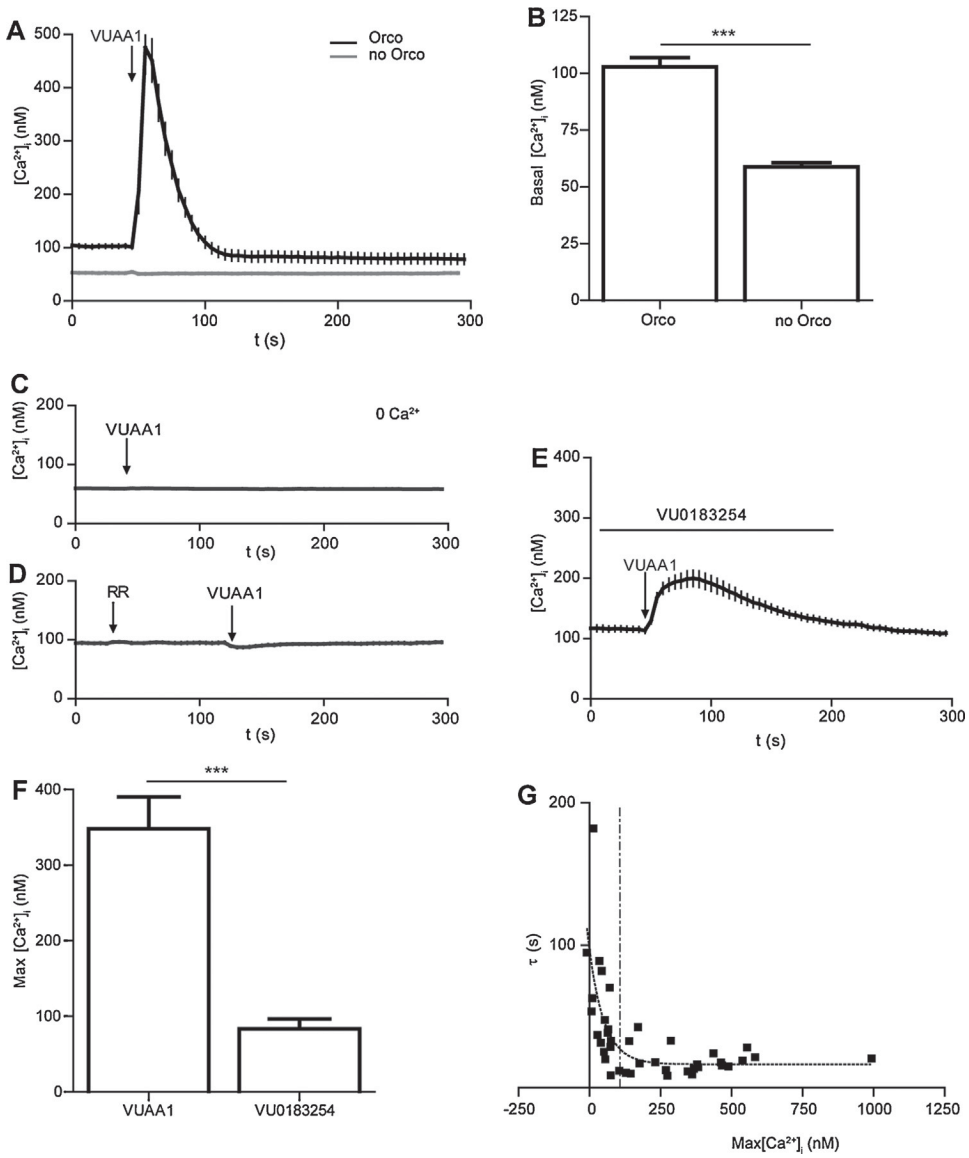

Fig. 3. Ca^{2+} responses in Orco-expressing CHO cells obtained with VUAA1. (A) Free calcium concentration $[Ca^{2+}]_i$ in response to VUAA1 application (100 μM) in Orco expressing ($n = 24$) and native CHO cells ($n = 24$). (B) Resting Ca^{2+} level as in (A). (C–E) $[Ca^{2+}]_i$ upon VUAA1 application (100 μM) with Ca^{2+} free bath solution (C, $n = 26$), in the presence of the cation channel blocker ruthenium red (RR, 100 μM)(D, $n = 26$), and with the OR antagonist VU0183254 (100 μM)(E, $n = 19$). (F) Maximum $[Ca^{2+}]_i$ as in (E). (G) Relationship between maximum $[Ca^{2+}]_i$ and time constants of decay upon VUAA1 stimulation. Hyperbola, regression curve, $R^2 = 0.5$; dotted line, minimum Ca^{2+} response used for further analysis. Unpaired *t*-test $^{***}p < 0.001$.

both (CaM NC) [22]. Given that the N- and C-terminal EF-hands of CaM differ in their affinity to Ca^{2+}, one would expect differential effects of the different mutations on size and/or duration of Ca^{2+} signals elicited upon Orco stimulation. However, all mutant CaM forms modified the Ca^{2+} signals similar to W7 with no difference in the phenotype of calcium responses between N and C terminal mutations (Fig. 5). The maximum of $[Ca^{2+}]_i$ increase was largely attenuated (Fig. 5E), while in parallel the decay time constant τ became larger (Fig. 5F). In contrast to conditions without overexpression, the average $[Ca^{2+}]_i$ rise was not changed for the mutant CaM forms (34 ± 3 nM, CaM wt, $n = 30$; 33 ± 4 nM, CaM N, $n = 29$; 27 ± 2 nM, CaM C, $n = 43$; 32 ± 5 nM; CaM NC; $n = 45$).

We next asked how CaM inhibition would affect the Ca^{2+} response upon OR stimulation in cells expressing heteromeric ORs. When Or22a was coexpressed with Orco, the Ca^{2+} signals elicited after VUAA1 stimulation appeared considerably prolonged in comparison with those obtained from solely Orco expressing cells (Fig. 6A). Heterologously expressed Orco and Or22a may form homomers (Orco/Orco, Or22a/Or22a) as well as heteromers (Or22a/Orco) [23]. In order to test whether there are different populations of Ca^{2+} responses in terms of decay kinetics we plotted the number of cells characterized by a given decay time constant (Fig. 6B). In cells co-expressing Or22a with Orco we found a large variation of τ, while in cells solely expressing Orco there was a rather narrow τ distribution. There was, however, no considerable overlap in the τ distributions as expected for a significant contribution of Orco monomers in the Or22a and Orco expressing cells (Fig. 6B). In Orco expressing cells we found a correlation between slow decay and weak Ca^{2+} responses (Fig. 3D). There was a similar relationship in cells coexpressing Or22a, yet with generally larger time constants (Fig. 6C). Taken together, a slow decay of Ca^{2+} responses in cells expressing Or22a/Orco might reflect an inherent property of heteromeric OR complexes.

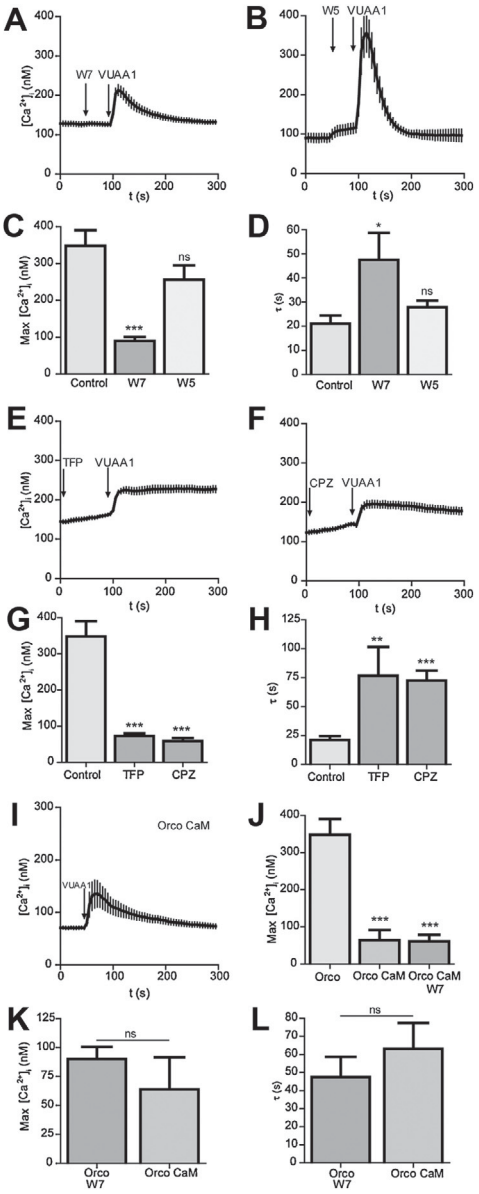

Fig. 4. CaM inhibition affects maximum and time course of Ca^{2+} responses obtained with VUAA1 in Orco-expressing CHO cells. (A and B) Effect of the potent CaM inhibitor W7 (10 μM, A, $n = 23$) and the weak CaM inhibitor W5 (10 μM, B, $n = 8$) on mean $[Ca^{2+}]_i$ upon application of VUAA1 (100 μM). (C, D) $[Ca^{2+}]_i$ maxima (C) and time constants of $[Ca^{2+}]_i$ decay (D) as in A and B. (E and F) Effect of the CaM inhibitors trifluoperazine (TFP, 10 μM)(E, $n = 22$) and chlorpromazine (CPZ, 25 μM)(F, $n = 21$) on responses to VUAA1. (G and H) $[Ca^{2+}]_i$ maxima (G) and time constants of $[Ca^{2+}]_i$ decay (H) as in E and F. (I–L) Effect of the point mutation K339N in Orco CaM on Ca^{2+} responses. Mean $[Ca^{2+}]_i$ upon application of VUAA1 (100 μM)(I, $n = 12$). $[Ca^{2+}]_i$ maxima for wt Orco ($n = 24$), Orco CaM without ($n = 12$) and with W7 preincubation ($n = 17$) (J); wt Orco in the presence of W7 ($n = 23$) and Orco CaM ($n = 12$)(K). (L) Time constants of $[Ca^{2+}]_i$ decay for wt Orco with W7 and Orco CaM. Unpaired *t*-test; $^*p < 0.05$; $^{***}p < 0.001$; ns, not significant.

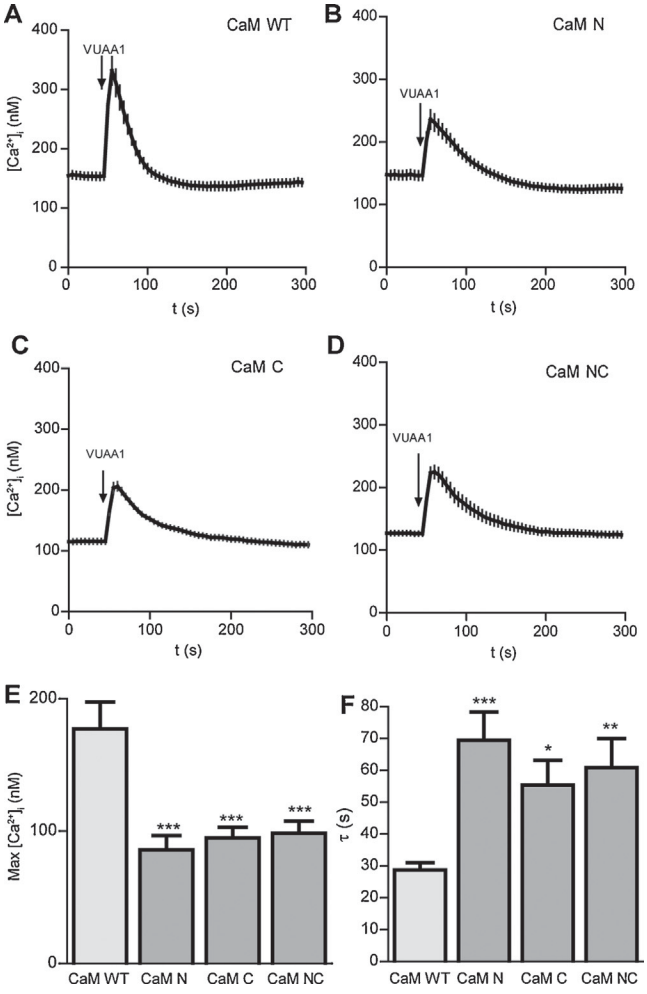

Fig. 5. Overexpression of CaM mutants affects maximum and time course of Ca^{2+} responses obtained with VUAA1 in Orco-expressing CHO cells. (A–D) Mean $[Ca^{2+}]_i$ upon application of VUAA1 (100 μM) in cells overexpressing CaM WT (A, $n = 30$), N-terminal (B, $n = 29$), C-terminal (C, $n = 43$) and N- plus C-terminal (NC, $n = 45$) CaM-EF-hand mutants. (E and F) $[Ca^{2+}]_i$ maxima (E) and time constants of $[Ca^{2+}]_i$ decay (F) as in (A–D). Non-parametric Kruskal–Wallis test with Dunn's multiple comparison; mutants versus control; $^*p < 0.05$; $^{**}p < 0.01$; $^{***}p < 0.001$.

Pre-incubation of Or22a expressing cells with W7 strongly reduced the maximum in $[Ca^{2+}]_i$ rise (Fig. 6D and E) but it did not affect the decay kinetics of the Ca^{2+} signal (Fig. 6F). Overexpression of CaM mutants affected the Ca^{2+} responses in a similar way as W7 (Fig. 6G–K).

We also co-expressed a couple of other odorant-specific receptor proteins with Orco, namely Or33a, Or47a and Or56a. Or47a represents, like Or22a, a food odor-detecting type. Or56a, the geosmin receptor [24], represents a receptor for a danger signal. Or33a is expressed in the same sensillum as Or56a and detects other odors of negative valence. The Ca^{2+} responses elicited by VUAA1 stimulation varied considerably in decay kinetics (Fig. 7A). While for Or33a the decay was as slow as for Or22a, the Ca^{2+} signals obtained with Or47a and Or56a appeared to be even more long lasting. In contrast to Or22a and Orco or solely Orco expressing cells, preincubation with W7 did not significantly affect the maximum in $[Ca^{2+}]_i$ rise after VUAA1 stimulation (Fig. 7B and C). In addition, for Or33a and Or47a, W7 did not change the decay kinetics of the Ca^{2+} signal (Fig. 7B and D). For Or56a, W7 accelerated the decay kinetics (Fig. 7B and D). The average rise in $[Ca^{2+}]_i$ determined from the area under curve became reduced from 73 ± 22 nM (Control) to 23 ± 2 nM (W7; $n = 19$, $^*p < 0.05$).

Taken together, inhibition of CaM functions was found to reduce the Ca^{2+} response of Orco channels upon agonist stimulation. For OrX/Orco heteromers, there was no consistent effect of impaired CaM activity on Ca^{2+} responses. For Or22a containing heteromers the Ca^{2+} responses appeared to be reduced while they became shortened for Or56a. For ORs comprising Or33a or Or47a CaM inhibition had no effect.

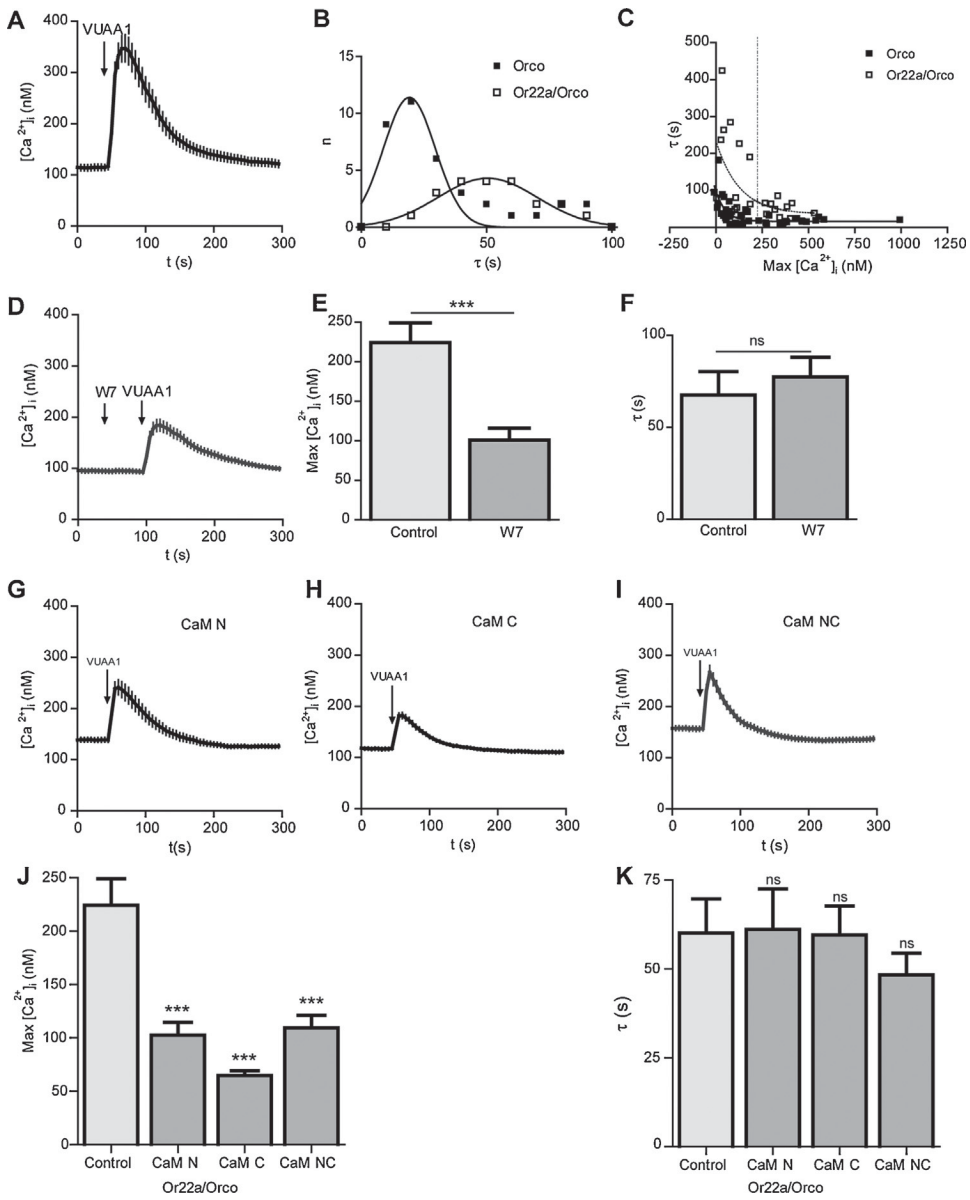

Fig. 6. CaM inhibition affects maximum but not the time course of Ca^{2+} responses obtained with VUAA1 in Orco- and Or22a-expressing CHO cells. (A) Mean $[Ca^{2+}]_i$ upon application of VUAA1 (100 μM). $n = 19$. (B) Distribution of cells (number n) with time constants of $[Ca^{2+}]_i$ decay in cells expressing Orco and Or22a/Orco indicated. Curves, fitted Gaussian distribution. (C) Relationship between maximum $[Ca^{2+}]_i$ and time constants of decay upon VUAA1 stimulation for cells expressing Orco and Or22a/Orco. Hyperbolas, regression curves, $R^2 = 0.5$ (Orco), 0.2 (Or22a/Orco); dashed line, minimum Ca^{2+} response for Or22a/Orco used for further analysis. (D) Mean $[Ca^{2+}]_i$ upon application of VUAA1 (100 μM) in the presence of W7 (10 μM) ($n = 27$). (E and F) $[Ca^{2+}]_i$ maxima (E) and time constants of $[Ca^{2+}]_i$ decay (F) as in A and D. (G–I) Effect of overexpression of CaM mutants on Ca^{2+} responses upon VUAA1 in Orco and Or22a expressing cells (N-terminal, G, $n = 27$; C-terminal, H, $n = 37$; NC terminal, I, $n = 27$). (J and K) $[Ca^{2+}]_i$ maxima (J) and time constants of $[Ca^{2+}]_i$ decay (K) as in A and G–I. Unpaired t-test; $^{***}p < 0.001$; ns, not significant.

4. Discussion

In the present study we investigated if and how CaM activity affects the Ca^{2+} response of insect ORs to agonist stimulation. For this purpose we developed a *Drosophila* antenna preparation allowing us to observe these signals under in situ conditions. CaM inhibition initially reduced the maximum of the Ca^{2+} signal obtained upon agonist application, but also prolonged this signal in the OSN cell bodies. This dual effect is similar to what was observed after CaM inhibition in the heterologous system with expression of only the Orco subunit of ORs (Fig. 4). This phenotype may reflect the predominant expression of Orco in the OSN cell body membrane [25]. Although our antenna preparation in principle also allows to observe dendritic regions of the OSNs (Fig. 1D), we failed in getting sufficiently resolved and mechanically stable fluorescence recordings at this level.

In a previous study we could show that repeated subthreshold odor stimulation of *Drosophila* OSNs led to OR sensitization [5]. This sensitization required Orco activation as a first step. It could be mimicked by processes activating Orco before odor stimulation and it could be suppressed by Orco inhibition. For example, flies expressing an Orco mutant with disrupted PKC phosphorylation that is insensitive to cAMP activation [26] did not sensitize [5]. The mechanism by which Orco activation leads to OR sensitization is presently unknown. Given the fact that Orco channels conduct Ca^{2+}, a role of CaM in mediating sensitization could not be excluded. Our results obtained after co-expression of OrX proteins and Orco show, however, no consistent effect of CaM on the various OR constructs,

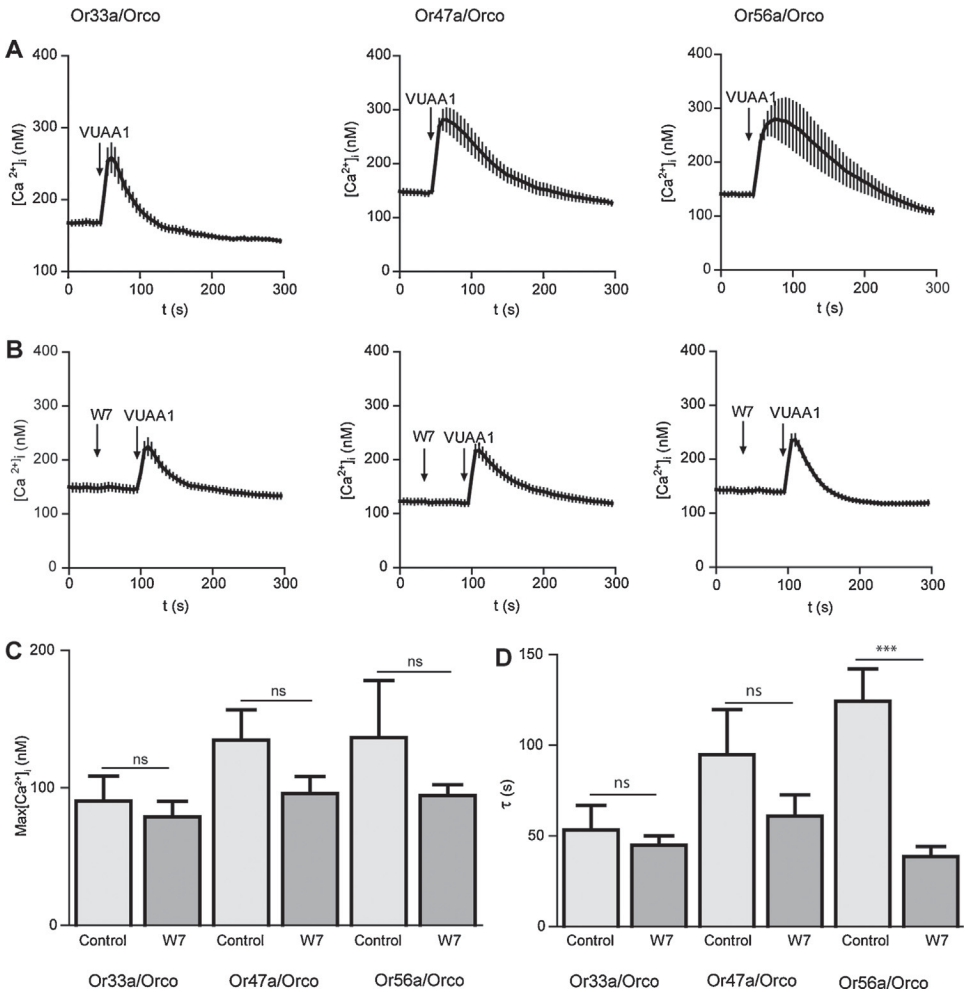

Fig. 7. CaM inhibition affects Ca^{2+} responses obtained with VUAA1 in Orco and various Or protein-expressing CHO cells differentially. (A and B) Mean $[Ca^{2+}]_i$ upon application of VUAA1 (100 μM) in control condition (A, $n = 13$ (Or33a), 17 (Or47a), 19 (Or56a)) and in the presence of W7 (B, $n = 15$ (Or33a), 27 (Or47a), 19 (Or56a)) in cells expressing the indicated ORs. (C and D) $[Ca^{2+}]_i$ maxima (C) and time constants of $[Ca^{2+}]_i$ decay (D) as in A and B. Unpaired *t*-test and Mann Whitney test; $^{*}p < 0.05$; $^{***}p < 0.001$; ns, not significant.

which was a prerequisite to provide a global mechanism of sensitization. The lack of a uniform modification of the Ca^{2+} response upon CaM inhibition in OrX/Orco heteromers may indicate that the regulation of this heteromeric receptor current is performed by Orco homomers. Their presence in the OSN membrane is indicated by recent observations [25,23]. Another explanation may be that the heterologous expression system misses some required player in the regulatory pathway.

The modulation of the Orco channel response by CaM inhibition suggests a stimulatory role of CaM activity on Orco function (Fig. 4). A tiny amount of Ca^{2+} influx obtained by weak Orco stimulation would thus be amplified. It remains to be shown which further downstream processes might lead to subsequent OR sensitization. A direct pacemaker activity of Orco can be excluded as we have observed that Orco activation via 8-bromo-cAMP did not accelerate the discharge rate of OSNs [5].

The present study provides evidence that CaM activity affects the function of Orco channels and may have specific effects on OrX/Orco couples. These results form the basis to answer further questions such as for the determinants of CaM action on Orco by mutation of candidate amino acids in the putative recognition motif. Other investigations should clarify whether there is an additional interaction between plasma membrane Ca^{2+} pump, CaM and the ORs.

Conflict of interest statement

All authors declare that they have no conflicts of interest.

Acknowledgements

The authors thank S. Neumann for orienting experiments with the fly antenna preparation, Drs. R. Schönherr and S.H. Heinemann for providing the CaM-EF-hand mutants, and Dr. Heinemann for helpful discussion on the manuscript. The study was supported by the Max Planck Society (LM, SK, BSH, DW) and the International Max Planck Research School (FM).

References

[1] F. Zufall, G.M. Shepherd, S. Firestein, Inhibition of the olfactory cyclic nucleotide gated ion channel by intracellular calcium, Proc. Biol. Sci. 246 (1991) 225–230.
[2] K. Sato, M. Pellegrino, T. Nakagawa, T. Nakagawa, L.B. Vosshall, K. Touhara, Insect olfactory receptors are heteromeric ligand-gated ion channels, Nature 452 (2008) 1002–1006.
[3] D. Wicher, R. Schäfer, R. Bauernfeind, M.C. Stensmyr, R. Heller, S.H. Heinemann, B.S. Hansson, Drosophila odorant receptors are both ligand-gated and cyclic-nucleotide-activated cation channels, Nature 452 (2008) 1007–1011.

[4] M.C. Larsson, A.I. Domingos, W.D. Jones, M.E. Chiappe, H. Amrein, L.B. Vosshall, Or83b encodes a broadly expressed odorant receptor essential for *Drosophila* olfaction, Neuron 43 (2004) 703–714.
[5] M.N. Getahun, S.B. Olsson, S. Lavista-Llanos, B.S. Hansson, D. Wicher, Insect odorant response sensitivity is tuned by metabotropically autoregulated olfactory receptors, PLoS ONE 8 (2013) e58889.
[6] T. Nakagawa, M. Pellegrino, K. Sato, L.B. Vosshall, K. Touhara, Amino acid residues contributing to function of the heteromeric insect olfactory receptor complex, PLoS ONE 7 (2012) e32372.
[7] P.L. Jones, G.M. Pask, D.C. Rinker, L.J. Zwiebel, Functional agonism of insect odorant receptor ion channels, Proc. Natl. Acad. Sci. U. S. A. 108 (2011) 8821–8825.
[8] M.J. Berridge, P. Lipp, M.D. Bootman, The versatility and universality of calcium signalling, Nat. Rev. Mol. Cell Biol. 1 (2000) 11–21.
[9] T. Budde, S. Meuth, H.C. Pape, Calcium-dependent inactivation of neuronal calcium channels, Nat. Rev. Neurosci. 3 (2002) 873–883.
[10] T.Y. Chen, K.W. Yau, Direct modulation by Ca^{2+}–calmodulin of cyclic nucleotide-activated channel of rat olfactory receptor neurons, Nature 368 (1994) 545–548.
[11] R. Rizzuto, T. Pozzan, Microdomains of intracellular Ca^{2+}: molecular determinants and functional consequences, Physiol. Rev. 86 (2006) 369–408.
[12] D.E. Clapham, Calcium signaling, Cell 131 (2007) 1047–1058.
[13] G.C. Faas, S. Raghavachari, J.E. Lisman, I. Mody, Calmodulin as a direct detector of Ca^{2+} signals, Nat. Neurosci. 14 (2011) 301–304.
[14] B.Z. Peterson, C.D. DeMaria, J.P. Adelman, D.T. Yue, Calmodulin is the Ca^{2+} sensor for Ca^{2+}-dependent inactivation of L-type calcium channels, Neuron 22 (1999) 549–558.
[15] Y. Song, K.D. Cygnar, B. Sagdullaev, M. Valley, S. Hirsh, A. Stephan, J. Reisert, H. Zhao, Olfactory CNG channel desensitization by Ca^{2+}/CaM via the B1b subunit affects response termination but not sensitivity to recurring stimulation, Neuron 58 (2008) 374–386.
[16] S. Antolin, J. Reisert, H.R. Matthews, Olfactory response termination involves Ca^{2+}-ATPase in vertebrate olfactory receptor neuron cilia, J. Gen. Physiol. 135 (2010) 367–378.
[17] B. Malnic, J. Hirono, T. Sato, L.B. Buck, Combinatorial receptor codes for odors, Cell 96 (1999) 713–723.
[18] K. Ukhanov, Y. Bobkov, B.W. Ache, Imaging ensemble activity in arthropod olfactory receptor neurons in situ, Cell Calcium 49 (2011) 100–107.
[19] T. Nakagawa, T. Sakurai, T. Nishioka, K. Touhara, Insect sex-pheromone signals mediated by specific combinations of olfactory receptors, Science 307 (2005) 1638–1642.
[20] A.S. Nichols, S. Chen, C.W. Luetje, Subunit contributions to insect olfactory receptor function: channel block and odorant recognition, Chem. Senses 36 (2011) 781–790.
[21] P.L. Jones, G.M. Pask, I.M. Romaine, R.W. Taylor, P.R. Reid, A.G. Waterson, G.A. Sulikowski, L.J. Zwiebel, Allosteric antagonism of insect odorant receptor ion channels, PLoS ONE 7 (2012) e30304.
[22] U. Ziechner, R. Schönherr, A.K. Born, O. Gavrilova-Ruch, R.W. Glaser, M. Malesevic, G. Kullertz, S.H. Heinemann, Inhibition of human ether a go–go potassium channels by Ca^{2+}/calmodulin binding to the cytosolic N- and C-termini, FEBS J. 273 (2006) 1074–1086.
[23] P.F. German, S. van der Poel, C. Carraher, A.V. Kralicek, R.D. Newcomb, Insights into subunit interactions within the insect olfactory receptor complex using FRET, Insect Biochem. Mol. Biol. 43 (2013) 138–145.
[24] M.C. Stensmyr, H.K. Dweck, A. Farhan, I. Ibba, A. Strutz, L. Mukunda, J. Linz, V. Grabe, K. Steck, S. Lavista-Llanos, D. Wicher, S. Sachse, M. Knaden, P.G. Becher, Y. Seki, B.S. Hansson, A conserved dedicated olfactory circuit for detecting harmful microbes in *Drosophila*, Cell 151 (2012) 1345–1357.
[25] R. Benton, S. Sachse, S.W. Michnick, L.B. Vosshall, Atypical membrane topology and heteromeric function of *Drosophila* odorant receptors in vivo, PLoS Biol. 4 (2006) e20.
[26] V. Sargsyan, M.N. Getahun, S. Lavista Llanos, S.B. Olsson, B.S. Hansson, D. Wicher, Phosphorylation via PKC regulates the function of the *Drosophila* odorant coreceptor, Front. Cell. Neurosci. 5 (2011) 5.

Manuscript V

Sensitization in heterologously expressed ORs

Sensitization in heterologously expressed ORs

Latha Mukunda*, Vardanush Sargsyan*, Bill S. Hansson, Dieter Wicher
**These authors contributed equally to the work*

Max Planck Institute for Chemical Ecology, Department Evolutionary Neuroethology, Hans-Knöll-St. 8, D-07745 Jena, Germany

Corresponding author: Dieter Wicher, Max Planck Institute for Chemical Ecology, Hans-Knöll-St. 8, D-07745 Jena, Germany, Tel.: +49 3641 571415, e-mail: dwicher@ice.mpg.de

Abstract:
Flying insects have developed a remarkably sensitive olfactory system that allows to detect faint and turbulent odor traces. Olfactory receptors exclusively occurring in flying insects are odorant receptors (ORs). They form heteromeric complexes of an odorant specific receptor protein (OrX) and a highly conserved co-receptor protein (Orco). The ORs form ligand gated ion channels that are tuned by intracellular signaling systems. Repetitive subthreshold odor stimulation of olfactory sensory neurons sensitizes insect ORs. This OR sensitization process requires Orco activity. In the present study we asked whether OR sensitization can be monitored with heterologously expressed OR proteins. Using electrophysiological and calcium imaging methods we demonstrate that *Drosophila* OR proteins expressed in CHO cells show sensitization upon repeated weak stimulation. This was found for OR channels formed by Orco as well as by Or56a and Orco. In addition we show that inhibition of calmodulin (CaM) in OR proteins expressing cells abolishes any sensitization. The use of heterologously expressed OR proteins appears to be suitable for further investigations of the mechanistic basis of OR sensitization.

Keywords: insect olfaction, odorant receptor, Drosophila, Orco, calmodulin, sensitization.

Introduction

Insects possess a highly sensitive olfactory system that allows to respond to dispersed and diluted odor plumes. The olfactory sensory neurons (OSNs) express two main families of 7-transmembrane proteins, odorant receptor (OR) and gustatory receptor (GR) proteins like metabotropic receptors and ionotropic receptors (IRs) which are related to ionotropic glutamate receptors (Stocker, 1994; Vosshall and Stocker, 2007; Benton et al., 2009). The occurrence of ORs is restricted to flying insects (Missbach et al., 2014). ORs form ligand-gated ion channels immediately activated by odorant binding to the receptor complex (Sato et al., 2008; Wicher et al., 2008). They are heterodimers composed of an odorant-specific OrX protein and an ubiquitous coreceptor (Orco), both of which contribute to ion channel pore and determine characteristics such as ion permeability (Nichols, 2011; Pask et al., 2011; Nakagawa et al., 2012). In addition, the ORs are controlled by intracellular signaling (Kain et al., 2008; Wicher et al., 2008; Deng et al., 2011; Sargsyan et al., 2011; Getahun et al., 2013). The sensitivity of ORs - but not of IRs - can be adjusted by metabotropic autoregulation (Getahun et al., 2013). Stimulation of OSNs with subthreshold odor concentrations can elicit a superthreshold response when the stimulus is repeated in a suitable time window. This OR sensitization required Orco activation (Getahun et al., 2013). For a recent review on the role of Orco in OR function see (Stengl and Funk, 2013).

The molecular mechanism leading to OR sensitization remains to be determined. The present study was aimed to find correlates to sensitization in heterologously expressed OR proteins. As Orco was found to play a central role in this process we first asked whether the Orco function was modified by repeated weak stimulation. Heterologously expressed Orco proteins form ion channels (Wicher et al., 2008) which can be activated by synthetic agonists (Jones et al., 2011; Chen et al., 2012) .We first used the patch clamp technique to register the currents passed by Orco channels. As Orco channels permeate cations including Ca^{2+}, we also performed Ca^{2+} imaging experiments without affecting the cell integrity. In previous experiments we have seen that the Orco response to synthetic agonist stimulation was modified by calmodulin (CaM) function. We thus asked in the present study whether CaM might play a role in the process of OR sensitization.

Materials and Methods:

Cell culture and calcium imaging

CHO cells stably expressing Orco and FACS (Fluorescent activated cell sorting) CHO cells were purchased from cytobox UG (Konstanz, Germany) and grown in cytobox™ CHO select medium

containing puromycin. The cells were grown on poly-L-lysine (0.01 %, Sigma-Aldrich, Steinheim, Germany) coated coverslips and cultured at a density of ~2 - 5×10^5 per four 35 mm dish.). The Or56a and Orco CaM mutant was transfected with 0.3 - 0.5 µg/well using X-treme GENE HP (Roche diagnostics, Mannheim, Germany) and Rotifect transfection kit (Roth, Karlsruhe, Germany).

For calcium imaging CHO cells were incubated in bath solution containing 5µM fura-2/acetomethylester (Molecular Probes, Invitrogen) for 30 min. Excitation of fura-2 at 340 and 380 nm was performed with a monochromator (Polychrome V, T.I.L.L. Photonics, Gräfelfing, Germany) coupled via an epifluorescence condenser into an Axioskop FS microscope (Carl Zeiss, Jena, Germany) with a water immersion objective (LUMPFL 40xW/IR/0.8; Olympus, Hamburg, Germany). Emitted light was separated by a 400-nm dichroic mirror and filtered with a 420-nm long-pass filter. Free intracellular Ca^{2+} concentration ($[Ca^{2+}]_i$) was calculated according to the equation $[Ca^{2+}]_i = K_{eff}(R-R_{min})/(R_{max}-R)$. K_{eff}, $R_{min,}$ and R_{max} were determined as mentioned in (Mukunda et al., 2014). Fluorescence images were acquired using a cooled CCD camera controlled by TILLVision 4.0 software (T.I.L.L. Photonics). The resolution was 640x480 pixels in a frame of 175x130 µm (40x/IR/0.8 objective). Image pairs were obtained by excitation for 150 ms at 340 nm and 380 nm; background fluorescence was subtracted.

VUAA1 (50 -100 µM) and the CaM inhibitors W7 (10 µM), CPZ (20 µM) were manually added via pipette (100 µl) with an interval of 75 s. Cells were continuously perfused with bath solution in the recording/perfusion chamber (RC-27, Warner Instruments Inc., and Hamden, CT, USA). For experiments cells the standard extracellular solution contained (in mM: 135 NaCl, 5 KCl, $1CaCl_2$, 1 $MgCl_2$, 10 HEPES, 10 glucose (pH 7.4, osmolarity 295 mOsmol/l).

Electrophysiology

Ion currents in Orco expressing FACS-CHO cells were measured with the patch clamp technique in the whole-cell configuration using an EPC10 patch-clamp amplifier controlled by the Patchmaster software (HEKA, Elektronik, Lambrecht, Germany). Experiments were performed at room temperature, series resistance and capacitive currents were compensated. Pipettes were made from borosilicate glass and had resistances of 2 - 4 MΩ. The pipette solution contained (in mM) 140 KCl, 4 NaCl, 2.2 $CaCl_2$, 2 Mg-ATP, 0.05 Na-GTP, 5 EGTA, 10 HEPES (pH 7.3), the bath solution was composed as described above. The pipette solution for comparing the buffering effect of EGTA vs BAPTA contained 50 nM free Ca^{2+} adjusted with the metal/chelator ratio (in

mM) 1 $CaCl_2$, 5 BAPTA and 1.6 $CaCl_2$, 5 EGTA (http://www.stanford.edu/~cpatton/webmaxc/webmaxcE.htm). The agonist VUAA1 (100 µM) was applied for 1 s with interval of 60 s under continuous perfusion. For agonist application the pneumatic picopump PV830 (World precision Instruments, USA) was used; cells were continuously perfused with bath solution in the recording/perfusion chamber (RC-27, Warner Instruments Inc., Hamden, CT, USA).

Chemicals

VUAA1 (N-(4-ethylphenyl)-2-((4-ethyl-5-(3-pyridinyl)-4H-1,2,4-triazol-3-yl)thio)acetamide) was synthesized by the working group "Mass Spectrometry/Proteomics" of the Max Planck Institute for Chemical Ecology (Jena, Germany). W-7 hydrochloride was purchased from Tocris bioscience (Wiesbaden-Nordenstadt, Germany) and Chlorpromazine hydrochloride (CPZ) from Sigma Aldrich (Steinheim, Germany).

Data analysis

For electrophysiology, IgorPro (WaveMetrics, Lake Oswego, OR, USA) was used. Statistical analysis was performed with Prism 4 (GraphPad Software, Inc., La Jolla, CA, USA).

Results

As OR sensitization requires Orco activation, we first asked whether repeated weak stimulation of Orco proteins expressed in CHO cells would lead to enhanced current responses. For this sake we performed patch clamp recordings in the whole cell configuration with near-threshold stimulation of Orco using the OR agonist VUAA1. A critical parameter in OSN sensitization process was the time span between two stimuli. Using subthreshold odor stimulation, an OR sensitization was observed for time spans between 10 s and 3 min (Getahun et al., 2013). Using a medium interval of 60 s, repeated near-threshold stimulation elicited an increased current production (Figure 1). For stimuli eliciting a robust first response (> 300 pA) we never observed an enhanced second response. Usually, the second response was attenuated representing an adaptation (not shown).

The $[Ca^{2+}]_i$ buffering plays an important role in regulating the Orco function (Sargsyan et al., 2011). A high degree of intracellular calcium buffering was seen to prevent Orco activation (Sargsyan et al., 2011). As the first Orco activation produces a Ca^{2+} influx and a too strong first stimulus could prevent a sensitization, we asked whether the speed of calcium buffering may affect the sensitization. For a given level $[Ca^{2+}]_i$ of 50 nM in the pipette solution adjusted with the

slow calcium buffer EGTA or with fast buffer BAPTA we compared the amount of current amplification. Using BAPTA the normalized second current response was 1.82 ± 0.48 (n = 9), for EGTA it was 1.44 ± 0.24 (n = 7) which was not significantly different.

We next tried to observe sensitization with excised patches to determine how this phenomenon is manifested at the level of single channels. Unfortunately we got no increases in the responses, both for inside out as well as outside out configuration. The possible reason for this might be a change in the regulatory environment due to patch excision, e.g.by a dephosphorylation or a loss of parts of a signaling cascade. We thus decided to perform further investigations with the non-invasive Ca^{2+} imaging technique. In a previous study we have characterized the Ca^{2+} responses of Orco channels expressed in CHO cells when stimulated with VUAA1 (Mukunda et al., 2014). Similar to the findings from patch-clamp experiments, a repeated stimulation after a near-threshold response results in an amplified Ca^{2+} signal in cells expressing Orco (Figure 2A, B).We also tested a complete OR construct composed of Or56a. Here the second stimulation also amplified the Ca^{2+} response (Figure 2C, D). The more prolonged VUAA1 responses are in line with the previous observation that OR responses are prolonged in comparison with Orco responses (Mukunda et al., 2014).

A previous study revealed a control of Orco function by CaM (Mukunda et al., 2014). Inhibition of CaM function reduced the Orco response upon VUAA1 stimulation and prolonged the response. Here we tested whether CaM might be involved in Orco sensitization. The double stimulation protocols were used in the presence of the CaM inhibitors W7 and chlorpromazine (CPZ) on Orco (Figure 3A-D). We also tested the Orco CaM mutant bearing point mutation in putative CaM binding site (Figure 3E, F) and the complete OR construct Or56a/Orco (Figure 3G, H). In all cases tested there was no significant potentiation of the response at the second stimulus (Figure 3). To support the findings obtained on the role of CaM with Ca^{2+} imaging we performed whole-cell patch-clamp experiments. When cells having shown sensitization by repeated VUAA1 stimulation were treated with W7, a double stimulation with the same protocol did not enhance the second current response, and both stimuli elicited a general weaker response (Figure 4A, B). Thus, both Ca^{2+} imaging and electrophysiological experiments support the view that CaM activity is required to establish OR sensitization.

Discussion

In our recent study using extracellular recording of *Drosophila* OSNs we showed that Orco activation is important for the regulation of insect OR sensitivity. Repetitive subthreshold odor

stimulations elicited sensitized OR responses in the OSNs (Getahun et al., 2013). In the present study we asked whether the sensitization phenomenon would also occur in heterologously expressed Or proteins. Indeed, repeated VUAA1 stimulation of Orco expressed in CHO cells induced an increase in the response. This sensitization phenomenon was observed both in electrophysiology recordings as well as calcium imaging experiments (Figure 1, 2).

CaM modulates the response of Orco channels to stimulation with VUAA1 (Mukunda et al., 2014). In the present study we could show that CaM inhibition abolished any sensitization in cells expressing Orco alone or together with the OrX protein Or56a (Figure 3, 4). Orco contains a putative CaM binding motif which is conserved across insect species (Mukunda et al., 2014). Similar to application of CaM inhibitors, repeated stimulation of cells expressing Orco CaM mutant (K339N) failed to show sensitization process (Figure 3E, F). It has been demonstrated that activation of Orco through intracellular signaling was necessary to sensitize the ORs (Getahun et al., 2013). In heterologously expressed *Drosophila* ORs, CaM does not show a generalized effect independent of the specific OrX proteins (Mukunda et al., 2014). Moreover the effect of CaM inhibition differed qualitatively between different OrX proteins. We thus can exclude that CaM activation due to Ca^{2+} influx via Orco activation directly leads to OR sensitization. There is thus a missing link between Orco activation and OR sensitization. Recently published studies report as yet unknown mechanisms regulating the OR function.

dATP8B, a phospholipid flippase was, for example, shown to be essential for an appropriate sensitivity of ORs, but not of IRS. It has been shown that mutation in the dATP8B gene strongly reduces the sensitivity of OR-expressing neurons (Liu et al., 2014). To understand the basis and the molecular mechanism of insect OR sensitization relies on the knowledge of further regulators of sensitivity. A study performed on heterologously expressed insect ORs revealed an amplification of odor induced calcium responses through activation of intracellular Ca^{2+} release channels (Ignatious Raja et al., 2014). A further analysis of intracellular calcium signaling using *in vivo* studies is required as it might play a role in olfactory signaling (Ignatious Raja et al., 2014).

Taken together, our study shows that repeated stimulation of heterologously expressed Orco caused an enhanced response, similar as observed in *Drosophila* OSNs (Getahun et al., 2013).We also provide evidence that the sensitization process can be abolished by CaM inhibition. This suggests that CaM may play a central role in mediating sensitization, but this contribution is not sufficient to completely explain this process. The heterologous expression system seems to be

suitable for further investigations to provide a more comprehensive view on the mechanisms involved in OR sensitization.

Acknowledgements

This study was supported by the Max Planck Society. The authors thank Sabine Kaltofen for assistance.

References

Benton, R., Vannice, K.S., Gomez-Diaz, C., and Vosshall, L.B. (2009). Variant Ionotropic Glutamate Receptors as Chemosensory Receptors in *Drosophila*. *Cell* 136**,** 149-162.

Deng, Y., Zhang, W., Farhat, K., Oberland, S., Gisselmann, G., and Neuhaus, E.M. (2011). The stimulatory Galpha(s) protein is involved in olfactory signal transduction in *Drosophila*. *PLoS One* 6**,** e18605.

Getahun, M.N., Olsson, S.B., Lavista-Llanos, S., Hansson, B.S., and Wicher, D. (2013a). Insect Odorant Response Sensitivity Is Tuned by Metabotropically Autoregulated Olfactory Receptors. *Plos One* 8.

Ignatious Raja, J.S., Katanayeva, N., Katanaev, V.L., and Galizia, C.G. (2014). Role of Go/i subgroup of G proteins in olfactory signaling of *Drosophila melanogaster*. *Eur J Neurosci* 39**,** 1245-1255.

Kain, P., Chakraborty, T.S., Sundaram, S., Siddiqi, O., Rodrigues, V., and Hasan, G. (2008). Reduced odor responses from antennal neurons of G(q)alpha, phospholipase Cbeta, and rdgA mutants in *Drosophila* support a role for a phospholipid intermediate in insect olfactory transduction. *J Neurosci* 28**,** 4745-4755.

Liu, Y.C., Pearce, M.W., Honda, T., Johnson, T.K., Charlu, S., Sharma, K.R., Imad, M., Burke, R.E., Zinsmaier, K.E., Ray, A., Dahanukar, A., De Bruyne, M., and Warr, C.G. (2014). The *Drosophila melanogaster* phospholipid flippase dATP8B is required for odorant receptor function. *PLoS Genet* 10**,** e1004209.

Missbach, C., Dweck, H.K.M., Vogel, H., Vilcinskas, A., Stensmyr, M.C., Hansson, B.S., and Grosse-Wilde, E. (2014). Evolution of insect olfactory receptors. *Elife* 3.

Mukunda, L., Miazzi, F., Kaltofen, S., Hansson, B.S., and Wicher, D. (2014). Calmodulin modulates insect odorant receptor function. *Cell Calcium* 55**,** 191-199.

Nakagawa, T., Pellegrino, M., Sato, K., Vosshall, L.B., and Touhara, K. (2012). Amino acid residues contributing to function of the heteromeric insect olfactory receptor complex. *PLoS One* 7**,** e32372.

Nichols, A.S.C., S. And Luetje, C. W. (2011). Subunit contributions to insect olfactory receptor function: channel block and odorant recognition. *Chem Senses* 36**,** 781-790.

Pask, G.M., Jones, P.L., Rützler, M., Rinker, D.C., and Zwiebel, L.J. (2011). Heteromeric anopheline odorant receptors exhibit distinct channel properties. *PloS one* 6**,** e28774.

Sargsyan, V., Getahun, M.N., Llanos, S.L., Olsson, S.B., Hansson, B.S., and Wicher, D. (2011). Phosphorylation via PKC Regulates the Function of the *Drosophila* Odorant Co-Receptor. *Front Cell Neurosci* 5**,** 5.

Sato, K., Pellegrino, M., Nakagawa, T., Nakagawa, T., Vosshall, L.B., and Touhara, K. (2008). Insect olfactory receptors are heteromeric ligand-gated ion channels. *Nature* 452**,** 1002-1006.

Stengl, M., and Funk, N.W. (2013). The role of the coreceptor Orco in insect olfactory transduction. *J Comp Physiol A* 199**,** 897-909.

Stocker, R.F. (1994). The organization of the chemosensory system in *Drosophila melanogaster*: a rewiew. *Cell Tissue Res* 275**,** 3-26.

Vosshall, L.B., and Stocker, R.F. (2007). Molecular architecture of smell and taste in *Drosophila*. *Annu Rev Neurosci* 30**,** 505-533.

Wicher, D., Schafer, R., Bauernfeind, R., Stensmyr, M.C., Heller, R., Heinemann, S.H., and Hansson, B.S. (2008). *Drosophila* odorant receptors are both ligand-gated and cyclic-nucleotide-activated cation channels. *Nature* 452**,** 1007-1011.

Figure legends

Figure 1: Current flow through Orco channels increases after repeated stimulation. (A) Representative trace of whole cell current recorded from a CHO cell expressing Orco. Currents were activated by application of the agonist VUAA1 (100 µM) (arrows). (B) Current amplitudes obtained as described in A (n = 23); mean ± SEM; paired t-test, * $p < 0.05$.

Figure 2: Rise in intracellular free Ca^{2+} concentration $[Ca^{2+}]_i$ due to current flow via Orco and Or56a/Orco channels increases upon repeated stimulation. (A, C) Averaged recordings of $[Ca^{2+}]_i$ in cells expressing Orco (A, n = 9) and Or56a/Orco (C, n = 20) stimulated with VUAA1 (A, 50 µM; B,100 µM)(arrows). (B, D) Maximum increase in $[Ca^{2+}]_i$ after 1st and 2nd application of VUAA1 as in A and C. Data represent mean ± SEM; paired t-test, ** $p < 0.01$, *** $p < 0.001$.

Figure 3: Calmodulin (CaM) inhibition abolishes increase in $[Ca^{2+}]_i$ rise upon repeated stimulation. (A-D) Effect of CaM inhibitors on the response to VUAA1 application (100 µM) in cells expressing Orco. Averaged recordings of $[Ca^{2+}]_i$ in presence of W7 (A, n = 15) and chlorpromazine (CPZ, C, n = 10) and maxima of $[Ca^{2+}]_i$ rise with W7 (B) and CPZ (D). (E, F) Averaged recordings of $[Ca^{2+}]_i$ (E) and maxima of $[Ca^{2+}]_i$ rise (F) in presence of W7 in cells expressing the Orco CaM mutant (n = 14). (G, H) Averaged recordings of $[Ca^{2+}]_i$ (G) and maxima of $[Ca^{2+}]_i$ rise (H) in presence of W7 in cells expressing Or56a/Orco (n = 43). Data represent mean ± SEM, paired t-test, ns not significant, *** $p < 0.001$.

Figure 4: The CaM inhibitor W7 abolishes enhanced current flow through Orco channels increases after repeated stimulation. (A) Representative traces of whole cell currents recorded from a cell expressing Orco. Currents were obtained by VUAA1 application in the absence (top) and in presence of W7 (bottom). (B) Current amplitudes obtained as described in A (Control, n = 8; W7, n = 8). Data represent mean ± SEM; paired t-test, ns not significant, ** $p < 0.01$.

Figure 1

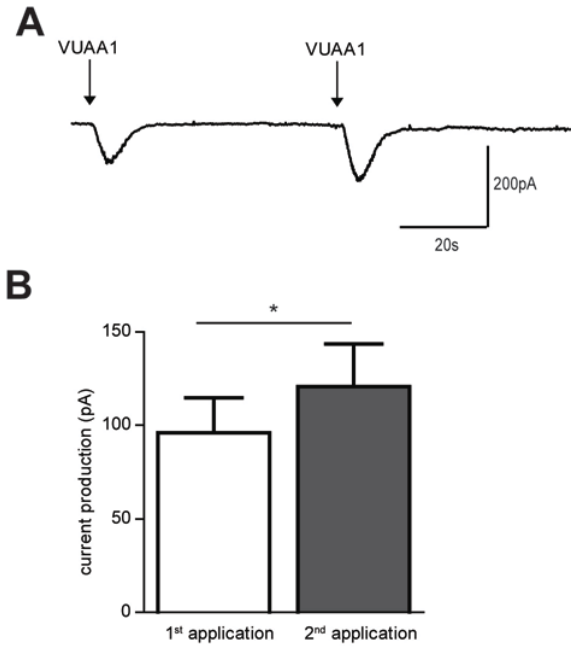

Figure 2

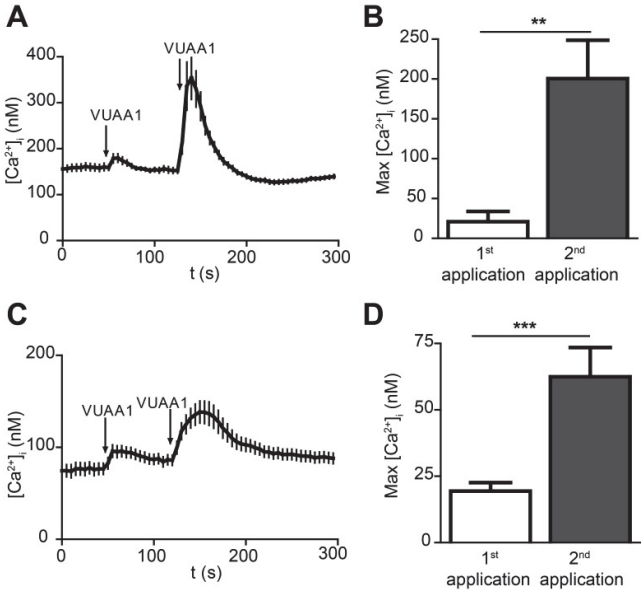

Figure 3

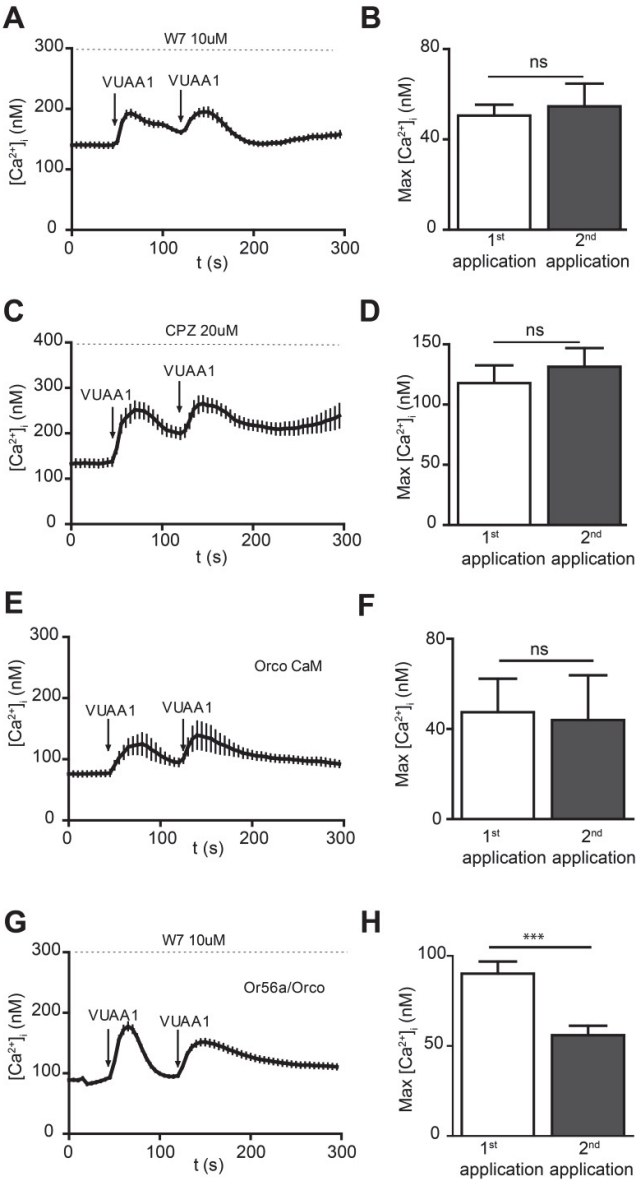
A
W7 10uM
VUAA1
VUAA1
[Ca2+]i (nM)
t (s)
B
ns
Max [Ca2+]i (nM)
1st application
2nd application
C
CPZ 20uM
VUAA1
VUAA1
[Ca2+]i (nM)
t (s)
D
ns
Max [Ca2+]i (nM)
1st application
2nd application
E
Orco CaM
VUAA1
VUAA1
[Ca2+]i (nM)
t (s)
F
ns
Max [Ca2+]i (nM)
1st application
2nd application
G
W7 10uM
Or56a/Orco
VUAA1
VUAA1
[Ca2+]i (nM)
t (s)
H
***
Max [Ca2+]i (nM)
1st application
2nd application

Figure 4

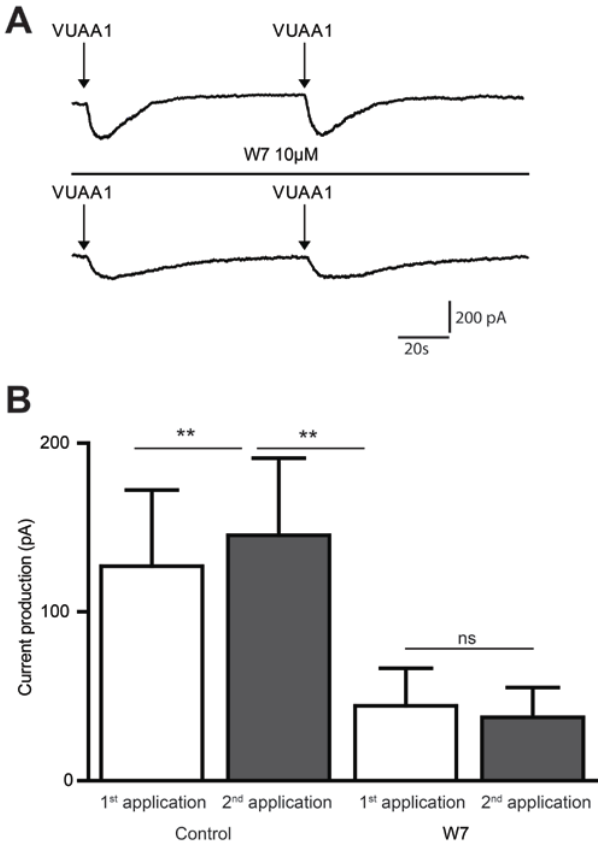
A
VUAA1
VUAA1
W7 10μM
VUAA1
VUAA1
200 pA
20s
B
**
**
200
100
0
Current production (pA)
ns
1st application
2nd application
1st application
2nd application
Control
W7

General Discussion

In the recent years considerable progress has been made in understanding the principles in olfactory signal process in insect OSNs. Work on molecular and cellular characterization of the olfactory process in insects has revealed both commonalities and fundamental differences between vertebrates and insects (Pellegrino and Nakagawa, 2009; Kaupp, 2010). The insect ORs, composed of a ligand-specific OrX protein and the Orco protein, act as ligand gated ion channels (Neuhaus et al., 2005; Benton et al., 2006; Sato et al., 2008; Wicher et al., 2008). In addition, these ORs are controlled by intracellular signaling (Wicher et al., 2008; Kain et al., 2009; Deng et al., 2011; Getahun et al., 2013; Ignatious Raja et al., 2014). The main objective of this thesis was to investigate certain aspects of function and regulation of selected insect ORs.

Function of synthetic Orco dimer construct

The stoichiometry and the number of subunits required to form the ion channel pore of OR or Orco channels is presently unknown. There is heteromeric interaction within the OrX-Orco complex (Neuhaus et al., 2005; Benton et al., 2006), but recent FRET experiments presented also evidence for homomeric interaction between Orco proteins (German et al., 2013). Likewise, reports on the purification of insect OR subunits indicate a potential dimer of a dimer formation of Orco and Or22a (Carraher et al., 2013).

To study the effect of oligomerisation of Orco proteins on channel characteristics, we engineered the simplest oligomeric structure of Orco, the Orco dimer (Orco di) (**manuscript 1**). We asked whether this construct would exhibit similar channel properties like Orco wild type (Orco wt). The Orco di construct and Orco wt were stably expressed in the CHO (Chinese Hamster ovary) cells and their functional properties were determined and compared by performing calcium imaging and patch clamp experiments. Both functional assays have demonstrated that Orco di is activated by the non-odor Orco agonists VUAA1 and OLC12. The Orco di expressing cells displayed membrane current in response to OLC12 stimulation and showed intracellular Ca^{2+} rise in response to VUAA1. The background activity of Orco di channel was similar to Orco wt which indicates a constitutive activity of the construct.

Pharmacological inhibition of calmodulin (CaM) using the CaM inhibitor W7 significantly reduced and prolonged $[Ca^{2+}]_i$ responses obtained upon Orco dimer stimulation. These changes are similar to those previously observed with Orco wt (Mukunda et al., 2014). Coexpression of Orco di and Or22a elicited Ca^{2+} responses in response to agonist VUAA1 as seen in cells expressing Orco 22a/Orco wt. This suggests an interaction of Orco di with OrX proteins. Taken together, Orco di construct shows similar ion channel properties as Orco wt. This result is compatible with the hypothesis that Orco wt may act as homodimer. But this view requires more support, e.g. by studies resolving the crystal structure of Orco complexes.

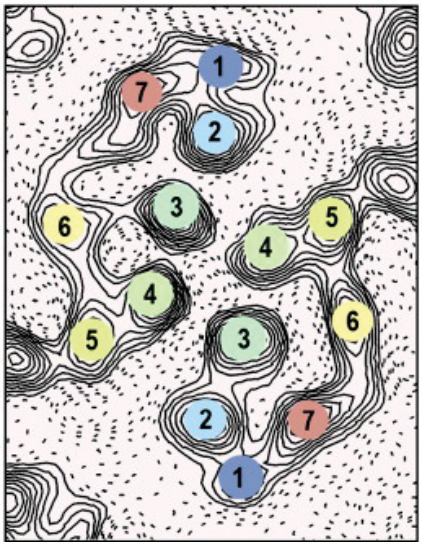

Figure 6: Projection structure of Channelrhodopsin-2 by electro crystallography studies showing the cation conductance pathway formed by third and the fourth TM helix (Mueller et al., 2011)

A recent protein crystallization study revealed the structure of the 7-TM light-gated ion channel Channelrhodopsin-2. The structure of this pore is shaped by two 7-TM monomers. The conductance pathway is located at the dimer interface on the 2-fold axis, lined by transmembrane helices 3 and 4 (Figure 6) (Mueller et al., 2011; Kato et al., 2012). This illustrates one possibility how a pore might be shaped by two Orco monomers.

Odorant receptor function

During insect flight, the perception of odors in the turbulent environment is achieved by arrays of OSNs. The signal for source detection arises from the chemoreceptors expressed in the OSNs. The OSNs express three types of insect chemoreceptors, odorant receptors (ORs), ionotropic glutamate-like receptors (IRs) and gustatory receptors (GRs). These receptor types differ in their response kinetics to brief stimuli (Getahun et al., 2012). The OSNs which express ORs are more sensitive compared to those expressing IRs and Gr expressing neurons (Getahun et al., 2012; Liu et al., 2014).

The ORs belong to the ancient family of chemosensory receptors (Robertson et al., 2003) and their occurrence is restricted to flying insects (Missbach et al., 2014). Insect ORs recognize biologically relevant volatile odorants and pheromones in air. The olfactory cues detected by ORs elicit appropriate behavior in insects. For example, BmOR1, a male specific pheromone receptor for bombykol elicits a full array of sexual behaviors in *B. mori* (Nakagawa et al., 2005); Odorant receptor Or19a which detects terpenes is necessary for oviposition behavior on citrus substrates in *Drosophila* (Dweck et al., 2013).

Similarly, the study in **manuscript 2** shows that the odorant receptor protein Or56a mediates innate avoidance behavior to toxic feeding and breeding substrates infected with bacteria and mold as it detects geosmin, a volatile compound released by those organisms (Becher et al., 2010). Or56a is exclusively activated by geosmin and is part of a functionally segregated olfactory circuit in *Drosophila* (Stensmyr et al., 2012). This sensitive detection system for geosmin is functionally conserved across the drosophilids which indicates a fundamental function for the survival of flies.

Pheromone receptors expressed in OSNs of *M. sexta* and *B. mori* belong to the most sensitive receptors known (Stengl, 2010). For example, the OSNs from *B. mori* can detect even a single pheromone molecule (Kaissling, 1987). A recent study using extracellular single sensillum recording showed that the *Drosophila* ORs can be sensitized through metabotropic autoregulation which requires Orco activation (Getahun et al., 2013). But it remains to be examined which signal transduction machinery is involved in the extreme sensitivity in moths. In **manuscript 3** we investigated the function of Orco in pheromone transduction of *M. sexta*. *In situ* tip recordings from pheromone-sensitive trichoid sensilla of intact *M. sexta* showed no evidence of ionotropic pathway (Nolte et al., 2013). With calcium imaging experiments we could demonstrate that heterologously expressed *Manduca* Orco proteins form a Ca^{2+}-permeable cation channel which is activated by the agonist VUAA1. It still remains to be examined which metabotropic regulation of Orco is involved in moths as demonstrated in *Drosophila* (Stengl and Funk, 2013)

Role of calmodulin in regulation of olfactory receptors

Ca^{2+} ions are important intracellular messengers and play a vital role in the control of intracellular biochemical processes. The cytosolic free intracellular Ca^{2+} concentration of 100 nM at rest can strongly rise when cells are stimulated. This requires a tight regulation as high concentrations are potentially dangerous for the cell. Cytosolic Ca^{2+} is regulated by many Ca^{2+} binding proteins among which calmodulin (CaM) is one of the most potent biochemically efficient regulators (Berridge et al., 2000).

Insect ORs act as non-selective cation channels which also conduct Ca^{2+} ions. The OR activation by odor stimulation causes increased calcium influx into the OSN. The work in **manuscript 4** was aimed to investigate the effects of CaM on insect ORs. We hypothesized that CaM might play an important role in peripheral olfactory signaling by regulating insect OR function. To specify the role of CaM in the regulation of insect OR function we used a heterologous expression system to express Orco and ORs composed of OrX/Orco proteins. Using Ca^{2+} imaging we examined the effect of CaM inhibition on the intracellular Ca^{2+} responses elicited by stimulation of the OR proteins. Pharmacological CaM inhibition and overexpression of CaM mutants (N terminal and C-terminal) showed that the Ca^{2+} responses from cells expressing Orco protein became weaker and were more prolonged. In addition, by screening for CaM binding sites in insect ORs, we identified the putative CaM binding motif ^{336}SAIKYWVER^{344} within the second intracellular loop of the Orco protein. This motif is highly conserved in Orco proteins from other insect species indicating an important functional role. A point mutation K339N within the putative CaM site affected the Ca^{2+} responses of the Orco protein as previously observed for CaM inhibition. But with heteromeric ORs, CaM inhibition showed a variable OrX protein-specific effect.

Taken together, this study using heterologous expression system provides substantial evidence that CaM activity affects the function of Orco channel and that the direct effect of CaM inhibition on OrX/Orco heteromers is differential and depends on the OrX protein. Since OR sensitization was dependent on Orco function (Getahun et al., 2013) we propose that CaM regulation of Orco may affect ORs via an as yet unknown mechanism.

Olfactory receptor sensitization

A recent study on insect odorant response sensitivity suggests that metabotropic regulation of Orco regulates the OR sensitization (Getahun et al., 2013). But the mechanism by which Orco activation leads to OR sensitization is not known. In **manuscript 5** we show that repeated stimulation induces enhanced responses in heterologously expressed OR proteins. The sensitization event was observed both in electrophysiological recordings as well as calcium imaging experiments. As described in manuscript 4, CaM modulates the responses of Orco channels to agonist stimulation. Hence we hypothesized that CaM might be also involved in Orco sensitization. We could show that sensitization was abolished when we applied CaM inhibitors or used the Orco CaM mutant (K339N). Furthermore, in presence of CaM inhibitor W7 the complete OR construct represented by Or56a/Orco did not show an increased response on second stimulation. Thus, these experiments support the view that CaM activity is required for mediating sensitization in insect ORs. To understand the molecular mechanism involved in insect OR sensitization it is essential to find more players involved in regulating the sensitivity of ORs. Recently published articles from Liu et al., and Ha et al., identify an aminophospholipid transferase, dATP8B as a critical factor for proper OR function and trafficking. Mutation in the dATP8B gene strongly reduces the sensitivity of OR expressing neurons, but not IRs (Ha et al., 2014; Liu et al., 2014).

In manuscript 4 and 5 we show that CaM plays a modulatory role in insect odorant receptor function. Free $[Ca^{2+}]_i$ is an important parameter that controls the function of Orco (Sargsyan et al., 2011). A recent study performed on heterologously expressed insect ORs revealed an amplification of odor induced calcium responses through activation of intracellular Ca^{2+} release channels (Ignatious Raja et al., 2014). Further *in vivo* studies on intracellular calcium signaling are required to understand its role in olfactory signaling.

Conclusions and future directions

In the past decade there has been much progress in understanding the basal function of insect olfaction. In addition to studies showing that insect OR complexes (OrX-Orco) form ligand gated ion channels (Sato et al., 2008; Smart et al., 2008; Wicher et al., 2008;

Yao and Carlson, 2010), there is also growing evidence for a slower and more sensitive metabotropic response induced by cAMP binding to Orco (Wicher et al., 2008; Kain et al., 2009; Deng et al., 2011). Furthermore, it has been shown that Orco which acts as an ion channel by itself also regulated by phosphorylation via PKC (Getahun et al., 2013; Sargsyan et al., 2011).

It is still unknown how the subunits of the OrX-Orco complex form an ion channel pore. For example, each subunit of this complex can build an independent ion channel or they could together form a pore. By constructing a synthetic Orco dimer we show in manuscript 1 that it functions as a channel with similar properties as Orco wt. This result is compatible with the hypothesis that the Orco wt channel is as a homodimer. In manuscript 4 we show that CaM plays a role in regulating insect OR function. We could show that CaM affects the function of Orco and that the regulation of ORs depends on the Orco regulation by CaM. Finally, the results from manuscript 5 indicate a role of CaM in the sensitization process of insect ORs as the disruption of CaM activity abolished the sensitization in heterologously expressed insect ORs.

Future mutational analysis of determinants of putative CaM binding site of OrX proteins might be helpful in understanding the details of CaM in mediating olfactory signaling. For example, the sensitive detection of geosmin by Or56a is important for fly's survival (manuscript 2). Our calcium imaging results in manuscript 4 indicate that normal function of CaM amplifies the Ca^{2+} influx during Or56a/Orco activation by geosmin. This leads to a new hypothesis that CaM might provide an intracellular amplification mechanism of a signal critical for survival of flies. Since OrX-Orco signaling is dependent on intracellular signaling there is a need for identification of other regulators involved in this complex signaling cascade. A recent report suggests a role of intracellular Ca^{2+} release in amplifying the odor response (Ignatious Raja et al., 2014). Thus, a further analysis of the role of $[Ca^{2+}]_i$ using *in vivo* studies should be performed.

Summary

Early flying insects evolved around 300 million years ago; since then, the insects have gained an overwhelming ability to adapt. They have become evolutionarily successful, hence the most diverse and dominant group of organisms on earth. Insects have an exquisite sensitive olfactory system that allows them to recognize and discriminate odor plumes even at extremely low concentrations in a turbulent environment. The detection and appropriate response to the chemical cues in the environment is essential for their survival. In the past decade there has been much progress in understanding the basal function of insect olfaction but what we still lack is a deep understanding of the mechanisms leading to the exceptional sensitivity of olfaction. This knowledge is important in providing links to the odor mediated behavior of the insects which leads to design of strategies for insect control. In order to design ways to regulate olfactory sensitivity in insects it is necessary to know the details of insect olfactory signal transduction pathway. The main objective of this thesis is to understand the function and regulation of insect olfactory receptors. To address our questions we employed pharmacological, molecular and physiological approaches on heterologously expressed insect olfactory receptors.

The insect odorant receptors (ORs) form heteromeric complexes composed of a ligand binding protein (OrX) and a highly conserved ubiquitous correceptor Orco. But the actual stoichiometry of this complex is unknown. Recent reports also suggest the presence of homomeric interactions between Orco proteins. In order to understand the function of Orco channel as an oligomer, we artificially engineered a minimal oligomeric construct, Orco dimer (Orco di) and expressed it in CHO (Chinese Hamster Ovary cells). Using calcium imaging and patch clamp techniques we show that the application of synthetic Orco agonists VUAA1 and OLC12 activate the Orco di construct and the Orco wt. Our results demonstrate that Orco di forms a calcium permeable ion channel. In addition, we show that Orco di also interacts with Or22a in a similar to Orco wt. Our experiments show that the functional properties of the Orco di construct are similar to those of Orco wt. These results are in line with view that Orco wt may form homodimers. However, our experimental design does not prove this hypothesis.

Detection of harmful substrates in the environment is necessary for the survival of the insects. Flies, for example avoid geosmin, a volatile compound produced by many toxic microbes and fungi. In our study, using calcium imaging and deorphanization techniques, we identify an odorant receptor, namely Or56a which exclusively detects geosmin thereby alerting the flies to the presence of harmful microbes. The activation of this receptor alerts the flies and triggers an immediate flight response.

Furthermore, we investigated the functional role of Orco in pheromone transduction in tobacco hornworm *Manduca sexta.* The pheromone receptors of *Manduca* are among the most sensitive receptors known. We expressed *Manduca* Orco in HEK293 (Human embryonic kidney) cells and were able to show by means of calcium imaging, that the Orco agonist VUAA1 leads to calcium influx. Thus we have shown that *Manduca* Orco protein acts as a Ca^{2+} permeable channel mediating the pheromone response as a pacemaker.

In addition to functional studies, this thesis provides insights on the regulation of insect olfactory receptor activity. In order to understand how intracellular calcium influx is regulated in the insects ORs we investigated the role of the ubiquitous Ca^{2+} binding protein calmodulin (CaM) in insect odorant receptor function. We identified a conserved putative CaM binding motif ^{336}SAIKYWVER^{344} in the second intracellular loop of Orco protein indicating an important functional role. Pharmacological inhibition and overexpression of CaM mutants in heterologously expressed insect ORs showed that inhibition of CaM activity affects Ca^{2+} response of Orco channel. The effect of CaM inhibition could be mimicked by a point mutation in the putative CaM site (K339N). But with heteromeric ORs, CaM inhibition affected the response of ORs in OrX specific manner. Given that, Orco is a ubiquitous constituent of insect ORs and the regulation of heteromers probably depends on the function of Orco, our results give ample evidence for CaM activity in modulating the function of insect odorant receptors. In a further study, where we replicated the process of sensitization event in heterologously expressed insect ORs, we observed that inhibition of CaM abolished this event. These results suggests a role of CaM in the Orco-mediated OR sensitization.

Zusammenfassung

Seit dem ersten Auftreten fliegender Insekten vor 300 Millionen Jahren haben sich die Insekten über die Erde ausgebreitet und eine erstaunliche Fähigkeit zur Anpassung an ökologische Nischen entwickelt. Insekten stellen die artenreichste Tiergruppe dar. Ihren evolutionären Erfolg verdanken sie nicht zuletzt ihrem hochentwickelten Geruchssinn, der es ihnen gestattet, Duftwolken geringster Konzentration in turbulenter Luftströmung wahrzunehmen und zu unterscheiden. Die Wahrnehmung chemischer Signale und die Auslösung einer angemessenen Verhaltensantwort darauf ist überlebenswichtig. Im vergangenen Jahrzehnt ist ein wesentlicher Fortschritt im Verständnis der grundlegenden Funktion olfaktorischer Rezeptoren der Insekten zu verzeichnen. Noch unverstanden sind gegenwärtig allerdings noch die Mechanismen, die die extreme Sensitivität der Geruchsrezeptoren bedingen. Die Kenntnis dieser kann zum Verständnis der Verhaltenssteuerung der Insekten beitragen und damit zur Entwicklung neuer Strategien deren Verhalten zu kontrollieren. Um Wege zu finden, wie man das Geruchsvermögen manipulieren kann, ist die Kenntnis der Signalverarbeitung erforderlich. Hauptziel der vorliegenden Arbeit war es, einen Beitrag zum Verständnis der Funktion und der Regulation von Geruchsrezeptoren der Insekten zu liefern. Zu diesem Zweck wurden molekulare, pharmakologische und physiologische Methoden eingesetzt, um heterolog exprimierte Geruchsrezeptoren zu untersuchen.

Insekten-Geruchsrezeptoren („odorant receptors, ORs) bilden Heteromere unbekannter Stöchiometrie aus einen duftspezifischen Protein (OrX) und einem universellen Korezeptorprotein (Orco). Kürzlich erschienene Arbeiten legen auch die Existenz homomerer Interaktionen zwischen Orco-Proteinen nahe. Um den Effekt einer Oligomerisierung von Orco-Proteinen auf deren Kanaleigenschaften zu studieren, stellten wir ein Orco-Dimerkonstrukt (Orco di) her und exprimierten dieses in CHO (chinese hamster ovary) Zellen. Unter Verwendung von Calciumimaging und Elektrophysiologie (Patch clamp) konnte die funktionelle Expression von Orco di gezeigt werden. Die Applikation der synthetischen Orco-Agonisten VUAA1 und OLC12 aktivierten Orco di in vergleichbarer Weise wie Orco. Orco di bildet mithin einen Ca^{2+}-permeablen Ionenkanal, ebenso konnten wir am Beispiel von Or22a zeigen, daß Orco di mit OrX-Proteinen interagiert. Damit wies Orco di vergleichbare Eigenschaften wie Orco auf, was

mit der Hypothese vereinbar ist, daß Orco-Kanäle aus Dimeren bestehen. Allerdings lässt sich diese Vermutung nicht mit unserem Versuchsansatz beweisen.

Das Aufspüren gefährlicher Substanzen in der Umwelt und deren Meidung ist auch für Insekten überlebenswichtig. Fliegen meiden beispielsweise Geosmin, ein flüchtiges Produkt toxischer Mikroben und Pilze. Es gelang uns, das für die Geosminwahrnehmung zuständige Rezeptorprotein als Or56a zu identifizieren. Die Aktivierung dieses Rezeptors alarmiert das Tier und löst eine unmittelbare Fluchtreaktion aus.

In einer weiteren Studie untersuchten wir den Beitrag von Orco für die Pheromonwahrnehmung des Tabakschwärmers *Manduca sexta*. Die Pheromonrezeptoren von *Manduca* zählen zu den sensitivsten Rezeptoren überhaupt. Wir exprimierten *Manduca* Orco in HEK293 (human embryonic kidney) Zellen und konnten mittels Calciumimaging zeigen, daß der Orco-Agonist VUAA1 zu einem Ca^{2+}-Einstrom führt. Damit ist gezeigt, daß das *Manduca* Orcoprotein einen Ca^{2+}- permeablen Kationenkanal bildet, der als Schrittmacher die Pheromonantwort vermittelt.

Ein weiterer Aspekt der vorgestellten Untersuchungen war der Regulation der Rezeptoraktivitätt gewidmet. Da die Rezeptoraktivierung zu einem Ca^{2+}-Einstrom führt, fragten wir, wie dieser Einstrom seinerseits reguliert wird und ob das Ca^{2+}-Bindeprotein Calmodulin (CaM) hierbei eine Rolle spielt. Wir identifizierten ein konserviertes, putatives CaM-Bindemotif ^{336}SAIKYWVER^{344} im zweiten intrazellulären Loop des Orco-Proteins, was auf eine funktionelle Rolle hindeutet. Mittels pharmakologischer Inhibition von CaM bzw. Überexpression von CaM-Mutanten konnten wir zeigen, daß CaM die Orco-Funktion modifiziert. Der Effekt der CaM-Inhibition konnte durch eine Punktmutation im CaM-Motiv in Orco (K339N) imitiert werden. Werden komplette OrX/Orco-Heteromere exprimiert, führt CaM-Inhibition zu einer OrX-spezifischen Modulation. Daher ist es unwahrscheinlich, daß CaM zu einer globalen Regulation der OR-Funktion führt. Die funktionelle Rolle der Orco-Modulation durch Orco ist zunächst noch unklar. In einer weiteren Studie beobachteten und untersuchten wir den Prozess der OR-Sensitisierung im heterologen Expressionssystem. Während wir unter Kontrollbedingungen bei wiederholter Stimulation eine erhöhte Antwort erhielten, entfiel dies bei Inhibition von CaM. Dieses Resultat deutet auf eine Rolle von CaM in der Orco-vermittelten OR-Sensitisierung.

References

Becher, P.G., Bengtsson, M., Hansson, B.S., and Witzgall, P. (2010). Flying the Fly: Long-range Flight Behavior of *Drosophila melanogaster* to Attractive Odors. *J Chem Ecol* 36**,** 599-607.

Benton, R., Sachse, S., Michnick, S.W., and Vosshall, L.B. (2006). Atypical membrane topology and heteromeric function of *Drosophila* odorant receptors in vivo. *Plos Biology* 4**,** 240-257.

Benton, R., Vannice, K.S., Gomez-Diaz, C., and Vosshall, L.B. (2009). Variant Ionotropic Glutamate Receptors as Chemosensory Receptors in *Drosophila*. *Cell* 136**,** 149-162.

Berridge, M.J., Lipp, P., and Bootman, M.D. (2000). The versatility and universality of calcium signalling. *Nat Rev Mol Cell Bio* 1**,** 11-21.

Buck, L., and Axel, R. (1991). A novel multigene family may encode odorant receptors: A molecular basis for odor recognition. *Cell* 65**,** 175-187.

Chen, S., and Luetje, C.W. (2012). Identification of New Agonists and Antagonists of the Insect Odorant Receptor Co-Receptor Subunit. *Plos One* 7.

Clyne, P.J., Warr, C.G., Freeman, M.R., Lessing, D., Kim, J.H., and Carlson, J.R. (1999). A novel family of divergent seven-transmembrane proteins: Candidate odorant receptors in *Drosophila*. *Neuron* 22**,** 327-338.

Deng, Y., Zhang, W., Farhat, K., Oberland, S., Gisselmann, G., and Neuhaus, E.M. (2011). The Stimulatory G alpha(s) Protein Is Involved in Olfactory Signal Transduction in *Drosophila*. *Plos One* 6.

Dweck, H.K.M., Ebrahim, S.A.M., Kromann, S., Bown, D., Hillbur, Y., Sachse, S., Hansson, B.S., and Stensmyr, M.C. (2013). Olfactory Preference for Egg Laying on Citrus Substrates in *Drosophila*. *Current Biology* 23**,** 2472-2480.

Faas, G.C., Raghavachari, S., Lisman, J.E., and Mody, I. (2011). Calmodulin as a direct detector of Ca^{2+} signals. *Nat Neurosci* 14**,** 301-304.

Gao, Q., and Chess, A. (1999). Identification of candidate *Drosophila* olfactory receptors from genomic DNA sequence. *Genomics* 60**,** 31-39.

German, P.F., Van Der Poel, S., Carraher, C., Kralicek, A.V., and Newcomb, R.D. (2013). Insights into subunit interactions within the insect olfactory receptor complex using FRET. *Insect Biochem Mol Biol* 43**,** 138-145.

Getahun, M.N., Olsson, S.B., Lavista-Llanos, S., Hansson, B.S., and Wicher, D. (2013). Insect Odorant Response Sensitivity Is Tuned by Metabotropically Autoregulated Olfactory Receptors. *Plos One* 8.

Getahun, M.N., Wicher, D., Hansson, B.S., and Olsson, S.B. (2012). Temporal response dynamics of *Drosophila* olfactory sensory neurons depends on receptor type and response polarity. *Front Cell Neurosci* 6.

Grienberger, C., and Konnerth, A. (2012). Imaging Calcium in Neurons. *Neuron* 73**,** 862-885.

Ha, T.S., Xia, R., Zhang, H., Jin, X., and Smith, D.P. (2014). Lipid flippase modulates olfactory receptor expression and odorant sensitivity in *Drosophila*. *Proc Natl Acad Sci U S A*.

Hansson, B.S. (1995). Olfaction in Lepidoptera. *Experientia* 51**,** 1003-1027.

Ignatious Raja, J.S., Katanayeva, N., Katanaev, V.L., and Galizia, C.G. (2014). Role of Go/i subgroup of G proteins in olfactory signaling of *Drosophila melanogaster*. *Eur J Neurosci* 39**,** 1245-1255.

Jones, P.L., Pask, G.M., Rinker, D.C., and Zwiebel, L.J. (2011). Functional agonism of insect odorant receptor ion channels (vol 108, pg 8821, 2011). *Proc Natl Acad Sci U S A* 108**,** 11298-11298.

Kain, P., Chandrashekaran, S., Rodrigues, V., and Hasan, G. (2009). *Drosophila* Mutants in Phospholipid Signaling Have Reduced Olfactory Responses as Adults and Larvae. *J Neurogenet* 23**,** 303-312.

Kaissling, K.-E. (1987). Stimulus transduction. In: Colbow K. Burnaby (Canada): Simon Fraser University: R.H. Wright lectures on insect olfaction).

Kato, H.E., Zhang, F., Yizhar, O., Ramakrishnan, C., Nishizawa, T., Hirata, K., Ito, J., Aita, Y., Tsukazaki, T., Hayashi, S., Hegemann, P., Maturana, A.D., Ishitani, R., Deisseroth, K., and Nureki, O. (2012). Crystal structure of the channelrhodopsin light-gated cation channel. *Nature* 482**,** 369-374.

Kaupp, U.B. (2010). Olfactory signalling in vertebrates and insects: differences and commonalities. *Nat Rev Neurosci* 11**,** 188-200.

Kumar, B.N., Taylor, R.W., Pask, G.M., Zwiebel, L.J., Newcomb, R.D., and Christie, D.L. (2013). A Conserved Aspartic Acid Is Important for Agonist (VUAA1) and Odorant/Tuning Receptor-Dependent Activation of the Insect Odorant Co-Receptor (Orco). *Plos One* 8.

Larsson, M.C., Domingos, A.I., Jones, W.D., Chiappe, M.E., Amrein, H., and Vosshall, L.B. (2004). Or83b encodes a broadly expressed odorant receptor essential for *Drosophila* olfaction. *Neuron* 43**,** 703-714.

Liu, Y.C., Pearce, M.W., Honda, T., Johnson, T.K., Charlu, S., Sharma, K.R., Imad, M., Burke, R.E., Zinsmaier, K.E., Ray, A., Dahanukar, A., De Bruyne, M., and Warr, C.G. (2014). The *Drosophila melanogaster* phospholipid flippase dATP8B is required for odorant receptor function. *PLoS Genet* 10**,** e1004209.

Lundin, C., Kall, L., Kreher, S.A., Kapp, K., Sonnhammer, E.L., Carlson, J.R., Von Heijne, G., and Nilsson, I. (2007). Membrane topology of the *Drosophila* OR83b odorant receptor. *Febs Letters* 581**,** 5601-5604.

Martin, S.R., Teleman, A.A., Bayley, P.M., Drakenberg, T., and Forsen, S. (1985). Kinetics of calcium dissociation from calmodulin and its tryptic fragments. A stopped- flow flurescence study using Quin 2 reveals a two domain structure. *Eur J Biochem* 151**,** 543-550.

Missbach, C., Dweck, H.K.M., Vogel, H., Vilcinskas, A., Stensmyr, M.C., Hansson, B.S., and Grosse-Wilde, E. (2014). Evolution of insect olfactory receptors. *Elife* 3.

Mukunda, L., Miazzi, F., Kaltofen, S., Hansson, B.S., and Wicher, D. (2014). Calmodulin modulates insect odorant receptor function. *Cell Calcium* 55**,** 191-199.

Mueller, M., Bamann, C., Bamberg, E., and Kuhlbrandt, W. (2011). Projection structure of channelrhodopsin-2 at 6 A resolution by electron crystallography. *J Mol Biol* 414**,** 86-95.

Nakagawa, T., Pellegrino, M., Sato, K., Vosshall, L.B., and Touhara, K. (2012). Amino Acid Residues Contributing to Function of the Heteromeric Insect Olfactory Receptor Complex. *Plos One* 7.

Nakagawa, T., Sakurai, T., Nishioka, T., and Touhara, K. (2005). Insect sex-pheromone signals mediated by specific combinations of olfactory receptors. *Science* 307**,** 1638-1642.

Neuhaus, E.M., Gisselmann, G., Zhang, W.Y., Dooley, R., Stortkuhl, K., and Hatt, H. (2005). Odorant receptor heterodimerization in the olfactory system of *Drosophila* melanogaster. *Nat Neurosci* 8**,** 15-17.

Nolte, A., Funk, N.W., Mukunda, L., Gawalek, P., Werckenthin, A., Hansson, B.S., Wicher, D., and Stengl, M. (2013). In situ Tip-Recordings Found No Evidence for an Orco-Based Ionotropic Mechanism of Pheromone-Transduction in Manduca sexta. *Plos One* 8.

Pellegrino, M., and Nakagawa, T. (2009). Smelling the difference: controversial ideas in insect olfaction. *J Exp Biology* 212**,** 1973-1979.

Robertson, H.M., Warr, C.G., and Carlson, J.R. (2003). Molecular evolution of the insect chemoreceptor gene superfamily in *Drosophila* melanogaster. *Proc Natl Acad Sci U S A* 100**,** 14537-14542.

Sanchez-Gracia, A., Vieira, F.G., and Rozas, J. (2009). Molecular evolution of the major chemosensory gene families in insects. *Heredity* 103**,** 208-216.

Sargsyan, V., Getahun, M.N., Llanos, S.L., Olsson, S.B., Hansson, B.S., and Wicher, D. (2011). Phosphorylation via PKC regulates the function of the *Drosophila* odorant co-receptor. *Front Cell Neurosci* 5.

Sato, K., Pellegrino, M., Nakagawa, T., Nakagawa, T., Vosshall, L.B., and Touhara, K. (2008). Insect olfactory receptors are heteromeric ligand-gated ion channels. *Nature* 452**,** 1002-U1009.

Schneider.D (1969). Insect Olfaction-Deciphering System for Chemical Messages. *Science* 163**,** 1031-&.

Schwaller, B. (2012). The Regulation of a Cell's Ca^{2+} Signaling Toolkit: The Ca^{2+} Homeostasome. *Adv Exp Med Biol* 740**,** 1-25.

Smart, R., Kiely, A., Beale, M., Vargas, E., Carraher, C., Kralicek, A.V., Christie, D.L., Chen, C., Newcomb, R.D., and Warr, C.G. (2008). *Drosophila* odorant receptors are novel seven transmembrane domain proteins that can signal independently of heterotrimeric G proteins. *Insect Biochem Mol Biol* 38**,** 770-780.

Steinbach, J.H., and Akk, G. (2011). Use of Concatemers of Ligand-Gated Ion Channel Subunits to Study Mechanisms of Steroid Potentiation. *Anesthesiology* 115**,** 1328-1337.

Stengl, M. (2010). Pheromone transduction in moths. *Front Cell Neurosci* 4.

Stengl, M., and Funk, N.W. (2013). The role of the coreceptor Orco in insect olfactory transduction. *J Comp Physiol A Neuroethol Sensory Neural Behav Physiol* 199**,** 897-909.

Stensmyr, M.C., Dweck, H.K.M., Farhan, A., Ibba, I., Strutz, A., Mukunda, L., Linz, J., Grabe, V., Steck, K., Lavista-Llanos, S., Wicher, D., Sachse, S., Knaden, M., Becher, P.G., Seki, Y., and Hansson, B.S. (2012). A Conserved Dedicated Olfactory Circuit for Detecting Harmful Microbes in *Drosophila*. *Cell* 151**,** 1345-1357.

Taylor, R.W., Romaine, I.M., Liu, C., Murthi, P., Jones, P.L., Waterson, A.G., Sulikowski, G.A., and Zwiebel, L.J. (2012). Structure-Activity Relationship of a Broad-Spectrum Insect Odorant Receptor Agonist. *Acs Chem Biol* 7**,** 1647-1652.

Tsung-Yu, C., and King-Wai, Y. (1994). Direct modulation by Ca^{2+}-calmodulin of cyclic nucleotide-activated channel of rat olfactory receptor neurons. *Nature* 368**,** 545-548.

Van Petegem, F., Chatelain, F.C., and Minor, D.L. (2005). Insights into voltage-gated calcium channel regulation from the structure of the Ca(V)1.2 IQ domain-Ca^{2+}/calmodulin complex. *Nat Struct Mol Biol* 12**,** 1108-1115.

Vosshall, L.B., Amrein, H., Morozov, P.S., Rzhetsky, A., and Axel, R. (1999). A spatial map of olfactory receptor expression in the *Drosophila* antenna. *Cell* 96**,** 725-736.

Vosshall, L.B., and Hansson, B.S. (2011). A Unified Nomenclature System for the Insect Olfactory Coreceptor. *Chem Senses* 36**,** 497-498.

Vosshall, L.B., and Stocker, R.E. (2007). Molecular architecture of smell and taste in *Drosophila*, in *Annu Rev of Neurosci*, 505-533.

Wicher, D., Schaefer, R., Bauernfeind, R., Stensmyr, M.C., Heller, R., Heinemann, S.H., and Hansson, B.S. (2008). *Drosophila* odorant receptors are both ligand-gated and cyclic-nucleotide-activated cation channels. *Nature* 452**,** 1007-U1010.

Wistrand, M., Kall, L., and Sonnhammer, E.L.L. (2006). A general model of G protein-coupled receptor sequences and its application to detect remote homologs. *Protein Sci* 15**,** 509-521.

Yao, C.A., and Carlson, J.R. (2010). Role of G-Proteins in Odor-Sensing and CO_2-Sensing Neurons in *Drosophila*. *J Neurosci* 30**,** 4562-4572.

Declaration of Independent Assignment

I declare in accordance with the conferral of the degree of doctor from the School of Biology and Pharmacy of Friedrich-Schiller-University Jena that the submitted thesis was written only with the assistance and literature cited in the text.

People who assisted in experiments, data analysis and writing of the manuscripts are listed as co-authors of the respective manuscripts. I was not assisted by a consultant for doctorate theses.

The thesis has not been previously submitted whether to the Friedrich-Schiller-University, Jena or to any other university.

Jena, June 17, 2014

Latha Mukunda Shivalingaiah

Curriculum vitae

Personal data

Name: **Latha Mukunda Shivalingaiah**
Date of birth: 01.01.1985
Address: 172,2nd C main, 8th block, Koramangala
Bangalore -560095, Karnataka, India
e-mail: lmukunda@ice.mpg.de
latha.mukunda@gmail.com

Education:

October 2009 to present, PhD student**,** Max Planck institute of Chemical Ecology, Germany Department of Evolutionary Neuroethology, Thesis: 'Function and regulation of insect olfactory receptors' Supervisors: PD Dr. D. Wicher and Prof. Dr. Bill. S. Hansson

Year 2007, Master of Science (Genetics) University of Mysore, India
Year 2005, Bachelors in Science (Chemistry, Botany, Zoology), University of Mysore, India

---

Work experience:

Year 2008-2009, Project assistant in Department of Molecular Reproduction and Developmental Biology, Indian Institute of Science (IISc) Bangalore, India
Advisors: Professor Sandhya. S. Visveswaraiah and Dr. Upendra Nongthomba
Research topic: Functional and physiological analysis of an evolutionary conserved phosphodiesterase gene using *Drosophila melanogaster* as a model organism using reverse genetics approach.

Awards:

SPP ISOT student travel grant (DFG Schwerpunktprogramm (SPP) 1392: Integrative Analysis of Olfaction) 2012

Publications :

Mukunda, L., Miazzi, F., Kaltofen, S.,Hansson,B., Wicher,D. (2014). Calmodulin modulates insect odorant receptor function. Cell Calcium, 55, 191-199.

Nolte, A., Funk, N., Mukunda, L., Gawalek, P., Werckenthin, A., Gawalek, P., Hansson, B., Wicher, D., Stengl, M. (2013). In situ tip-recordings found no evidence for an Orco-based ionotropic mechanism of pheromone-transduction in *Manduca sexta*. PLoS One, 8(5): e62648.

Stensmyr, M. C., Dweck, H., Farhan, A., Ibba, I., Strutz, A., Mukunda, L., Linz, J., Grabe, V., Steck, K., Lavista Llanos, S., Wicher, D., Sachse, S., Knaden, M., Becher, P. G., Seki, Y., Hansson, B. (2012). A conserved dedicated olfactory circuit for detecting harmful microbes in *Drosophila*. Cell, 151(6), 1345-1357.

Oral presentation

Mukunda L. Sniffing around ion channels. 10th IMPRS Symposium, MPI for Chemical Ecology, Dornburg, DE, Feb 2011

Mukunda L. Dissecting ion channels in vivo. Chemical Ecology 2010 Mini-Symposium, Jena, DE, Sep 2010

Poster presentation

Miazzi F. *, Mukunda L., Kaltofen S., Hansson B.S., Wicher D. Calmodulin modulates insect odorant receptor function. SAB meeting 2014, MPI for Chemical Ecology, Jena, DE, May 2014

Mukunda L.*, Miazzi F., Hansson B.S., Wicher D. Calmodulin affects the insect odorant receptor function. ICE Symposium, MPI for Chemical Ecology, Jena, DE, Sep 2013

Mukunda L.*, Sargsyan V., Lavista Llanos S., Hansson B.S., Wicher D. Functional properties of oligomeric constructs of the *Drosophila* Odorant Co-receptor Orco. 10th Göttingen Meeting of the German Neuroscience Society, Göttingen, DE, Mar 2013

Nolte A.*, Mukunda L., Funk N., Gawalek P., Körte S., Wicher D., Hansson B.S., Stengl M. Modulation of Pheromone responses in antennal trichoid sensilla of the hawkmoth *Manduca Sexta* by Orco agonism and antagonism. 10th Göttingen Meeting of the German Neuroscience Society, Göttingen, DE, Mar 2013

Mukunda L.*, Lavista Llanos S., Hansson B.S., Wicher D. Oligomerization of the *Drosophila* Orco channel. XVI International Symposium on Olfaction and Taste (ISOT), Stockholm, SE, Jun 2012

Mukunda L.*, Oligomerisation study in *Drosophila* Orco channel. 11th IMPRS Symposium, MPI for Chemical Ecology, Dornburg, DE, Feb 2012

Mukunda L.*, Lavista Llanos S., Wicher D., Hansson B.S. Dissecting ion channel properties of OR83b. Neuro DoWo (22nd Neurobiology PhD Student Workshop), Universtität Bonn, Bonn, DE, Jul 2011

Mukunda L.* Deciphering olfactory mechanism in *Drosophila melanogaster*. 9th IMPRS Symposium, MPI for Chemical Ecology, Dornburg, DE, Feb 2010

Richa Tyagi.*, Avinash R. Shenoy., Latha M. Shivalingaiah.,Upendra Nongthomba.,Sandhya S. Visweswariah. Biochemical analysis and function of the 239FB gene family: From flies to man. EMBO meeting Amsterdam, Netherlands Aug 2009

Courses attended:

Neurobiology course: Insect Neurobiology course Feb 1st to Feb 12th 2010, Division of Chemical Ecology, SLU Alnarp , (Swedish University of Agricultural Sciences), Alnarp 230 53 Sweden

Acknowledgements

They say
'It's not where you end up that means as much
As the road that you travel along.
And it's not the result that counts as much
As the progress that makes you strong.
Since it's not the destination. . . *It's the journey.'*

This journey through my PhD would not have been possible without the contribution and support from many people throughout the years. I would like to convey my gratitude to all those who helped me to come so far.

First and foremost I would like to thank my supervisors Bill Hansson and Dieter Wicher for accepting me as a student in this department. Thanks for all the advice and guidance throughout my doctoral training. I have always admired you both for your unique qualities. I am very glad to have worked under you as a student.

To Bill, you are the best Boss ever. It's great to be a part of your scientific family. Thank you so much for being so kind and friendly. Thanks for all the support and words of encouragement especially when I was frustrated and struggling with my projects.

Big thanks to Dieter for the everyday supervision during my PhD. This work would not have been possible without your outstanding scientific expertise and your constant support and help. Thanks for all the helpful discussions and your patience with me especially with my stupid mistakes.

I would like to thank Prof. Stefan Heinemann for the external supervision and valuable inputs during committee meetings.

Thanks to Prof. Monika Stengl and Marcus Stensmyr for their project collaborations.

Thanks to all the patch lab members Sabine, Vard, Fabio, Susie, Sarah, Kerstin and Nico. Vard and Kerstin thank you for helping with patch clamp set up and Nico for calcium imaging. Fabio, thanks for all the help and the fun times in the lab.

Sabine, I owe you special thanks for preparing all the countless cell plates and for ordering chemicals whenever I needed them. Also thank you for your help with my apartment and health insurance issues.

Sofia thanks for all the helpful discussions with my projects. Thanks a lot for all the stroop wafles and the Argentinian mate cup.

Regi, Thank you for being so sweet to me all the time. Don't forget your kleines freund.

Swetlana, thank you for helping me with all the administrative issues.

To all my past and present officemates Sofia, Jaime, Elisa, Anna, Elisabeth, Franzi, Yoichi and Kathrin thanks for the friendly atmosphere.

I wish to thank all the present and past members of the Hansson family for all the warmth and good times. Thanks for all the delicious cakes and especially for the fun and dancing during group

retreats. It was a pleasure working with all of you. I have always loved this department and I will miss you all a lot.

Thanks to Max Planck society for funding my doctoral work and thanks to SPP (1392) for ISOT travel grant.

Thanks to Daniel and the IT department for all the technical help.

Special thanks to Myroslava for all the yummy chocolates, cookies, cakes, road trips and most importantly your warmth and affection. Tara, Lucie and Peter thank you for all the good energy during the initial years of my PhD.

To all my good friends in Jena especially Samay, Abith, Tulsi, Sailen, Glen and Shraddha thank you all for the fun times and the awesome Indian food you guys cooked.

Samay, Thank you for always being there for me and thank you for being so wonderful.

To all my close friends across the miles thank you for all the optimism.

Very special thanks to all the members of my huge family, thank you for your endless support and affection.

Above all I would like to thank my eldest brother for being my guardian angel. Thank you for giving me education and help me fulfil my dreams. Without you I wouldn't have reached this stage of my journey.